

# **Evaluate, Modify, and Adapt the ConcreteWorks Software for Iowa's Use**

**Final Report  
March 2020**

---

**IOWA STATE UNIVERSITY**  
**Institute for Transportation**

**Sponsored by**  
Iowa Highway Research Board  
(IHRB Project TR-712)  
Iowa Department of Transportation  
(InTrans Project 16-581)

## **About the Institute for Transportation**

The mission of the Institute for Transportation (InTrans) at Iowa State University is to develop and implement innovative methods, materials, and technologies for improving transportation efficiency, safety, reliability, and sustainability while improving the learning environment of students, faculty, and staff in transportation-related fields.

## **Iowa State University Nondiscrimination Statement**

Iowa State University does not discriminate on the basis of race, color, age, ethnicity, religion, national origin, pregnancy, sexual orientation, gender identity, genetic information, sex, marital status, disability, or status as a US veteran. Inquiries regarding nondiscrimination policies may be directed to the Office of Equal Opportunity, 3410 Beardshear Hall, 515 Morrill Road, Ames, Iowa 50011, telephone: 515-294-7612, hotline: 515-294-1222, email: eooffice@iastate.edu.

## **Disclaimer Notice**

The contents of this report reflect the views of the authors, who are responsible for the facts and the accuracy of the information presented herein. The opinions, findings and conclusions expressed in this publication are those of the authors and not necessarily those of the sponsors.

The sponsors assume no liability for the contents or use of the information contained in this document. This report does not constitute a standard, specification, or regulation.

The sponsors do not endorse products or manufacturers. Trademarks or manufacturers' names appear in this report only because they are considered essential to the objective of the document.

## **Iowa DOT Statements**

Federal and state laws prohibit employment and/or public accommodation discrimination on the basis of age, color, creed, disability, gender identity, national origin, pregnancy, race, religion, sex, sexual orientation or veteran's status. If you believe you have been discriminated against, please contact the Iowa Civil Rights Commission at 800-457-4416 or the Iowa Department of Transportation affirmative action officer. If you need accommodations because of a disability to access the Iowa Department of Transportation's services, contact the agency's affirmative action officer at 800-262-0003.

The preparation of this report was financed in part through funds provided by the Iowa Department of Transportation through its "Second Revised Agreement for the Management of Research Conducted by Iowa State University for the Iowa Department of Transportation" and its amendments.

The opinions, findings, and conclusions expressed in this publication are those of the authors and not necessarily those of the Iowa Department of Transportation.

### Technical Report Documentation Page

|                                                                                                                                                                                                                                                                                                                                                                                                                                                                                                                                                                                                                                                                                                                                                                                                                                                                                                                                                                                                                                                                                                                                                                                                                                                                                                                                                                                                                                                                                                                                                                                                                                                                                                                                                                                                                                                                                                                                                                                                                                                                                                                                                                                                                                         |                                                                    |                                                                        |                        |
|-----------------------------------------------------------------------------------------------------------------------------------------------------------------------------------------------------------------------------------------------------------------------------------------------------------------------------------------------------------------------------------------------------------------------------------------------------------------------------------------------------------------------------------------------------------------------------------------------------------------------------------------------------------------------------------------------------------------------------------------------------------------------------------------------------------------------------------------------------------------------------------------------------------------------------------------------------------------------------------------------------------------------------------------------------------------------------------------------------------------------------------------------------------------------------------------------------------------------------------------------------------------------------------------------------------------------------------------------------------------------------------------------------------------------------------------------------------------------------------------------------------------------------------------------------------------------------------------------------------------------------------------------------------------------------------------------------------------------------------------------------------------------------------------------------------------------------------------------------------------------------------------------------------------------------------------------------------------------------------------------------------------------------------------------------------------------------------------------------------------------------------------------------------------------------------------------------------------------------------------|--------------------------------------------------------------------|------------------------------------------------------------------------|------------------------|
| <b>1. Report No.</b><br>IHRB Project TR-712                                                                                                                                                                                                                                                                                                                                                                                                                                                                                                                                                                                                                                                                                                                                                                                                                                                                                                                                                                                                                                                                                                                                                                                                                                                                                                                                                                                                                                                                                                                                                                                                                                                                                                                                                                                                                                                                                                                                                                                                                                                                                                                                                                                             | <b>2. Government Accession No.</b>                                 | <b>3. Recipient's Catalog No.</b>                                      |                        |
| <b>4. Title and Subtitle</b><br>Evaluate, Modify, and Adapt the ConcreteWorks Software for Iowa's Use                                                                                                                                                                                                                                                                                                                                                                                                                                                                                                                                                                                                                                                                                                                                                                                                                                                                                                                                                                                                                                                                                                                                                                                                                                                                                                                                                                                                                                                                                                                                                                                                                                                                                                                                                                                                                                                                                                                                                                                                                                                                                                                                   |                                                                    | <b>5. Report Date</b><br>March 2020                                    |                        |
|                                                                                                                                                                                                                                                                                                                                                                                                                                                                                                                                                                                                                                                                                                                                                                                                                                                                                                                                                                                                                                                                                                                                                                                                                                                                                                                                                                                                                                                                                                                                                                                                                                                                                                                                                                                                                                                                                                                                                                                                                                                                                                                                                                                                                                         |                                                                    | <b>6. Performing Organization Code</b>                                 |                        |
| <b>7. Author(s)</b><br>Kejin Wang (orcid.org/0000-0002-7466-3451), Yogiraj Sargam (orcid.org/0000-0001-9980-3038), Kyle Riding (orcid.org/0000-0001-8083-554X), Mahmoud Faytarouni (orcid.org/0000-0003-4231-158X), Charles Jahren (orcid.org/0000-0003-2828-8483), and Jay Shen (orcid.org/0000-0002-8201-5569)                                                                                                                                                                                                                                                                                                                                                                                                                                                                                                                                                                                                                                                                                                                                                                                                                                                                                                                                                                                                                                                                                                                                                                                                                                                                                                                                                                                                                                                                                                                                                                                                                                                                                                                                                                                                                                                                                                                        |                                                                    | <b>8. Performing Organization Report No.</b><br>InTrans Project 16-581 |                        |
| <b>9. Performing Organization Name and Address</b><br>Institute for Transportation<br>Iowa State University<br>2711 South Loop Drive, Suite 4700<br>Ames, IA 50010-8664                                                                                                                                                                                                                                                                                                                                                                                                                                                                                                                                                                                                                                                                                                                                                                                                                                                                                                                                                                                                                                                                                                                                                                                                                                                                                                                                                                                                                                                                                                                                                                                                                                                                                                                                                                                                                                                                                                                                                                                                                                                                 |                                                                    | <b>10. Work Unit No. (TRAIS)</b>                                       |                        |
|                                                                                                                                                                                                                                                                                                                                                                                                                                                                                                                                                                                                                                                                                                                                                                                                                                                                                                                                                                                                                                                                                                                                                                                                                                                                                                                                                                                                                                                                                                                                                                                                                                                                                                                                                                                                                                                                                                                                                                                                                                                                                                                                                                                                                                         |                                                                    | <b>11. Contract or Grant No.</b>                                       |                        |
| <b>12. Sponsoring Organization Name and Address</b><br>Iowa Highway Research Board<br>Iowa Department of Transportation<br>800 Lincoln Way<br>Ames, IA 50010                                                                                                                                                                                                                                                                                                                                                                                                                                                                                                                                                                                                                                                                                                                                                                                                                                                                                                                                                                                                                                                                                                                                                                                                                                                                                                                                                                                                                                                                                                                                                                                                                                                                                                                                                                                                                                                                                                                                                                                                                                                                            |                                                                    | <b>13. Type of Report and Period Covered</b><br>Final Report           |                        |
|                                                                                                                                                                                                                                                                                                                                                                                                                                                                                                                                                                                                                                                                                                                                                                                                                                                                                                                                                                                                                                                                                                                                                                                                                                                                                                                                                                                                                                                                                                                                                                                                                                                                                                                                                                                                                                                                                                                                                                                                                                                                                                                                                                                                                                         |                                                                    | <b>14. Sponsoring Agency Code</b><br>IHRB Project TR-712               |                        |
| <b>15. Supplementary Notes</b><br>Visit <a href="https://intrans.iastate.edu/">https://intrans.iastate.edu/</a> for color pdfs of this and other research reports.                                                                                                                                                                                                                                                                                                                                                                                                                                                                                                                                                                                                                                                                                                                                                                                                                                                                                                                                                                                                                                                                                                                                                                                                                                                                                                                                                                                                                                                                                                                                                                                                                                                                                                                                                                                                                                                                                                                                                                                                                                                                      |                                                                    |                                                                        |                        |
| <b>16. Abstract</b><br><p>The early-age thermal development in mass concrete has a significant impact on the performance and long-term serviceability of mass concrete structures, such as bridge foundations. Great efforts have been made on predicting and controlling the thermal development in mass concrete. ConcreteWorks has been increasingly used for this purpose. However, previous research in Iowa indicated that, although user-friendly, the public ConcreteWorks program has some features that do not fit Iowa concrete well. The present research aimed at modifying the ConcreteWorks software for Iowa's use, particularly for the prediction of thermal behavior of mass concrete elements with a smallest dimension of 6.5 feet or less.</p> <p>In this study, the input and output parameters of ConcreteWorks that need to be modified for Iowa's use were identified. The key properties (heat of hydration, thermal conductivity, mechanical properties, etc.) of typical Iowa concrete mixes required by ConcreteWorks for thermal predictions were tested. The Iowa environmental data and Iowa Department of Transportation (DOT) temperature differential limits were incorporated into the modified ConcreteWorks program. An initial soil temperature model was added. Thermal analyses were conducted on a real-time mass concrete project (the I-35 NB to US 30 WB [Ramp H] bridge) using both the unmodified and modified ConcreteWorks software as well as 4C-Temp&amp;Stress software, and the predicted temperature developments were compared with those monitored from the field site.</p> <p>The results indicate that the modified ConcreteWorks software predicts the early-age temperature profile, maturity, and strength of Iowa mass concrete quite well. As many default data in the public ConcreteWorks software are replaced with Iowa concrete values, the modified software is even more user-friendly and reliable for Iowa's use. A hands-on workshop on learning how to use ConcreteWorks was welcomed by Iowa engineers. Recommendations are made in this report for effective use of the modified ConcreteWorks software in Iowa and for further research in this area.</p> |                                                                    |                                                                        |                        |
| <b>17. Key Words</b><br>4C-Temp&Stress—ConcreteWorks—mass concrete—thermal analysis                                                                                                                                                                                                                                                                                                                                                                                                                                                                                                                                                                                                                                                                                                                                                                                                                                                                                                                                                                                                                                                                                                                                                                                                                                                                                                                                                                                                                                                                                                                                                                                                                                                                                                                                                                                                                                                                                                                                                                                                                                                                                                                                                     |                                                                    | <b>18. Distribution Statement</b><br>No restrictions.                  |                        |
| <b>19. Security Classification (of this report)</b><br>Unclassified.                                                                                                                                                                                                                                                                                                                                                                                                                                                                                                                                                                                                                                                                                                                                                                                                                                                                                                                                                                                                                                                                                                                                                                                                                                                                                                                                                                                                                                                                                                                                                                                                                                                                                                                                                                                                                                                                                                                                                                                                                                                                                                                                                                    | <b>20. Security Classification (of this page)</b><br>Unclassified. | <b>21. No. of Pages</b><br>138                                         | <b>22. Price</b><br>NA |





# **EVALUATE, MODIFY, AND ADAPT THE CONCRETEWORKS SOFTWARE FOR IOWA'S USE**

**Final Report  
March 2020**

**Principal Investigator**

Kejin Wang, Professor  
Institute for Transportation, Iowa State University

**Co-Principal Investigators**

Kyle Riding, Associate Professor  
Department of Civil and Coastal Engineering, Kansas State University  
Chuck Jahren, Professor  
Civil, Construction, and Environmental Engineering, Iowa State University  
Jay Shen, Associate Professor  
Civil, Construction, and Environmental Engineering, Iowa State University

**Research Assistants**

Yogiraj Sargam and Mahmoud Faytarouni

**Authors**

Kejin Wang, Yogiraj Sargam, Kyle Riding, Mahmoud Faytarouni, Charles Jahren, and Jay Shen,

Sponsored by  
Iowa Highway Research Board and  
Iowa Department of Transportation  
(IHRB Project TR-712)

Preparation of this report was financed in part  
through funds provided by the Iowa Department of Transportation  
through its Research Management Agreement with the  
Institute for Transportation  
(InTrans Project 16-581)

A report from  
**Institute for Transportation**  
**Iowa State University**  
2711 South Loop Drive, Suite 4700  
Ames, IA 50010-8664  
Phone. 515-294-8103 / Fax. 515-294-0467  
<https://intrans.iastate.edu/>



## TABLE OF CONTENTS

|                                                                   |      |
|-------------------------------------------------------------------|------|
| ACKNOWLEDGMENTS .....                                             | xi   |
| EXECUTIVE SUMMARY .....                                           | xiii |
| 1. INTRODUCTION .....                                             | 1    |
| Problem Statement .....                                           | 1    |
| Goals and Objectives .....                                        | 1    |
| Tasks Conducted .....                                             | 2    |
| Scope of Report .....                                             | 2    |
| 2. SOFTWARE REVIEW .....                                          | 4    |
| ConcreteWorks Review .....                                        | 4    |
| 4C-Temp&Stress Review .....                                       | 7    |
| Comparison of Inputs and Prediction Models .....                  | 9    |
| 3. EXPERIMENTS AND TEST METHODS .....                             | 13   |
| Materials and Mixes .....                                         | 13   |
| Tests and Methods .....                                           | 16   |
| 4. RESULTS AND DISCUSSION .....                                   | 30   |
| Properties of Fresh Concrete .....                                | 30   |
| Properties of Hardened Concrete .....                             | 30   |
| Semi-Adiabatic Calorimetry .....                                  | 42   |
| Thermal Conductivity .....                                        | 44   |
| Coefficient of Thermal Expansion .....                            | 45   |
| 5. FIELD INVESTIGATION .....                                      | 46   |
| Investigation before Placement of Concrete .....                  | 48   |
| Investigation during Placement of Concrete .....                  | 53   |
| Investigation after Placement of Concrete .....                   | 57   |
| 6. CONCRETEWORKS MODIFICATIONS .....                              | 69   |
| Modifications in Input .....                                      | 69   |
| Modifications in Output .....                                     | 74   |
| 7. THERMAL ANALYSIS USING CONCRETEWORKS AND 4C .....              | 77   |
| Analysis of the Field Mix .....                                   | 77   |
| Analysis of Laboratory Mixes .....                                | 88   |
| 8. WORKSHOP AND SOFTWARE DOWNLOAD DETAILS .....                   | 106  |
| 9. CONCLUSIONS AND RECOMMENDATIONS .....                          | 108  |
| REFERENCES .....                                                  | 111  |
| APPENDIX A. CALIBRATION OF ISOTHERMAL CALORIMETER .....           | 113  |
| APPENDIX B. STEPS FOR BUILDING A SEMI-ADIABATIC CALORIMETER ..... | 115  |

|                                                                                |     |
|--------------------------------------------------------------------------------|-----|
| APPENDIX C. CALIBRATION OF SEMI-ADIABATIC CALORIMETER.....                     | 119 |
| APPENDIX D. PROCEDURE TO ASSEMBLE THE THERMAL CONDUCTIVITY<br>TEST SETUP ..... | 121 |
| APPENDIX E. CALIBRATION OF THERMAL CONDUCTIVITY APPARATUS .....                | 123 |

## LIST OF FIGURES

|                                                                                                                                                                                                                                                                     |    |
|---------------------------------------------------------------------------------------------------------------------------------------------------------------------------------------------------------------------------------------------------------------------|----|
| Figure 2.1. Temperature prediction model in ConcreteWorks .....                                                                                                                                                                                                     | 5  |
| Figure 2.2. Flowchart of the thermal stress modeling in ConcreteWorks .....                                                                                                                                                                                         | 6  |
| Figure 2.3. Process of performing an analysis in 4C-Temp & Stress program .....                                                                                                                                                                                     | 9  |
| Figure 3.1. Aggregate gradation curves: ASTM C33 (top) and 8/18 gradation (bottom) .....                                                                                                                                                                            | 15 |
| Figure 3.2. Isothermal calorimeter (left) and channels for holding samples (right) .....                                                                                                                                                                            | 18 |
| Figure 3.3. Arrhenius plot .....                                                                                                                                                                                                                                    | 21 |
| Figure 3.4. Semi-adiabatic calorimeter .....                                                                                                                                                                                                                        | 22 |
| Figure 3.5. Thermal conductivity test setup .....                                                                                                                                                                                                                   | 26 |
| Figure 3.6. Coefficient of thermal expansion test equipment .....                                                                                                                                                                                                   | 28 |
| Figure 4.1. Compressive strength development .....                                                                                                                                                                                                                  | 31 |
| Figure 4.2. Compressive strength – TTF best-fit curve .....                                                                                                                                                                                                         | 33 |
| Figure 4.3. Rate of heat generation (Mix 1) .....                                                                                                                                                                                                                   | 34 |
| Figure 4.4. Cumulative heat (Mix 1) .....                                                                                                                                                                                                                           | 35 |
| Figure 4.5. Rate of heat and cumulative heat (Mix 2) .....                                                                                                                                                                                                          | 36 |
| Figure 4.6. Rate of heat and cumulative heat (Mix 3) .....                                                                                                                                                                                                          | 37 |
| Figure 4.7. Rate of heat and cumulative heat (Mix 4) .....                                                                                                                                                                                                          | 38 |
| Figure 4.8. Arrhenius plots for activation energy .....                                                                                                                                                                                                             | 40 |
| Figure 4.9. Measured semi-adiabatic (top) and calculated adiabatic temperature (bottom) .....                                                                                                                                                                       | 43 |
| Figure 4.10. Temperature development during thermal conductivity test .....                                                                                                                                                                                         | 44 |
| Figure 5.1. Location of the I-35 to US 30 Bridge .....                                                                                                                                                                                                              | 46 |
| Figure 5.2. Locations of all six piers .....                                                                                                                                                                                                                        | 47 |
| Figure 5.3. Dimensions of all six piers .....                                                                                                                                                                                                                       | 47 |
| Figure 5.4. Subsurface profile of Pier 4 job site (left), Thickness of layers (top right), and<br>Excavated soil (bottom right) .....                                                                                                                               | 48 |
| Figure 5.5. Limestone subbase with steel bearing H-piles (left) and front elevation of<br>footing with subbase (right) .....                                                                                                                                        | 49 |
| Figure 5.6. Formwork used in Pier 4 footing .....                                                                                                                                                                                                                   | 50 |
| Figure 5.7. Locations of temperature sensors installed in Pier 4 footing .....                                                                                                                                                                                      | 50 |
| Figure 5.8. Data loggers (left), primary and backup sensors (center), and measurement of<br>sensor locations (right) .....                                                                                                                                          | 51 |
| Figure 5.9. Predicted maximum temperature at the core, ambient temperature, and<br>temperature differential compared to Iowa DOT specified limits .....                                                                                                             | 53 |
| Figure 5.10. Pouring concrete using pump (left) and compaction using vibrator (right) .....                                                                                                                                                                         | 54 |
| Figure 5.11. Weather station at job site .....                                                                                                                                                                                                                      | 55 |
| Figure 5.12. Casting cylindrical specimens (left) and curing specimens in field conditions<br>at the job site (right) .....                                                                                                                                         | 56 |
| Figure 5.13. Insulation blanket over formwork .....                                                                                                                                                                                                                 | 56 |
| Figure 5.14. Recorded temperature data of all sensors .....                                                                                                                                                                                                         | 59 |
| Figure 5.15. Differential temperature in concrete footing with age .....                                                                                                                                                                                            | 59 |
| Figure 5.16. Temperature (top) and relative humidity (bottom) variations with age .....                                                                                                                                                                             | 62 |
| Figure 5.17. Insulation and formwork removal stage: Day 0 Insulation blanket (top left),<br>Day 5. Formwork removed from three sides (top right), Day 10 Exposed<br>concrete surface (bottom left), and Day 12 Footing backfilled with soil (bottom<br>right) ..... | 63 |

|                                                                                                                                                |     |
|------------------------------------------------------------------------------------------------------------------------------------------------|-----|
| Figure 5.18. Compressive strength development (left) and compressive strength-TTF curve (right).....                                           | 65  |
| Figure 5.19. Variation of temperature in thermal conductivity test.....                                                                        | 66  |
| Figure 5.20. Rate of heat generation at different temperatures.....                                                                            | 67  |
| Figure 5.21. Measured semi-adiabatic and calculated true adiabatic temperature for field specimen (left) and laboratory specimen (right) ..... | 68  |
| Figure 6.1. Analysis duration increased to 30 days .....                                                                                       | 69  |
| Figure 6.2. Four new Iowa cities incorporated into ConcreteWorks .....                                                                         | 70  |
| Figure 6.3. One-dimensional analysis added to ConcreteWorks .....                                                                              | 71  |
| Figure 6.4. Default cement chemical/physical properties in new ConcreteWorks .....                                                             | 71  |
| Figure 6.5. Default hydration parameters in new ConcreteWorks .....                                                                            | 72  |
| Figure 6.6. Insulated steel formwork added to new ConcreteWorks.....                                                                           | 72  |
| Figure 6.7. Insulated formwork R-value .....                                                                                                   | 73  |
| Figure 6.8. New soil temperature calculation model incorporated into ConcreteWorks.....                                                        | 74  |
| Figure 6.9. Iowa DOT mass concrete temperature differential limits shown in the output.....                                                    | 74  |
| Figure 6.10. Iowa DOT mass concrete temperature differential limits incorporated into new ConcreteWorks.....                                   | 75  |
| Figure 6.11. Thermocouple locations in the old ConcreteWorks .....                                                                             | 76  |
| Figure 6.12. Thermocouple locations picked by exact position in new ConcreteWorks .....                                                        | 76  |
| Figure 7.1. Input data in the new ConcreteWorks (field mix).....                                                                               | 78  |
| Figure 7.2. Maximum temperature comparisons for field mix .....                                                                                | 79  |
| Figure 7.3. Temperature profiles at installed thermocouple locations (field mix) .....                                                         | 81  |
| Figure 7.4. Differential temperature analysis (field mix) .....                                                                                | 84  |
| Figure 7.5. Maturity comparisons for field mix.....                                                                                            | 86  |
| Figure 7.6. Compressive strength comparisons for field mix .....                                                                               | 87  |
| Figure 7.7. Probability density for cracking probability classification in ConcreteWorks .....                                                 | 87  |
| Figure 7.8. Cracking probability prediction for field mix .....                                                                                | 88  |
| Figure 7.9. ConcreteWorks input for Mix I-20.....                                                                                              | 90  |
| Figure 7.10. Temperature at the core of footing (Mix 1).....                                                                                   | 91  |
| Figure 7.12. Cracking probability prediction for Mix 1 .....                                                                                   | 93  |
| Figure 7.13. Temperature at the core of footing (Mix 2).....                                                                                   | 94  |
| Figure 7.14. Differential temperature comparisons for Mix 2.....                                                                               | 95  |
| Figure 7.15. Cracking probability prediction for Mix 2 .....                                                                                   | 96  |
| Figure 7.16. Temperature at the core of footing (Mix 3).....                                                                                   | 97  |
| Figure 7.17. Differential temperature comparisons for Mix 3.....                                                                               | 98  |
| Figure 7.18. Cracking probability prediction for Mix 3 .....                                                                                   | 99  |
| Figure 7.19. Temperature at the core of footing (Mix 4).....                                                                                   | 100 |
| Figure 7.20. Differential temperature comparisons for Mix 4.....                                                                               | 101 |
| Figure 7.21. Cracking probability prediction for Mix 4 .....                                                                                   | 102 |
| Figure 7.22. Maximum temperature comparison of laboratory mixes .....                                                                          | 103 |
| Figure 7.23. Maximum temperature differential comparison of laboratory mixes.....                                                              | 104 |
| Figure 7.24. Maturity and compressive strength comparison of laboratory mixes .....                                                            | 105 |
| Figure 8.1. Mass concrete fundamentals workshop.....                                                                                           | 107 |
| Figure B.1. Specimen holder .....                                                                                                              | 115 |
| Figure B.2. Thermocouple wires through drilled hole.....                                                                                       | 115 |
| Figure B.3. Cut-off at steel chamber edge .....                                                                                                | 116 |

|                                                                                                                                                         |     |
|---------------------------------------------------------------------------------------------------------------------------------------------------------|-----|
| Figure B.4. Use of foam sealant.....                                                                                                                    | 116 |
| Figure B.5. Alignment of foam with steel chamber.....                                                                                                   | 117 |
| Figure B.6. Acrylic sheet finish .....                                                                                                                  | 117 |
| Figure B.7. Semi-adiabatic calorimeter .....                                                                                                            | 118 |
| Figure D.1. Specimen preparation .....                                                                                                                  | 121 |
| Figure D.2. Iron disks for holding the rod .....                                                                                                        | 121 |
| Figure E.1. Reference material (UHMWPE).....                                                                                                            | 123 |
| Figure E.2. Thermal conductivity test for UHMWPE with temperature development during<br>the test (left) and measured $k$ of four test runs (right)..... | 124 |

## LIST OF TABLES

|                                                                                             |     |
|---------------------------------------------------------------------------------------------|-----|
| Table 2.1. Comparison of inputs in ConcreteWorks and 4C .....                               | 10  |
| Table 2.2. Comparison of prediction models used in ConcreteWorks and 4C.....                | 11  |
| Table 3.1. Concrete mix proportions .....                                                   | 13  |
| Table 3.2. Chemical composition of cementitious materials (%).....                          | 14  |
| Table 3.3. Properties of aggregate .....                                                    | 14  |
| Table 3.4. Cement paste mix proportions .....                                               | 19  |
| Table 4.1. Properties of fresh concrete .....                                               | 30  |
| Table 4.2. Split tensile strength and E-modulus at 28 days .....                            | 31  |
| Table 4.3. Maturity calculations for Mix 1 .....                                            | 32  |
| Table 4.4. Coefficients $a$ and $b$ of best-fit strength-maturity equation .....            | 33  |
| Table 4.5. Hydration curve parameters and $E_a$ values of all mixes .....                   | 41  |
| Table 4.6. Hydration parameters from semi-adiabatic calorimetry .....                       | 42  |
| Table 4.7. 95% confidence interval for mean thermal conductivity.....                       | 45  |
| Table 4.8. CTE values of concrete mixes .....                                               | 45  |
| Table 5.1. Iowa DOT maximum temperature differential limits .....                           | 52  |
| Table 5.2. Concrete mix proportion.....                                                     | 54  |
| Table 5.3. Fresh properties of Pier 4 footing concrete.....                                 | 55  |
| Table 5.4. Comparison of measured and predicted temperature .....                           | 60  |
| Table 5.5. Weather conditions at Pier 4 site .....                                          | 61  |
| Table 5.6. Cement and fly ash properties .....                                              | 64  |
| Table 5.7. Aggregate properties.....                                                        | 64  |
| Table 5.8. $H_u$ , Curve parameters and activation energy from isothermal calorimetry ..... | 67  |
| Table 7.1. Comparison of measured and predicted concrete temperature for field mix.....     | 77  |
| Table 7.2. Comparison of maximum temperature at thermocouple locations for field mix.....   | 82  |
| Table 7.3. Maximum temperature comparisons for laboratory mixes.....                        | 103 |
| Table 8.1. Presentations at the Mass Concrete Fundamentals workshop .....                   | 106 |
| Table A.1. Calibration factors for eight channels of isothermal calorimeter.....            | 114 |
| Table C.1. Calibration factors for semi-adiabatic calorimeter.....                          | 120 |





## **ACKNOWLEDGMENTS**

The authors would like to acknowledge the Iowa Department of Transportation (DOT) and the Iowa Highway Research Board (IHRB) for sponsoring this project.

The project technical advisory committee members were Ahmad Abu-Hawash, Todd Hanson, James Nelson, Wayne Sunday, and Curtis Carter. The authors gratefully acknowledge their valuable suggestions throughout the course of this project.

The help provided by the National Concrete Pavement Technology (CP Tech) Center research engineer Robert R. Steffes and graduate students at Iowa State University (ISU) during the field investigations are also greatly appreciated.



## EXECUTIVE SUMMARY

High temperature differentials in a mass concrete member at the early age may cause thermal cracking, thereby impacting its long-term durability. To minimize the risk of cracking, temperature prediction tools are often used to assist decision makers and determine preventive measures. ConcreteWorks is a computer program that helps analyze and manage the temperature of early-age mass concrete in specific geographical locations (e.g., Texas).

This project aimed to evaluate, modify, and adapt the ConcreteWorks software for use in Iowa. The long-term goals are to improve the longevity and performance of mass concrete constructed in Iowa with an emphasis on bridge foundations. The following major research activities were carried out as part of this project:

- Measure key properties of mass concrete mixes commonly used in Iowa in the laboratory
- Investigate a real-time mass concrete project (I-35 NB to US 30 WB bridge footing)
- Modify ConcreteWorks based on the test and field data and with suggestions from the technical advisory committee
- Conduct thermal analyses using ConcreteWorks and another software program, 4C-Temp&Stress, for laboratory and field concrete mixes
- Refine ConcreteWorks based on analysis results and feedback and review comments from the project team
- Develop recommendations

Observations from the tests on commonly used mass concrete mixes in Iowa are presented in this report. Various modifications (e.g., modifying default values, incorporating a soil temperature model, adding Iowa weather stations, extending temperature analysis duration to 30 days) were accomplished in ConcreteWorks and are presented herein. A comparative thermal analysis using three computer programs (old and modified ConcreteWorks and 4C) revealed that the modified ConcreteWorks better predicts the early-age temperature profile, maturity, strength, and cracking probability of Iowa mass concrete. Recommendations for an effective use of this modified ConcreteWorks are also presented in this report.



# **1. INTRODUCTION**

## **Problem Statement**

Early-age thermal development in concrete has a significant impact on the performance and long-term serviceability of mass concrete structures such as bridge foundations. In mass concrete placements, high thermal differentials between the concrete surface and the interior can result in large temperature-induced stresses, which increase the risk of early-age cracking (ACI 2006, Riding et al. 2006). This can cause durability problems such as delayed ettringite formation (DEF) and increased reinforcing steel corrosion risk due to thermal cracking (Riding et al. 2006).

The number of structural members considered to be mass concrete has increased in recent years. To minimize the risk of cracking, a range of preventive measures could be taken and, for that, the temperature development within the structure must be known. Many studies have been carried out and a few finite element-based analysis software applications have been developed to predict this temperature development.

A previous research project sponsored by the Iowa Department of Transportation (DOT) analyzed two such computer software programs—ConcreteWorks and 4C-Temp&Stress—and recommended that ConcreteWorks is much easier to use than 4C-Temp&Stress and capable of predicting the general trend of thermal development of mass concrete elements (focused on structural elements with the smallest dimension of 6.5 feet or less). However, the same investigation also indicated there are some features in the ConcreteWorks program that do not fit typical Iowa concrete construction situations appropriately.

For example, some units are in the metric system, some default input data (e.g., materials and properties) do not align with Iowa mass concrete materials and practice, there is no consideration of cooling pipe systems, and the program provides limited temperature output up to 14 days and cracking potential up to 7 days only. The outputs do not provide sufficient information on the degree (e.g., stress-to-strength ratio) or probability of cracking. The software application also lacks the flexibility to create new construction methods or edit outputs (Shaw et al. 2011).

## **Goals and Objectives**

This research project was intended to evaluate, modify, and adapt the ConcreteWorks software application to enhance its usefulness for mass concrete construction activities in Iowa. The long-term goals are to improve the longevity and performance of Iowa bridge foundations and other mass concrete structures by better understanding the thermal behavior of Iowa mass concrete, properly managing temperature development in mass concrete, and reducing concrete thermal cracking potential. The following objectives were set to reach these goals:

- Identify the parameters and modification methods that are necessary for adapting the software for use in Iowa
- Investigate the key properties of typical Iowa mass concrete mixes that are required by

- ConcreteWorks as input data
- Evaluate the usefulness of the modified software on an actual mass concrete project
- Provide rational recommendations for the Iowa concrete industry to effectively use the modified ConcreteWorks software application
- Provide insight regarding how to refine Iowa specifications and requirements for mass concrete analysis, potentially eliminating unwarranted analysis affects and reducing construction costs

## **Tasks Conducted**

The following tasks were accomplished as part of this research:

- Task 1* Review the current ConcreteWorks software application and identify the parameters to be modified
- Task 2* Test the key properties of mass concrete mixes commonly used in Iowa
- Task 3* Modify the ConcreteWorks software based on the outputs of Task 2
- Task 4* Refine the modified ConcreteWorks software through an analysis of a previous mass concrete project
- Task 5* Conduct thermal analysis on an actual mass concrete project using the modified software
- Task 6* Conduct thermal analysis on the same actual mass concrete project using the 4C-Temp&Stress program and compare the results with those obtained from Task 5
- Task 7* Develop recommendations for the effective use of the modified ConcreteWorks software application

## **Scope of Report**

This report documents the investigation performed to complete the above-mentioned tasks.

*Chapter 1* outlines the problem statement, goals and objectives, and tasks conducted.

*Chapter 2* presents a brief review of the two software applications used in this research, ConcreteWorks and 4C-Temp&Stress. A comparison of the models used in both the applications for various calculations, such as heat development, thermal conductivity, specific heat, and mechanical properties development, is also presented.

*Chapter 3* describes the methods of the laboratory experiments and tests conducted: isothermal calorimetry, semi-adiabatic calorimetry, thermal conductivity, coefficient of thermal expansion and others.

*Chapter 4* presents the results of the experiments performed on the four concrete mixes tested in the laboratory as part of Task 2. The observations are also analyzed and discussed in this chapter.

*Chapter 5* reports the investigation of the construction of Pier 4 of the I-35 NB to US 30 WB bridge in Ames, Iowa. The investigation was subdivided and is reported in three parts: before, during, and after the placement of concrete.

*Chapter 6* describes the modifications made in the ConcreteWorks program based on the laboratory tests and field investigation.

*Chapter 7* presents the results of the thermal analysis performed using ConcreteWorks and 4C on the concrete mixes in the laboratory and on the job site. The analysis results from the two studies are also compared.

*Chapter 8* covers workshop and software download details.

*Chapter 9* summarizes and concludes this research work. Recommendations for effective use of the modified ConcreteWorks program are also presented.

## **2. SOFTWARE REVIEW**

### **ConcreteWorks Review**

ConcreteWorks is a software package developed at the Concrete Durability Center at the University of Texas. This software package was designed to assist with concrete mix proportioning, thermal analysis, and chloride diffusion service life evaluation of concrete. It can also be used to analyze the early-age thermal development and cracking potential of mass concrete and assist in the design of mass concrete placements (Riding 2007). Additionally, it contains design modules for several structural concrete applications, including bridge decks types, precast concrete beams, and concrete pavements. ConcreteWorks input data include the following parameters.

- Concrete material properties (cementitious properties, mix proportions, etc.)
- Structural parameters (shape, dimension, and subgrade condition)
- Construction parameters (concrete placement temperature, casting rate, curing/insulation methods, formwork removal time)
- Environmental parameters (ambient temperature variation, relative humidity, etc.)

The outputs of ConcreteWorks include predicting the maximum temperature within a unit, maximum temperature differential, maturity and compressive strength with respect to time, and a cracking potential. Additional details are available in the user manual (Riding et al. 2017).

ConcreteWorks utilizes the finite difference method to analyze the thermal development of mass concrete elements. To complete the thermal analysis of a mass concrete member, the software considers the material constituents, mix proportion, geometry, formwork type, and environmental conditions (Meeks and Folliard 2013) as shown in Figure 2.1.



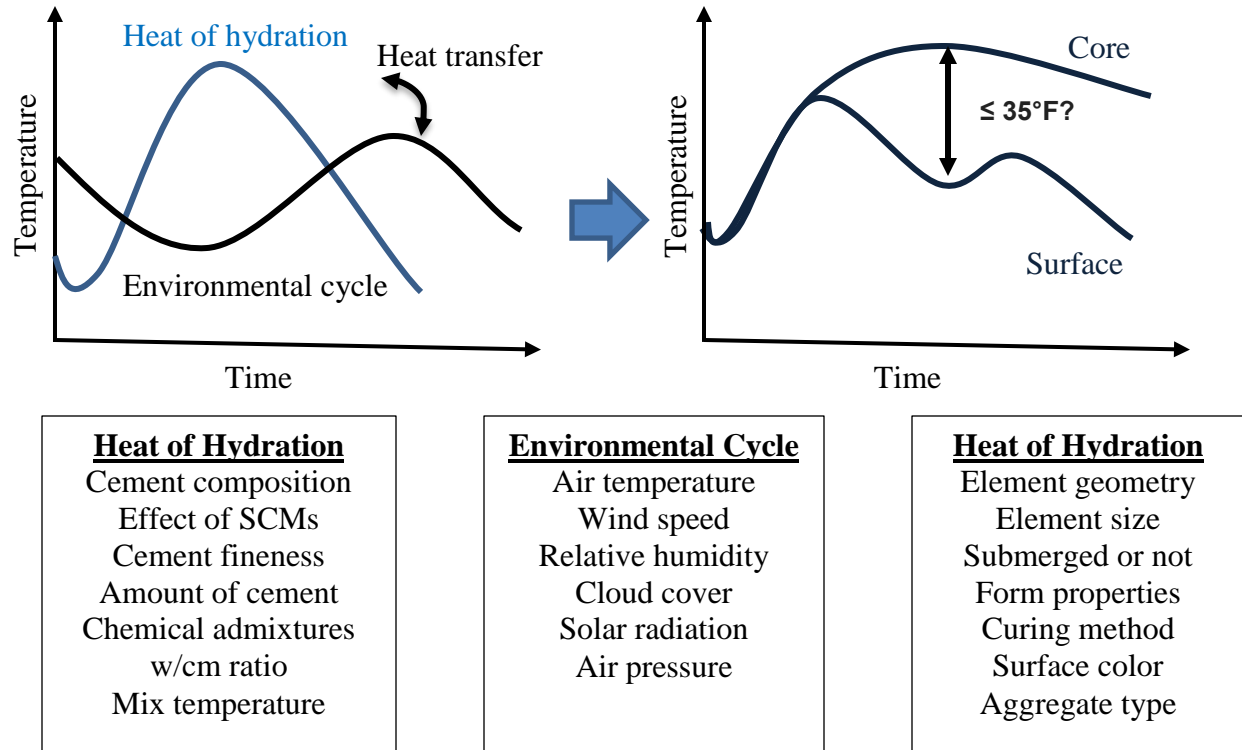


**Figure 2.1. Temperature prediction model in ConcreteWorks**

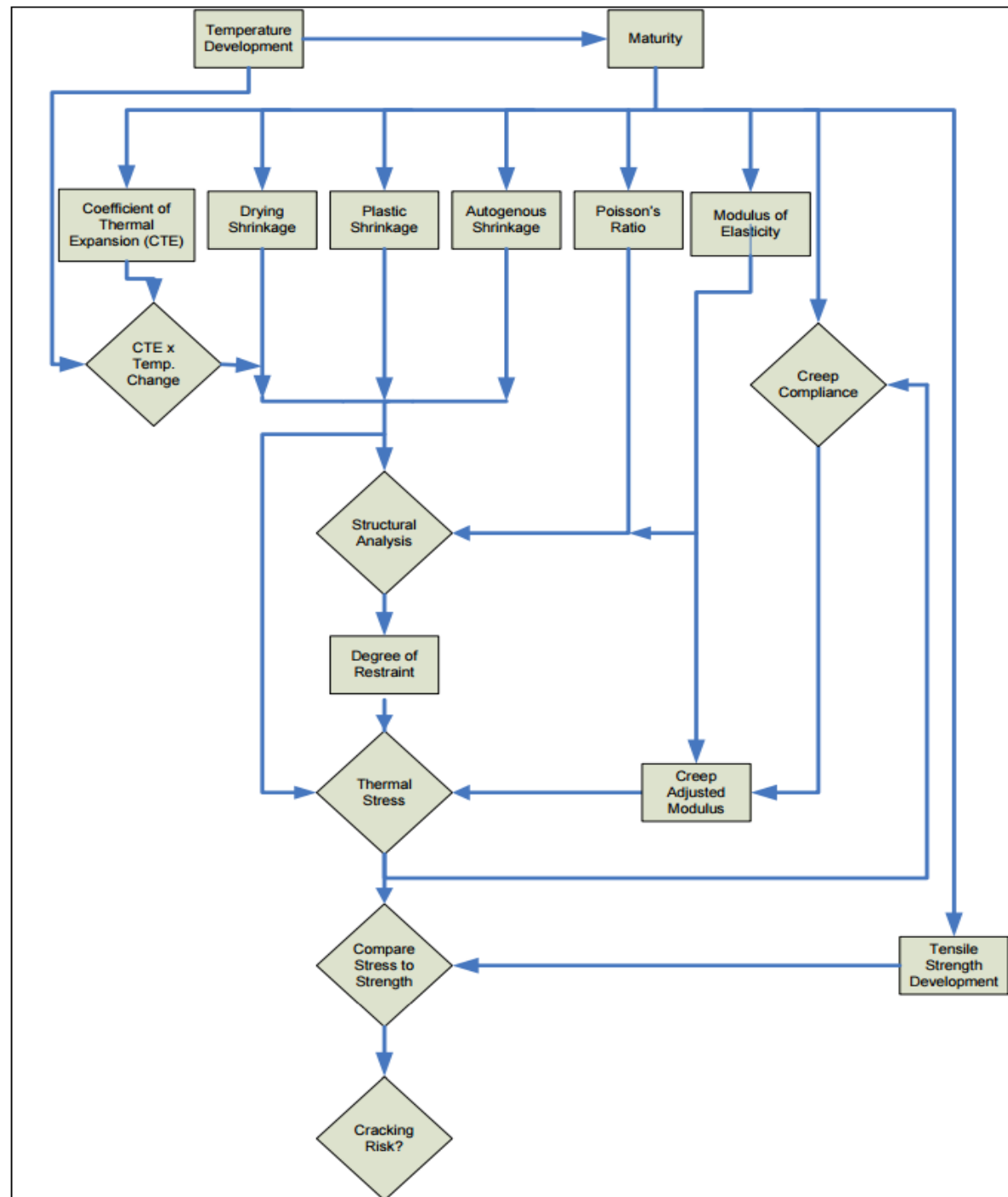
The ConcreteWorks program also considers the thermal energy generated from the process of cement hydration and the changes in the thermal energy in the placement and in the temperature of the concrete with time (Riding 2007). In addition, conduction, convection, evaporation, cooling, radiation, irradiation, and cement hydration are also considered to quantify the thermal energy entering ( $E_{in}$ ), exiting ( $E_{out}$ ), and being generated ( $E_{gen}$ ) in the volume, as follows:

$$\Delta E = E_{in} - E_{out} + E_{gen}$$

Where,  $\Delta E$  = change in thermal energy stored in the control volume,  $E_{in}$  = thermal energy entering control volume,  $E_{out}$  = thermal energy leaving control volume, and  $E_{gen}$  = thermal energy generated within control volume.

The finite difference method is employed to numerically evaluate the variation in temperature inside a mass concrete structure. In this method, a volume of concrete is divided into sufficiently small volumes with assumed constant thermal properties over that time step. For each volume, the energy conservation law is used to relate the temperature at each corner of this volume to the physical properties of the volume. The relations for each individual volume are then assembled using equilibrium balance amongst adjacent volumes to express the behavior of the entire structure.

ConcreteWorks considers the changing early-age properties of materials (elastic modulus, strength, Poisson's ratio, and coefficient of thermal expansion), differential temperature development, and creep, and uses non-linearity in thermal stress modeling (Riding 2007). Figure 2.2 shows a flowchart of the relationship between the various parameters in the thermal stress modeling of concrete structures as used by ConcreteWorks.



© Riding 2007

**Figure 2.2. Flowchart of the thermal stress modeling in ConcreteWorks**

In order to calculate the thermal stresses, the concrete member degree of hydration (DOH) and temperature development is first calculated. Next, the DOH and temperature development is used to calculate the strains the concrete would undergo in case of a restraint, including the changing early-age properties. After that, the concrete elastic stress is calculated from the free shrinkage strains and mechanical properties by performing a structural analysis. Stress relaxation is then applied to the concrete elastic stress. Finally, a failure criterion, such as the stress to tensile strength ratio, is used to determine the cracking risk (Riding et al. 2017).

The software has a built-in statistical predictive model to calculate the variables needed to perform the calculations. Some examples include a built-in 30-year historical weather model, the use of cement chemistry typical of the cement type, the ability to calculate hydration parameters from the cement chemistry, and, finally, the model for calculating heat transfer constants based on aggregate classification.

In all cases, the program allows the user to overwrite programmatically determined values with those obtained from laboratory testing. Doing so improves the overall accuracy of the resulting temperature prediction (Meeks and Folliard 2013).

In the previous Iowa Mass Concrete for Bridge Foundations Study that Iowa State University's Institute for Transportation (InTrans) conducted for the Iowa DOT, the ConcreteWorks program was used to study the temperature development profile in the concrete placed for the WB I-80 and US 34 bridge over the Missouri River in Iowa (Shaw et al. 2014). The results indicated that the program is capable of predicting the maximum temperature and maximum temperature difference of placements as well as the thermal development of placements at discrete locations with regard to time to a reasonable degree. The project report concludes that, on average, ConcreteWorks underestimates the maximum temperature of a placement by 12.3°F, and overestimates the maximum temperature difference by 1.9°F. The researchers recommended some adjustments to the inputs and outputs to ensure that the results are conservative and to increase the analysis duration from 14 days to 30 days (Shaw et al. 2014).

#### **4C-Temp&Stress Review**

4C-Temp & Stress is a finite element (FE) computer program developed by the Danish Technological Institute to conduct thermal, maturity, and stress analysis for concrete structures. The software automatically transforms the physical concrete structure defined by the user into formulations operated by using a finite element method. A set of triangular plane elements representing the defined geometry is used to compute the temperature and stress following a quadratic variation. The software calculates the time-dependent concrete temperatures and the corresponding thermal stresses considering the influence of other significant parameters on the thermal state of concrete. These are the parameters used: heat of hydration, thermal boundary conditions, time of casting, heating wires or cooling pipes, and environmental factors (wind and radiation). The numerical simulations provided by this software help to obtain the temperatures that typically develop due to hydration of cement in concrete and, therefore, assist in planning concrete casting in order to reduce the risk of cracks induced from thermal stresses.

The software's development of temperatures and stresses are obtained from transient analysis, i.e., as a function of place and time. When conducting thermal analysis, the external temperature, type of insulation, internal heat generation by the materials, and the thermal boundary conditions, all reflect necessary inputs for successful analysis. These latter inputs along with external loads and supports, thermal expansion, stiffness and strength properties developed as a function of maturity, and creep and relaxation of materials are also considered necessary for subsequent stress analysis. It is noteworthy to mention that stress analysis is typically performed based on inputs given for thermal analysis and its corresponding results. However, if the interest is on evaluating stresses without considering the thermal impact, the stress analysis will be based on external loads only.

The software uses certain computational assumptions to simplify the numerical simulations, particularly on those employed in the thermal analysis. For example, the location of the minimum temperature is considered as that at the top surface of the concrete structure, and the maximum temperature is considered as that at mid-center. The top surface temperature is considered as an ambient temperature, which equals an averaged 7-day temperature and is defined through a sinusoidal curve during the entire duration of the analysis. This sinusoidal curve assumes a constant wind speed instead of actual weather conditions, where the temperature history varies and differs from one day to another. The definition of the temperature difference is that between the location of mid-center and the top surface sensor located three inches below the surface. Another default input assumption is on the nonlinear convergence criteria that are typically defined as 0.001. This convergence value deems large for nonlinear calculations. Thus, it is advised to reduce this value at the start of the analysis further, and if convergence problems occur, the limit can be increased accordingly.

The 4C software consists of three major workspaces: Project Editor, Project Solver, and Result Viewer. Project Editor is where parts of the project like concrete geometry, calculation parameters, and mix-material database are defined. In this workspace, the concrete geometry is drawn, and the boundary conditions along with construction insulations are assigned. Further, a proper concrete mix design is established and specified to the desired geometry. Once the latter is carried out, the next step would be transforming the concrete geometry to finite element formulations by generating triangular mesh distributions. This step is done under the Project Solver workspace. The default values can be used for the mesh size. Users also have the option to modify the mesh sizes. Subsequently, the analysis is conducted, and the results can be viewed in the Results Viewer workspace. The results of the analysis are displayed either in x-y diagrams or as isocurves. At any specified time and place after casting, the results can be presented. The major steps in the above-discussed workspaces are illustrated in Figure 2.3.

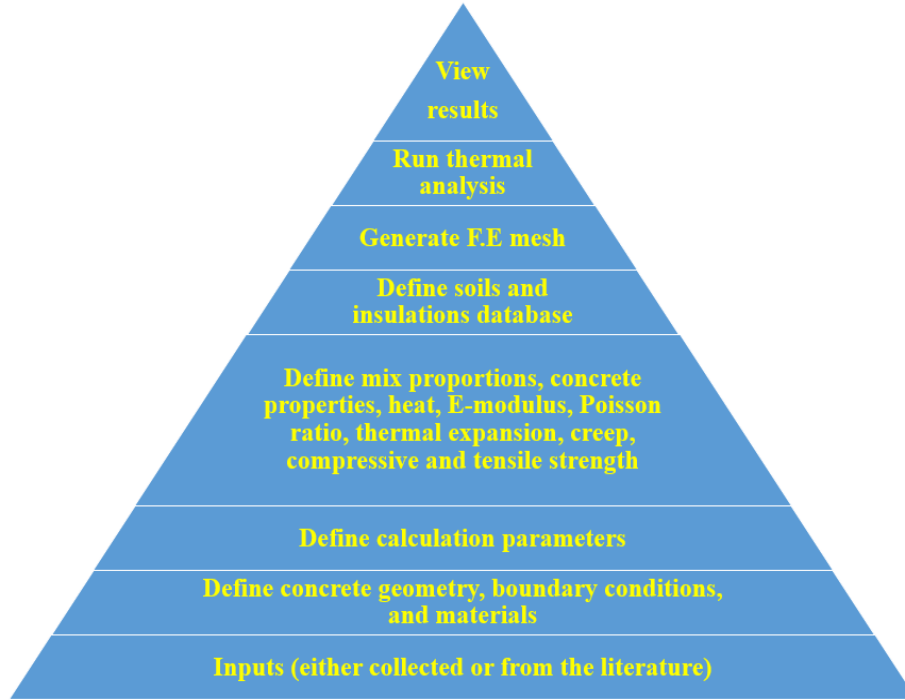


**Figure 2.3. Process of performing an analysis in 4C-Temp & Stress program**

Concrete, insulation, formwork, and materials databases are easily built, and the computational software time is very effective and allows for a relatively longer period of analysis. The software is capable of providing the maximum, minimum, and average temperatures at any specified place (point) in the desired volume, or alternatively, the maximum, minimum, and average temperatures of the volume.

The software includes many inputs that for some users could be considered a downside since it will require them to be keener in collecting information and making reasonable assumptions. A few additional shortcomings of the software can be discussed. Although the software allows a longer analysis period, this option is not available when the volume of the considered geometry is large, when a finer mesh is used, or when cement content is high. In addition, the predicted results from the software may not be in good agreement with the actual measurements because a constant or a sine curve is defined to represent the ambient temperature, while, in reality, the ambient temperature changes day by day. Lastly, and in the Result Viewer, only the longest edge of the concrete at the mid-span is typically shown, and no perpendicular or diagonal cross-section results can be estimated and displayed.

### **Comparison of Inputs and Prediction Models**

The two software applications used in this study and discussed in the earlier sections have been developed by different developers, so there is a multitude of differences in their thermal and stress analyses approaches. This section presents some of the differences in their inputs and the prediction models used for thermal and stress analysis of mass concrete members. Table 2.1 shows a comparison of the inputs used in ConcreteWorks and 4C, and Table 2.2 presents the

difference in the prediction models used in the software applications for various parameters including heat development, thermal conductivity, and others.

**Table 2.1. Comparison of inputs in ConcreteWorks and 4C**

| <b>Input</b>                           | <b>ConcreteWorks</b>                                                                                                                | <b>4C-Temp&amp;Stress</b>                                                     |
|----------------------------------------|-------------------------------------------------------------------------------------------------------------------------------------|-------------------------------------------------------------------------------|
| <b>Mix proportion</b>                  | Separate supplementary cementitious material (SCM) input is required with its type (fly ash/slag/silica fume) and their CaO content | Only total mineral additives content is required                              |
| <b>Cement/SCM chemical composition</b> | Type of cement and its chemical/physical properties are required as input                                                           | Type of cement and its chemical/physical properties are not required as input |
| <b>Maturity functions</b>              | The user can choose between the Nurse-Saul and Equivalent age methods                                                               | There is no option to choose a maturity method                                |

**Table 2.2. Comparison of prediction models used in ConcreteWorks and 4C**

| Property                         | ConcreteWorks Model                                                                                                                                                                                                                                                                                                                                                                                                                                                                                                                                                                                                                                                                                                                                                                                                                                                                | 4C-Temp&Stress Model                                                                                                                                                                                                                                                                                                                                                                                                                                                                 |
|----------------------------------|------------------------------------------------------------------------------------------------------------------------------------------------------------------------------------------------------------------------------------------------------------------------------------------------------------------------------------------------------------------------------------------------------------------------------------------------------------------------------------------------------------------------------------------------------------------------------------------------------------------------------------------------------------------------------------------------------------------------------------------------------------------------------------------------------------------------------------------------------------------------------------|--------------------------------------------------------------------------------------------------------------------------------------------------------------------------------------------------------------------------------------------------------------------------------------------------------------------------------------------------------------------------------------------------------------------------------------------------------------------------------------|
| Thermal conductivity ( $k$ )     | <ul style="list-style-type: none"> <li>Assumes a linear decrease of conductivity with the degree of hydration (Schindler 2002)</li> <li><math>k_c(\alpha) = k_{uc} (1.33 - 0.33\alpha)</math>; where <math>k_c</math> is the concrete thermal conductivity (W/m-K), <math>\alpha</math> is the degree of hydration, and <math>k_{uc}</math> is the ultimate hardened concrete thermal conductivity</li> </ul>                                                                                                                                                                                                                                                                                                                                                                                                                                                                      | <ul style="list-style-type: none"> <li>Assumes fixed values of conductivity</li> <li>Fresh and hardening concrete, <math>k = 8</math> KJ/m-h-°C</li> <li>Hardened concrete, <math>k = 6</math> KJ/m-h-°C</li> </ul>                                                                                                                                                                                                                                                                  |
| Specific heat                    | <ul style="list-style-type: none"> <li>Specific heat is dependent on the amount of concrete constituents, degree of hydration, and temperature (Van Breugel 1998)</li> <li><math>C_p(\alpha) = \frac{1}{\rho} [W_c \alpha (t_e) C_{cef} + W_c (1 - \alpha (t_e)) C_c + W_a C_a + W_w C_w]</math>; where, <math>C_p(\alpha)</math> = Specific heat of concrete mix, J/Kg °C; <math>\rho</math> = unit weight of concrete mix, Kg/m<sup>3</sup>; <math>W_c</math>, <math>W_a</math>, <math>W_w</math> = amount by weight of cement, aggregate, and water respectively, Kg/m<sup>3</sup>; <math>C_c</math>, <math>C_a</math>, <math>C_w</math> = specific heat of cement, aggregate, and water respectively, J/Kg °C; <math>C_{cef}</math> = fictitious specific heat of hydrated cement, J/Kg °C = <math>8.4 T_c + 339</math>; <math>T_c</math> = temperature of concrete</li> </ul> | <ul style="list-style-type: none"> <li>Specific heat is dependent only on the amount of concrete constituents</li> <li><math>c_{p,conc.} = \frac{\sum_{i=1}^n m_i \cdot c_{p,i}}{\sum_{i=1}^n m_i}</math>; where <math>c_{p,conc}</math> = specific heat of concrete mix; <math>m_i</math> = content of concrete constituent <math>i</math>; <math>c_{p,i}</math> = specific heat of concrete constituent <math>i</math>; <math>n</math> = number of concrete constituent</li> </ul> |
| Heat development                 | <ul style="list-style-type: none"> <li><math>Q_h(t) = H_u C_c (\frac{\tau}{t_e})^\beta (\frac{\beta}{t_e}) \alpha(t_e) e^{\frac{E_a}{R} \cdot (\frac{1}{T_c} + \frac{1}{T_r})}</math>; where <math>Q_h(t)</math> = rate of heat generation, W/m<sup>3</sup>; <math>H_u</math> = total heat available, J/Kg; <math>C_c</math> = cementitious content of concrete mix, Kg/m<sup>3</sup>; <math>E_a</math> = apparent activation energy of the concrete mix, J/mol; <math>\alpha_u</math>, <math>\beta</math>, and <math>\tau</math> = hydration curve parameters (Schindler 2004)</li> </ul>                                                                                                                                                                                                                                                                                         | <ul style="list-style-type: none"> <li><math>Q(M) = Q_\infty \exp \left[ -\left(\frac{\tau_e}{M}\right)^\alpha \right]</math>; where <math>Q(M)</math> = heat development at maturity <math>M</math>; <math>Q_\infty</math> = total heat development; <math>\tau_e</math> = time constant; <math>\alpha</math> = curvature parameter; <math>M</math> = maturity</li> </ul>                                                                                                           |
| Compressive strength development | <ul style="list-style-type: none"> <li><math>fc(te) = f_{cult} \exp \left[ -\left(\frac{\tau_s}{te}\right)^{\beta_s} \right]</math>; where <math>fc(te)</math> = compressive strength development at equivalent age <math>te</math>; <math>f_{cult}</math> = ultimate compressive strength fit parameter; <math>\tau_s</math> = fit parameter; <math>\beta_s</math> = fit parameter (Viviani 2005)</li> </ul>                                                                                                                                                                                                                                                                                                                                                                                                                                                                      | <ul style="list-style-type: none"> <li><math>fc(te) = f_{cult} \exp \left[ -\left(\frac{\tau_s}{te}\right)^{\beta_s} \right]</math>; where <math>fc(te)</math> = compressive strength development at equivalent age <math>te</math>; <math>f_{cult}</math> = ultimate compressive strength fit parameter; <math>\tau_s</math> = fit parameter; <math>\beta_s</math> = fit parameter</li> </ul>                                                                                       |

| Property                         | ConcreteWorks Model                                                                                                                                                                                                                                                                                                                                                                                                                                                                                                                                                                                                                                                     | 4C-Temp&Stress Model                                                                                                                                                                                                                                                                                           |
|----------------------------------|-------------------------------------------------------------------------------------------------------------------------------------------------------------------------------------------------------------------------------------------------------------------------------------------------------------------------------------------------------------------------------------------------------------------------------------------------------------------------------------------------------------------------------------------------------------------------------------------------------------------------------------------------------------------------|----------------------------------------------------------------------------------------------------------------------------------------------------------------------------------------------------------------------------------------------------------------------------------------------------------------|
| Tensile strength development     | <ul style="list-style-type: none"> <li>• <math>f_t = l(f_c^m)</math>; where <math>f_t</math> is the tensile strength; <math>l</math> and <math>m</math> are fit parameters</li> </ul>                                                                                                                                                                                                                                                                                                                                                                                                                                                                                   | <ul style="list-style-type: none"> <li>• Same model as compressive strength development</li> </ul>                                                                                                                                                                                                             |
| Elastic modulus development      | <ul style="list-style-type: none"> <li>• <math>E = k(f_c)^n</math>; where <math>E</math> is the elastic modulus; <math>f_c</math> is the compressive strength; <math>k</math> and <math>n</math> are the model parameters</li> </ul>                                                                                                                                                                                                                                                                                                                                                                                                                                    | <ul style="list-style-type: none"> <li>• Same model as compressive strength development</li> </ul>                                                                                                                                                                                                             |
| Poisson's ratio development      | <ul style="list-style-type: none"> <li>• Assumes variation of Poisson's ratio with the degree of hydration</li> <li>• <math>\nu(r) = 0.18 \sin\left(\frac{\pi \cdot r}{2}\right) + 0.5e^{-10r}</math>; where <math>r</math> is the degree of hydration (De Schutter and Taerwe 1996)</li> </ul>                                                                                                                                                                                                                                                                                                                                                                         | <ul style="list-style-type: none"> <li>• <math>\nu(M) = \nu_o - (\nu_o - \nu_\infty) \cdot \exp\left[-\left(\frac{\tau_e}{M}\right)^\alpha\right]</math>; where <math>\nu_o</math> is the Poisson's ratio of fresh concrete and <math>\nu_\infty</math> is the Poisson's ratio of hardened concrete</li> </ul> |
| Coefficient of thermal expansion | <ul style="list-style-type: none"> <li>• Assumes constant coefficient of thermal expansion</li> <li>• Calculated from the mix proportion and aggregate type</li> <li>• <math>\alpha_{cteh} = \frac{\alpha_{ca} \cdot v_{ca} + \alpha_{fa} \cdot v_{fa} + \alpha_p \cdot v_p}{v_{ca} + v_{fa} + v_p}</math>; where <math>\alpha_{cteh}</math> is the hardened concrete CTE; <math>\alpha_{ca}</math>, <math>\alpha_{fa}</math>, and <math>\alpha_p</math> are CTE of coarse, fine aggregate, and cement paste; <math>v_{ca}</math>, <math>v_{fa}</math>, and <math>v_p</math> are volume of coarse, fine aggregate, and cement paste (Emanuel and Leroy 1977)</li> </ul> | <ul style="list-style-type: none"> <li>• Assumes constant coefficient of thermal expansion</li> </ul>                                                                                                                                                                                                          |



### 3. EXPERIMENTS AND TEST METHODS

The default input data in ConcreteWorks were to be calibrated with those of the commonly used concrete mixtures for Iowa mass concrete construction. Various tests were performed on these mixes in the Portland Cement Concrete (PCC) Pavement and Materials Research Laboratory at Iowa State University. Test methods and experiments are discussed in the following sections.

#### Materials and Mixes

Four different concrete mixes were tested in the laboratory for their mechanical and thermal properties. The mixes commonly used for mass concrete construction in Iowa were selected for this study based on advice from the technical advisory committee (TAC). Four different types of cement—Type I, IP (25), IS (20), and I/II—and two types of supplementary cementitious materials (SCMs)—Class C fly ash and ground-granulated blast-furnace slag (GGBFS)—were used. Type IP (25) cement includes 25% Class F fly ash and Type IS (20) includes 20% Grade 120 slag. All four concrete mixes had a 20% replacement of cement by Class C fly ash, while Mix 4 had an additional replacement of cement by 30% with Grade 100 GGBFS. The fine-to-coarse aggregate ratio was selected as 50:50 and a water-binder ratio of 0.43 was used for all of the mixes. The mix proportions (with constituent materials in pounds per cubic yard of concrete) are presented in Table 3.1.

**Table 3.1. Concrete mix proportions**

| <b>Materials</b> | <b>Mix 1 (Type I Cement)<br/>lb/yd<sup>3</sup></b> | <b>Mix 2 (Type IP(25) Cement)<br/>lb/yd<sup>3</sup></b> | <b>Mix 3 (Type IS (20) Cement)<br/>lb/yd<sup>3</sup></b> | <b>Mix 4 (Type I/II Cement)<br/>lb/yd<sup>3</sup></b> |
|------------------|----------------------------------------------------|---------------------------------------------------------|----------------------------------------------------------|-------------------------------------------------------|
| Cement           | 474                                                | 474                                                     | 474                                                      | 296                                                   |
| Fly Ash          | 119                                                | 119                                                     | 119                                                      | 119                                                   |
| GGBFS            | 0                                                  | 0                                                       | 0                                                        | 178                                                   |
| Fine Aggregate   | 1,518                                              | 1,507                                                   | 1,513                                                    | 1,511                                                 |
| Coarse Aggregate | 1,532                                              | 1,521                                                   | 1,527                                                    | 1,526                                                 |
| Water            | 255                                                | 255                                                     | 255                                                      | 255                                                   |

In this report, the four concrete mixes are denoted as follows.

1. Mix 1 – I-20FA
2. Mix 2 – IP-20FA
3. Mix 3 – IS-20FA
4. Mix 4 – I/II-20FA-30S

Siliceous river sand as fine aggregate and 1-inch NMSA limestone as coarse aggregate were used for all mixes. Based on the values obtained from regular specific gravity tests performed on

aggregate batches, mix proportions were modified accordingly for the variation in specific gravity values. The following sections present the properties of the materials used.

### *Cementitious Materials*

Concrete mixes contained different cementitious materials as outlined previously. Different types of cement were used. ASTM C618 Class C fly ash was used in all four mixes with 20% replacement of cement, while Mix 4 had an additional 30% replacement of cement by GGBFS. Material data sheets were provided by the manufacturer showing the chemical composition of the material and also the physical properties. Table 3.2 shows the chemical compositions of all of the cementitious materials.

**Table 3.2. Chemical composition of cementitious materials (%)**

| <b>Material<br/>Cement Type</b> | <b>SiO<sub>2</sub></b> | <b>Al<sub>2</sub>O<sub>3</sub></b> | <b>Fe<sub>2</sub>O<sub>3</sub></b> | <b>CaO</b> | <b>MgO</b> | <b>SO<sub>3</sub></b> | <b>Na<sub>2</sub>O</b> | <b>K<sub>2</sub>O</b> | <b>Others</b> | <b>LOI</b> |
|---------------------------------|------------------------|------------------------------------|------------------------------------|------------|------------|-----------------------|------------------------|-----------------------|---------------|------------|
| I                               | 19.22                  | 5.30                               | 2.48                               | 63.40      | 2.88       | 2.82                  | 0.04                   | 0.51                  | 0.39          | 2.70       |
| IP (25)                         | 31.00                  | 8.72                               | 3.92                               | 46.20      | 2.68       | 3.33                  | 0.24                   | 0.84                  | 0.62          | 2.20       |
| IS (20)                         | 23.27                  | 5.47                               | 2.76                               | 59.44      | 3.80       | 3.15                  | 0.12                   | 0.62                  | 0.80          | 0.56       |
| I/II                            | 20.05                  | 4.34                               | 3.05                               | 63.18      | 2.24       | 3.18                  | 0.09                   | 0.68                  | 0.85          | 2.55       |
| Fly Ash                         | 36.09                  | 18.83                              | 5.85                               | 25.85      | 5.76       | 1.58                  | 1.78                   | 0.48                  | -             | 0.34       |
| GGBFS                           | 38.80                  | 7.91                               | 0.49                               | 38.37      | 10.64      | 2.54                  | -                      | 0.43                  | 0.91          | -          |

### *Aggregates*

The coarse aggregate source was Martin Marietta – Ames, and 1-inch NMSA limestone coarse aggregate was used for all four concrete mixes. River sand from Hallett Materials, Ames was used as the fine aggregate. The tests to determine the properties of both coarse and fine aggregates (gradation, specific gravity, absorption, dry rodded unit weight [DRUW], fineness modulus, etc.) were performed in the laboratory. All tests were performed by following the relevant ASTM standards. For example, ASTM C128-15 was followed for saturated-surface-dry (SSD) specific gravity tests. Based on the values of these tested parameters as shown in Table 3.3, concrete mix designs were modified accordingly before mixing.

**Table 3.3. Properties of aggregate**

| <b>Material</b> | <b>Specific Gravity</b> | <b>Absorption, %</b> | <b>Moisture Content, %</b> | <b>DRUW, lb/ft<sup>3</sup></b> | <b>Fineness Modulus</b> |
|-----------------|-------------------------|----------------------|----------------------------|--------------------------------|-------------------------|
| Limestone CA    | 2.7                     | 0.71                 | 0.13                       | 98.24                          | -                       |
| River Sand      | 2.68                    | 1.1                  | 1.15                       | -                              | 2.92                    |

The specific gravity of sand and coarse aggregate were 2.68 and 2.7, respectively. The DRUW of limestone aggregate was measured to be 98.24 lb/ft<sup>3</sup> and the fineness modulus of sand was determined to be 2.92.

Following ASTM C33 (2003), sieve analysis was performed for the coarse and fine aggregates to determine their grading. The gradation curves are shown in Figure 3.1.

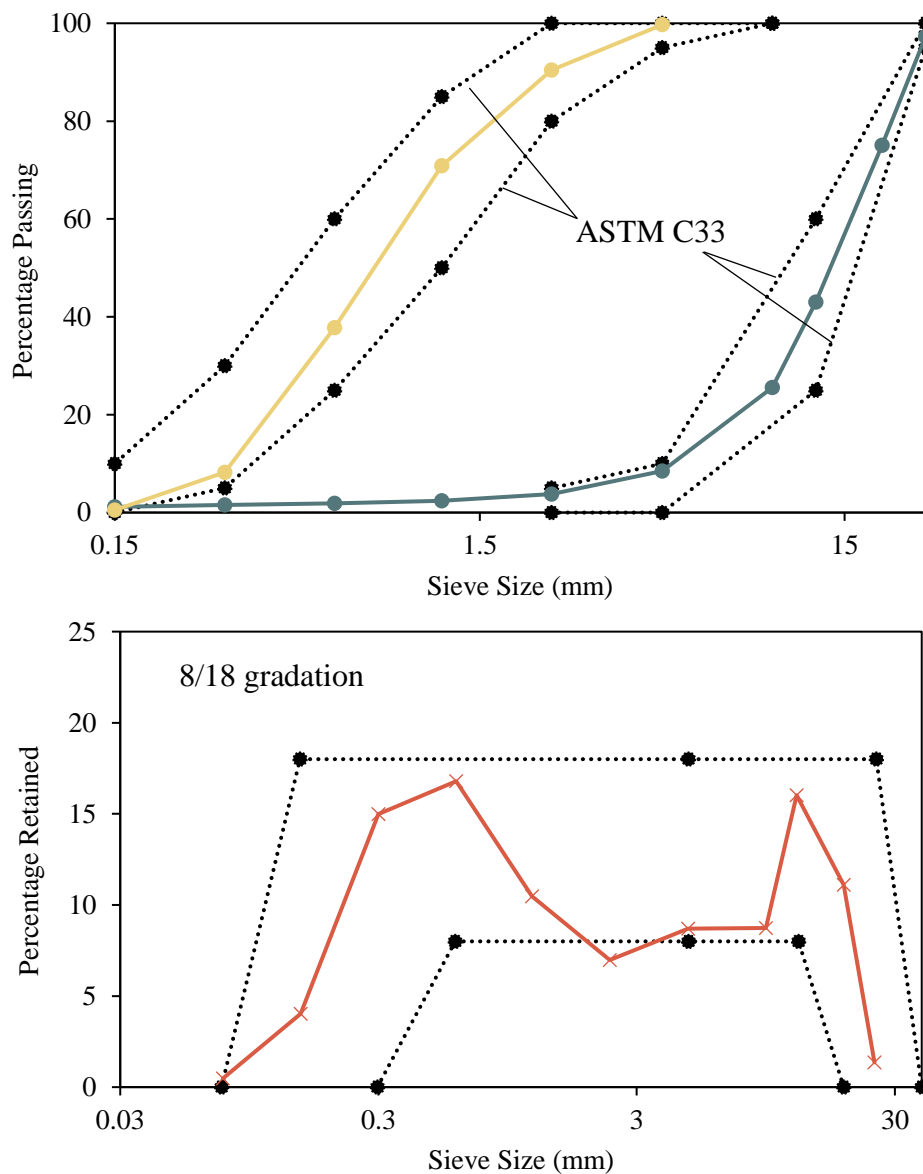


**Figure 3.1. Aggregate gradation curves: ASTM C33 (top) and 8/18 gradation (bottom)**

As evident from the curves in Figure 3.1, both coarse and fine aggregate gradation met the criteria as per ASTM C33. However, certain gap grading was visible from the 8/18 gradation curve.

### *Chemical Admixtures*

A low range water reducer (LRWR), BASF MasterPozzolith 322N, was used in sample comparison testing. As recommended by the manufacturer and the Iowa DOT, the dosage was kept to 3 fl oz. per 100 lbs. of cementitious materials. An air-entraining admixture (AEA), DARAVAIR 100, was also used. As recommended, the dosage was kept to 1 fl oz. per 100 lbs. of cementitious materials.

## **Tests and Methods**

### *Fresh Properties*

Concrete mixes were prepared using a drum mixer in the laboratory. Properties of fresh concrete such as slump, air content, and unit weight were then tested by following the standard test procedures per ASTM C143/C143M (2015), ASTM C231/231M (2010), and ASTM C138/C138M-13, respectively.

### *Mechanical Properties*

As required by the ConcreteWorks program, the mechanical properties of the four concrete mixes were tested in the laboratory as follows.

#### Compressive Strength

Compressive strength tests were performed on 4×8 in. cylindrical specimens as per the ASTM C39 (2016) test procedure. The Test Mark Industries testing apparatus available in the laboratory was used for this purpose. Three specimens of each mix were moist-cured at 74°F and tested at curing ages of 1, 3, 7, 14, and 28 days.

#### Split Tensile Strength

The test for split tensile strength of concrete mixes was performed on 28-day moistcured 4×8 in. cylindrical specimens following the ASTM C496 (2011) test procedure. Three specimens were tested for each mix and the mean was taken as the split tensile strength of the concrete mix.

#### Elastic Modulus

The static modulus of elasticity of the concrete mixes in compression was also tested using 28-day moist-cured 4×8 in. cylindrical specimens following the ASTM C469/C469M (2014) test procedure.

## Maturity

The maturity method is a technique for estimating concrete strength based on the assumption that samples of a given concrete mixture attain equal strengths if they attain an equal value of the maturity index. The maturity index is an indicator of maturity that is calculated from the temperature history of the cementitious mixture by using a maturity function ASTM C1074 (2015).

As per ASTM C1074, there are two methods for the computing maturity index from the measured temperature history of concrete:

- Nurse-Saul
- Equivalent age

Because of its simplicity, the Nurse-Saul method is frequently used in the field, and it is for this reason that this method was used for this investigation.

The temperature-time factor is calculated as follows:

$$M(t) = \sum (T_a - T_o) \Delta t \quad (1)$$

Where  $M(t)$  is the temperature-time factor at age  $t$  (in °F –hours),  $\Delta t$  is the time interval (in hours),  $T_a$  is the average concrete temperature during time interval  $\Delta t$ , and  $T_o$  is the datum temperature (in °F). Following the ASTM C39 (2016) standard procedure, 23 4×8 in. cylindrical specimens were prepared as per the mixture proportions for each of the four mixes. iButton temperature sensors were embedded in two specimens and all the specimens were moist-cured in a temperature and humidity controlled room at 74°F. The temperature of the concrete specimens was recorded at an interval of 45 minutes. Three specimens of each mix were tested at 1, 3, 7, 14, 28, 56, and 90 days for compressive strength as per ASTM C39 (2016). At each test age, the temperature-time factor (TTF) was calculated using a datum temperature of 14°F, and compressive strength was plotted as a function of TTF. The compressive strength-maturity relationship for each mix was then developed by performing a regression analysis to determine a best-fit equation to the data. The best-fit equation for all of the mixes was found to be of the form where compressive strength is a linear function of the logarithm of maturity index (in this case TTF) as given in equation (2).

$$S = a + b \log(M) \quad (2)$$

Where  $S$  is the compressive strength (in psi),  $M$  is the maturity index (TTF), and  $a$  and  $b$  are coefficients. The ConcreteWorks program allows the user to choose between two methods (Nurse-Saul and equivalent age) for computing the maturity index. Based on the selected method, relevant parameters can be edited. For example, values of the coefficients  $a$  and  $b$  can be entered manually if the Nurse-Saul method is selected for maturity calculations.

## *Isothermal Calorimetry*

Calorimetry is the measurement of heat and the rate of heat generation. An isothermal calorimeter measures heat and the rate of heat generation at a constant temperature. For this research, an eight-channel isothermal calorimeter (shown in Figure 3.2) that was available in the laboratory was used to measure heat generation of cement pastes.

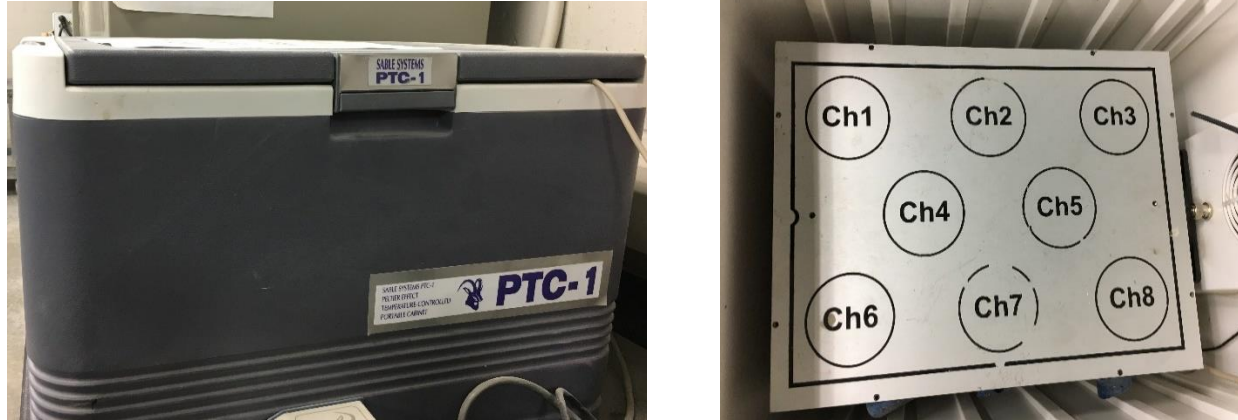


**Figure 3.2. Isothermal calorimeter (left) and channels for holding samples (right)**

As illustrated in Figure 3.2, each unit has an aluminum sample holder, which rests on a heat flow sensor (Peltier) that is placed on a common heat sink of a large block of aluminum. On the other side of the heat sink is another heat flow sensor and a 129-g aluminum block. The aluminum block is used as a reference to reduce the noise signal in this conduction calorimeter. When a sample is placed in the unit, the heat produced by hydration flows rapidly to its surroundings. The main route for heat exchange between the sample and the surroundings is through the heat flow detector. The heat flow, caused by the temperature difference across the sensor, creates a voltage signal proportional to the amount of heat flow. This voltage signal is then converted to the rate of heat evolution by applying a calibration factor based on the reference material (aluminum).

For analyzing the effect of temperature on the heat of hydration of cement, four different temperatures, 10, 20, 30, and 40°C, were selected for this project. Two different samples of pastes were prepared for each of the four mixes—one containing a LRWR and the other without any water reducer. All of the samples were prepared keeping the water-binder ratio the same as that in the corresponding concrete mix. Table 3.4 shows the proportions for the cement paste mixes that were tested in this experiment.

**Table 3.4. Cement paste mix proportions**

| Mix | Cement       |            | Class C Fly Ash |    | GGBFS |    | Water      |
|-----|--------------|------------|-----------------|----|-------|----|------------|
|     | Type         | Amount (g) | %               | g  | %     | g  | Amount (g) |
| 1   | Type I       | 40         | 20              | 10 | -     | -  | 21.5       |
| 2   | Type IP (25) | 40         | 20              | 10 | -     | -  | 21.5       |
| 3   | Type IS (20) | 40         | 20              | 10 | -     | -  | 21.5       |
| 4   | Type I/II    | 25         | 20              | 10 | 30    | 15 | 21.5       |

In order to bring the temperature of constituent materials to the desired mixing temperature, all of the materials (cement, fly ash, GGBFS, water, and water reducer) were first kept in separate containers in the calorimeter for approximately 5 hours. When the temperature of the mixing materials had approximately reached the desired value, the materials were taken out and mixed to form the paste as soon as possible. The paste specimens weighing 71.5 g each were then loaded into eight different channels of the isothermal calorimeter. The samples were loaded as soon as they were ready. The produced heat was then conducted from the sample to the heat sink, and the temperature gradient across the heat detector produced a voltage proportional to the heat flow. After the samples were placed into the calorimeter, the pre-programmed calorimeter started taking readings immediately. The readings were taken at an interval of 1 minute for approximately 100 hours.

Before performing the calorimetry tests, the calorimeter was calibrated. The calibration procedure aimed to obtain the baseline of calorimeter and calibration factors for each of the 8 cells at each of four temperatures 10, 20, 30, and 40°C. The steps for the calibration procedure are given in Appendix A. After the calibration factors were determined, calorimetry tests were conducted following the procedure discussed above. The data was recorded in mV at every 1-minute interval for approximately 100 hours. Then, equation (3) was used to determine the rate of heat generation in mW/g of cement.

$$P = \frac{(R-B)CF}{W_s/(1+\frac{s}{c}+\frac{w}{c})} \quad (3)$$

Where  $P$  is the rate of heat generation (in mW/g),  $R$  is data reading (mV),  $B$  is the calibrated baseline (mV),  $CF$  is the calibration factor (mW/mV),  $W_s$  is weight of the sample (g),  $s$  is weight of sand (g),  $c$  is weight of cement (g), and  $w$  is weight of water (g). The rate of heat generation (in mW/g) at every 1-minute interval is converted to the total heat generated in J/h and cumulative heat is then calculated by adding heat generated in each interval.

#### *Determination of Activation Energy*

Accurate prediction of temperature development in mass concrete requires an estimate of temperature sensitivity of the hydration of cementitious materials. The most commonly used method for characterizing this is the determination of activation energy using the Arrhenius equation. In the classical interpretation, activation energy is the energy barrier between the

reactant and product for a single reaction system. Cementitious systems involve multiple reactions that occur simultaneously, interact with each other, and change with time. The measurement of  $E_a$  for cementitious systems represents a globally averaged temperature sensitivity of the mixture; this empirically determined value is often referred to as the “apparent” activation energy (Riding et al. 2011). The modified ASTM C1074 procedure (Poole et al. 2007) was adopted here for determination of apparent activation energy.

Degree of hydration (DOH) of cementitious material at a specific time,  $t$ , is determined by taking the ratio of heat evolved at time  $t$  to the total amount of heat available as follows.

$$\alpha(t) = \frac{H(t)}{H_u} \quad (4)$$

Where  $\alpha(t)$  is the degree of hydration at time  $t$ ,  $H(t)$  is cumulative heat of hydration from time 0 to  $t$  (J/g), and  $H_u$  is total heat available for reaction (J/g).

Total heat available for reaction,  $H_u$ , is calculated from the material components and chemical compositions as follows.

$$H_u = H_{cem} \cdot p_{cem} + 461 \cdot p_{slag} + 1800 \cdot p_{FA-CaO} \cdot p_{FA} \quad (5)$$

$$H_{cem} = 500 \cdot p_{C3S} + 260 \cdot p_{C2S} + 866 \cdot p_{C3A} + 420 \cdot p_{C4AF} + 624 \cdot p_{SO3} + 1186 \cdot p_{FreeCa} + 850 \cdot p_{MgO} \quad (6)$$

Where  $H_{cem}$  is heat of hydration of cement (J/g),  $P_{cem}$  is cement mass to total cementitious content ratio,  $P_{slag}$  is slag mass to total cementitious content ratio,  $P_{FA-CaO}$  is fly ash CaO mass to total fly ash content ratio,  $P_{FA}$  is fly ash mass to total cementitious content ratio,  $P_{C3S}$ ,  $P_{C2S}$ ,  $P_{C3A}$ ,  $P_{C4AF}$ ,  $P_{SO3}$ ,  $P_{FreeCa}$ , and  $P_{MgO}$  are the cement composition-total cement content weight ratios.

As suggested by a number of researchers, an exponential function can be used to characterize cement hydration based on the degree of hydration data. The most commonly used relationship is a three-parameter model given below.

$$\alpha(t) = \alpha_u \cdot e^{-\left[\frac{\tau^\beta}{t}\right]} \quad (7)$$

Where  $\alpha(t)$  is the degree of hydration at time,  $t$ ,  $\alpha_u$  is the ultimate degree of hydration,  $\beta$  is the hydration shape parameter, and  $\tau$  is the hydration time parameter (hours).  $\alpha_u$ ,  $\beta$ , and  $\tau$  in equation (7) are three hydration curve parameters used to characterize DOH of cementitious materials. A larger  $\alpha_u$  indicates a higher magnitude of ultimate DOH, and a larger  $\tau$  implies a larger delay of hydration. Since  $\beta$  represents the slope of the major linear part of the hydration shape, a larger  $\beta$  implies a higher hydration rate at the linear portion of hydration curves.



The hydration curve parameters and the apparent activation energy are calculated according to the modified ASTM C1074 procedure as outlined in Methods for Calculating Apparent Activation Energy of Cementitious Systems (Poole et al. 2007). The steps of the calculation are as follows:

1. The hydration curve parameters  $\alpha_u$ ,  $\beta$ , and  $\tau$  in equation (7) are fit using the least squares approach for the cementitious system degree of hydration calculated from the cumulative isothermal heat of the hydration curve at 20°C using equations (4) through (6) for a particular concrete mix.
2. Following Step 1, parameters are fit at other temperatures, 10, 30, and 40°C as well. Since it has been shown in the literature that the ultimate degree of hydration  $\alpha_u$  and shape parameter  $\beta$  are independent of temperature, values of these two parameters at 10, 30, and 40°C are kept equal to the values found at 20°C. The value of the hydration time parameter  $\tau$  is changed for each temperature to fit the cumulative isothermal heat of hydration values at each temperature.
3. The four different  $\tau$  values fit to the cumulative isothermal heat of hydration curves are then plotted on an Arrhenius plot.
4. The apparent activation energy ( $E_a$ ) is then calculated as the slope of a best-fit line to the four points on the Arrhenius plot multiplied by the natural gas constant,  $R$  (Figure 3.3).

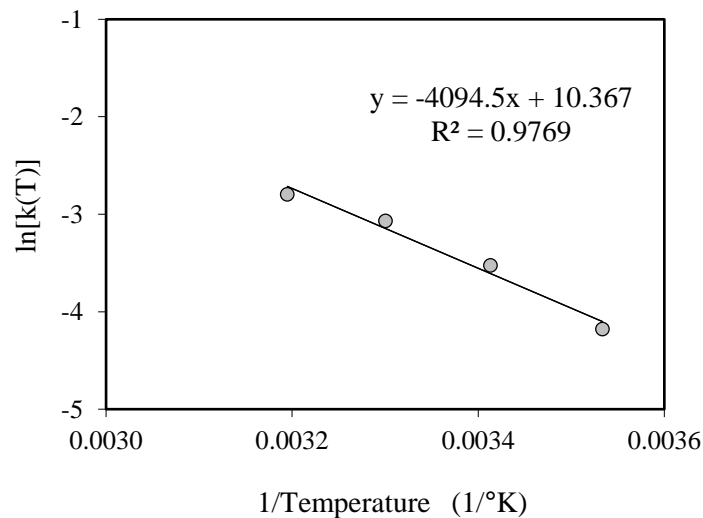


**Figure 3.3. Arrhenius plot**

The hydration curve parameters and  $E_a$  for all four concrete mixes are calculated from their respective isothermal calorimetry test data. The ConcreteWorks program allows the user to manually enter the value of calculated apparent activation energy (in J/mol).

### *Semi-Adiabatic Calorimetry*

Accurate characterization of the temperature rise in a concrete element requires an estimate of the adiabatic temperature rise of the concrete mixture. Adiabatic calorimetry requires an adiabatic process in which no heat is gained or lost to the system's surroundings. Because of the difficulty and the expensive equipment needed to eliminate heat gain or loss in an adiabatic calorimetry test, semi-adiabatic calorimetry is commonly used. From the semi-adiabatic calorimetry test results, the adiabatic temperature rise can be calculated. Even though the semi-adiabatic calorimetry test is a common test, there is no standard test method for it. This study followed the guidelines outlined in the prominent literature (Poole 2007). Based on these guidelines, a semi-adiabatic calorimeter was developed in the Iowa State University PCC Laboratory. The steps for building the calorimeter are presented in Appendix B. Figure 3.4 shows a diagram with the details of the calorimeter on the left and the finished apparatus on the right.

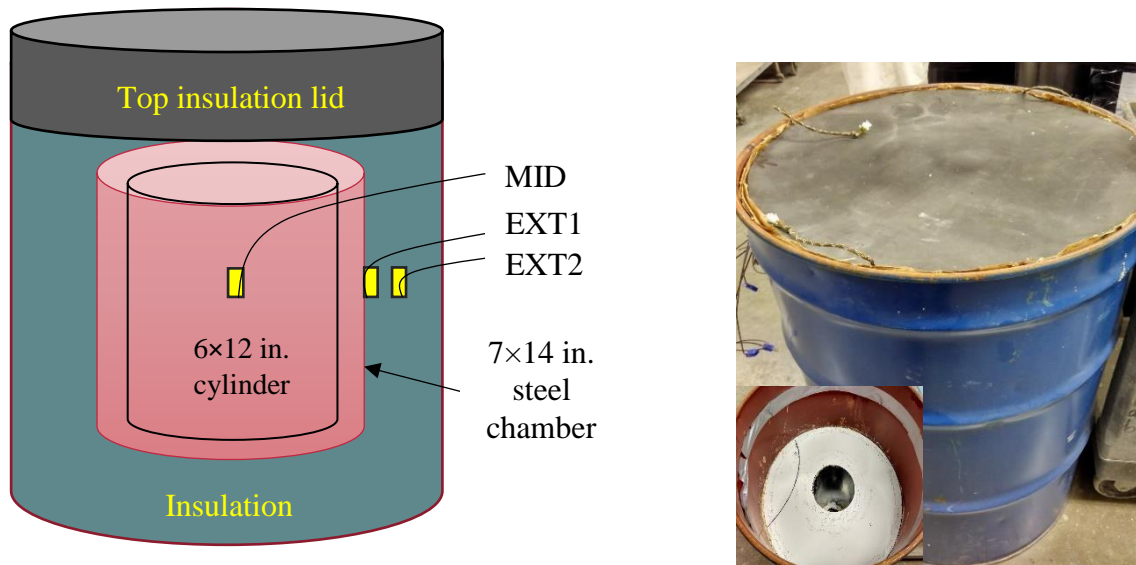


**Figure 3.4. Semi-adiabatic calorimeter**

A 24×34 in. cylindrical drum was used to build the semi-adiabatic calorimeter, as shown in Figure 3.4. Aeromarine insulation foam was used as the insulating material for the drum calorimeter. The top insulation lid was also prepared using the same insulation foam. For installing the 7×14 in. steel chamber in the middle of the drum, galvanized steel sheeting was used. Fresh concrete was poured into the 6×12 in. cylinder placed inside this chamber. The temperature was measured using Type T thermocouples at three locations: one at the center of the concrete specimen (MID), one at the surface of the steel chamber (EXT1), and one at an inch away from the chamber surface in the insulation (EXT2). The MID thermocouple was placed 6 inches into the center of the fresh concrete specimen. A plug-in for this thermocouple was installed at the edge of the steel chamber opening. For connecting thermocouple wires to the data logger, a hole was drilled in the middle of the drum surface through which the wires were taken out.

The test setup was kept in a closed room where temperature variations were limited. Concrete specimens for each of four mixes were prepared as per ASTM C192 (2016) and placed in the calorimeter as soon as possible. The data was recorded using a Pico Technology USB TC-08 data logger for 160 hours at 15-minute intervals. To measure the heat loss from the calorimeter, it was calibrated before the test. The calibration procedure is covered in Appendix C.

### Determination of Adiabatic Temperature Rise

After the determination of the calibration factors, the test was performed on each of four concrete mixes one by one and their semi-adiabatic temperature data were recorded. It was required to calculate the adiabatic temperature rise of the concrete mixture from the recorded semi-adiabatic temperature data. Since no standard testing procedure is currently available, the steps outlined in Hydration Study of Cementitious Materials using Semi-Adiabatic Calorimetry (Poole 2007) were followed closely to determine the adiabatic temperature rise. The steps are covered below.

1. Before placing the concrete sample inside the steel chamber of the calorimeter, its weight is recorded. The time from mixing of water to cement to the time the concrete mixture is kept inside the calorimeter is also recorded. An effort is made to keep this time period to a maximum of 30 minutes.
2. To estimate the true adiabatic temperature, the equivalent age needs to be calculated. The equivalent age is computed at each time step according to equation (8) using the mixture apparent activation energy as calculated from the isothermal calorimetry.

$$t_e(T_r) = \sum_0^t e^{-\frac{E_a}{R} \cdot (\frac{1}{T_c} - \frac{1}{T_r})} \cdot \Delta t \quad (8)$$

Where  $t_e(T_r)$  is the equivalent age at reference temperature (hr),  $T_r$  is the reference temperature of concrete (°K),  $T_c$  is temperature of concrete (°K),  $E_a$  is the apparent activation energy of the concrete mixture (J/mol),  $R$  is the natural gas constant (8.314 J/mol/K), and  $\Delta t$  is the time step.

3. The degree of hydration is calculated using the equivalent age of the mixture and the hydration parameters  $\alpha_u$ ,  $\beta$ , and  $\tau$  as per the three-parameter exponential function given by equation (9).

$$\alpha(t_e) = \alpha_u \cdot e^{-[\frac{\tau}{t_e}]^\beta} \quad (9)$$

Where  $\alpha(t_e)$  is the degree of hydration at equivalent age  $t_e$ ;  $\alpha_u$ ,  $\beta$ , and  $\tau$  are hydration curve parameters, and  $t_e$  is the equivalent age.

4. At each time step, the heat evolved is calculated using the hydration parameters and the ultimate heat of hydration, which was previously estimated using equations (5) and (7). The

heat evolved is quantified using equation (11), which is a combination of equations (8), (9), and (10).

$$\alpha(t) = \frac{H(t)}{H_u} \quad (10)$$

$$Q_h(t) = H_u C_c \left(\frac{\tau}{t_e}\right)^\beta \left(\frac{\beta}{t_e}\right) \alpha(t_e) e^{\frac{E_a}{R} \cdot \left(\frac{1}{T_c} + \frac{1}{T_r}\right)} \quad (11)$$

Where  $Q_h(t)$  is the rate of heat generation (W/m<sup>3</sup>),  $H_u$  is the total heat available (J/Kg),  $C_c$  is the cementitious content of concrete mix (Kg/m<sup>3</sup>),  $E_a$  is the apparent activation energy of the concrete mix (J/mol),  $\alpha_u$ ,  $\beta$ , and  $\tau$  are the hydration curve parameters.

5. The specific heat of the concrete mix, which is used to determine the change in temperature, is then calculated using equation (12)

$$C_p(\alpha) = \frac{1}{\rho} [W_c \alpha(t_e) C_{cef} + W_c (1 - \alpha(t_e)) C_c + W_a C_a + W_w C_w] \quad (12)$$

Where  $C_p(\alpha)$  is the specific heat of concrete mix (J/Kg °C),  $\rho$  is the unit weight of concrete mix (Kg/m<sup>3</sup>);  $W_c$ ,  $W_a$ , and  $W_w$  are the amount by weight of cement, aggregate, and water, respectively in Kg/m<sup>3</sup>;  $C_c$ ,  $C_a$ ,  $C_w$  are the specific heat of cement, aggregate, and water respectively, in J/Kg °C,  $C_{cef}$  is the fictitious specific heat of hydrated cement in J/Kg °C ( $C_{cef} = 8.4 T_c + 339$ ), and  $T_c$  is the temperature of the concrete. As evident from equation (12), the specific heat of the concrete mix is assumed to vary with the degree of hydration.

6. With the specific heat value, the change in temperature at each time step is calculated as given in equation (13).

$$\Delta T = \frac{Q_h(t) \cdot \Delta t}{\rho \cdot C_p(\alpha)} \quad (13)$$

Where the terms have meaning as specified for previous equations.

7. Starting from the original measured concrete temperature ( $T_c$ ), the change in temperature calculated in Step 6 ( $\Delta T$ ) at each time step is summed up. The resulting temperature is the “false” adiabatic temperature ( $T_{adia}^*$ ) as shown by equation (14).

$$T_{adia}^* = T_c + \Delta T \quad (14)$$

The false adiabatic temperature does not take into account the hydrating process of concrete and therefore it is lower than the “true” adiabatic temperature. However, it is important as it is used to model the temperature in the concrete cylinder in the semi-adiabatic calorimeter.

8. For calculating the true adiabatic temperature of concrete mix, the losses from the semi-adiabatic calorimeter during the test need to be calculated. Equation (14) is used to account for the heat transfer from concrete using the measured temperature differential between external thermocouples EXT1 and EXT2 and the calibration factors  $C_{f1}$  and  $C_{f2}$ . The change in concrete temperature from the losses is calculated using equation (15).

$$\Delta T_c = \frac{\Delta q_h \cdot \Delta t}{\rho_c \cdot C_p(\alpha) \cdot V_c} \quad (15)$$

Where  $\Delta T_c$  is the change in concrete temperature from the losses ( $^{\circ}\text{C}$ );  $\rho_c$  is the unit weight of concrete mix ( $\text{kg}/\text{m}^3$ ),  $C_p(\alpha)$  is the specific heat of the concrete mix ( $\text{J}/\text{kg} \cdot ^{\circ}\text{C}$ ),  $V_c$  is the volume of the concrete sample ( $\text{m}^3$ ), and  $\Delta t$  is the time step (s).

9. To determine the modeled semi-adiabatic concrete temperature ( $T_c^*$ ), the sum of changes in temperature from losses at each time step is subtracted from the false adiabatic temperature ( $T_{adia}^*$ ) as shown in equation (16).

$$T_c^* = T_{adia}^* - \sum \Delta T_c \quad (16)$$

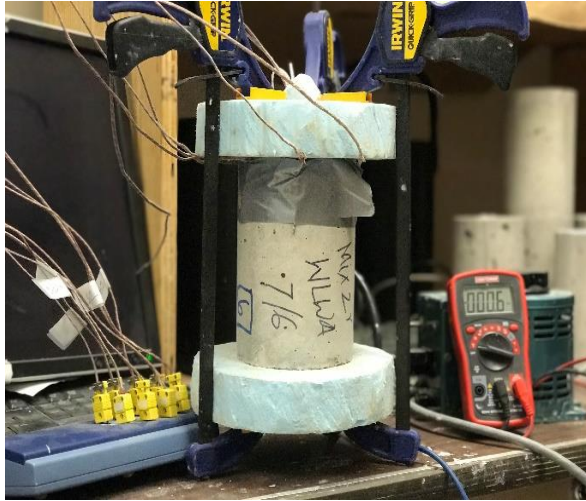
The solver function in Microsoft Excel is then used to compare the measured concrete temperature to the modeled concrete temperature and, using the coefficient of determination ( $R^2$ ), the best-fit hydration parameters  $\alpha_u$ ,  $\beta$ , and  $\tau$  are determined.

Using the best-fit hydration parameters found in Step 10, the true adiabatic temperature ( $T_{adia}$ ) is then modeled.

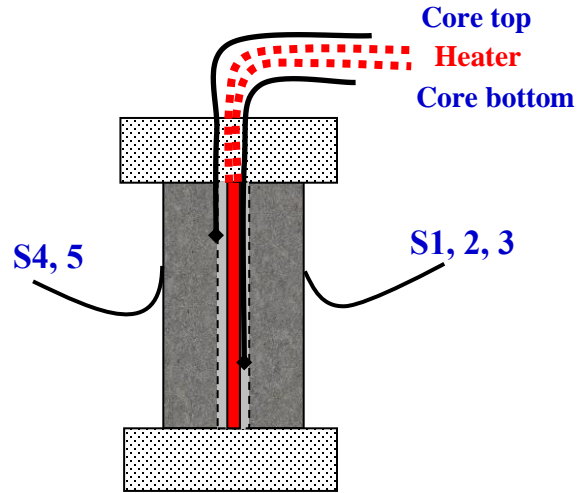
ConcreteWorks software allows the user to manually enter the values of calculated hydration parameters and total heat  $H_u$ .

### *Thermal Conductivity*

As the temperature prediction models also consider the heat conduction property of materials, the thermal conductivity of each type of concrete needs to be measured for this purpose. There are two popular methods of measuring the thermal conductivity of concrete: the guarded hot plate method and the Arizona State University (ASU) cylindrical specimen method (ASTM 2004). Since the guarded hot plate method is not recommended for highly heterogeneous materials like concrete and because of the simplicity of the ASU cylindrical specimen test method (Carlson et al. 2010), the latter was used in this research. Figure 3.5 shows the test setup assembled in the researchers' laboratory.



(a) Complete Test Setup



(b) Location of Sensors

Bai 2013

**Figure 3.5. Thermal conductivity test setup**

Also shown in the figure is the location of the temperature sensors. A total of seven sensors were installed to measure the temperature of the concrete specimen during the test and one sensor measured the ambient temperature. The test was performed in a closed temperature and humidity-controlled room. Three 4×6 in. specimens of each mix with a 0.5-in. diameter hole through the center of each was cast and moist-cured for 28 days at 74°F.

The specimens were dried in an oven for 24 hours. These steps were followed for the test:

1. The test setup is assembled as shown in Figure 3.5.
2. Silicone-based high thermal conductivity paste ( $k = 2.3 \text{ W/m-K}$ ) manufactured by Omega Engineering, Inc. is poured evenly into the central 0.5-in. diameter core of the specimen and a cartridge heater is inserted into the core.
3. Eight temperature sensors (Type K thermocouples) are installed as shown in Figure 3.5(b) as follows:
  - (a) One sensor at one third from the top into the core of the specimen (Core top)
  - (b) One sensor at one third from the bottom into the core of the specimen (Core bottom)
  - (c) Five sensors at the surface of the specimen (S1, S2, S3, S4, and S5)
  - (d) One sensor to measure the room temperature
4. Two 1.5 in. thick styrofoam insulation sheets are placed at the top and bottom of the cylindrical specimen and the entire setup is held together using three bar clamps.
5. The thermocouples are connected to a Pico Technology data logger for recording temperature development during the test.

6. The heater is connected to a voltage regulator, which is connected to a power source.
7. A multimeter is also connected in series for measuring the applied voltage.
8. The resistance of the heater is measured and a pre-determined voltage of 21.7 V is applied to the heater.
9. The data recording starts at this point.

Note that Appendix D also summarizes the materials and equipment required and the procedure for assembling the complete test setup.

The input voltage is controlled using a voltage regulator such that the temperature in the core reaches around 50°C. The input voltage for the experiments in this research was determined to be 21.7 V and hence the input power was 8.13 W. The data logger records temperature data of all eight sensors at 2-minute intervals. The thermal conductivity is calculated every half hour until it changes less than 2%, which is considered to be a steady state. It was observed in the experiments that it took about 2.5 hours for the concrete to reach a steady state.

It was required to check the accuracy of the test method so that the test results could be validated. For this purpose, an ultra-high molecular weight polyethylene (UHMWPE) material was selected as a “known” reference sample, since it has a low thermal conductivity range, and it was tested using the same apparatus. The method is presented in Appendix E.

Thermal conductivity  $k$  is defined by Fourier’s law of heat conduction as follows:

$$\frac{Q}{A} = -k \frac{dT}{dx} \quad (17)$$

Where  $Q/A$  is the steady-state conduction heat flux (W/m<sup>2</sup>),  $dT/dx$  is the steady-state temperature gradient, and  $k$  is the thermal conductivity (W/m-K). An important factor when measuring thermal conductivity in materials is establishing a one-dimensional heat flow. By thermally isolating the top and bottom of the cylindrical specimen in the method adopted here, the losses are reduced such that uniform one-dimensional heat flow in the radial direction is achieved for the most part. Other researchers that performed the tests on concrete samples using the same test method suggested that heat loss through the top and bottom insulation is less than 2% when high thermal conductivity paste is used in the core of the specimen (Carlson et al. 2010). The heat is transferred horizontally through the specimen more than the vertical heat transfer since the thermal conductivity of the styrofoam (0.02 W/m-K) insulating sheet is less than that of Omega paste (2.3 W/m-K). Therefore, that potential of heat loss has been negated and equation (17) was used for the calculation of thermal conductivity.

$$k = \frac{(VI) \cdot \ln(r_2/r_1)}{2\pi L (T_1 - T_2)} \quad (18)$$

Where  $k$  is the thermal conductivity (W/m-K),  $VI$  is the power input to the heater (W),  $r_2$  is the inner radius (m),  $r_1$  is the outer radius (m),  $L$  is the length of the specimen (m),  $T_1$  is the average temperature in the core of the specimen (K), and  $T_2$  is the average temperature on the surface of the specimen (K). The  $k$  value is calculated every half hour during the test, and when it changes less than 2%, it is considered a steady state and the value at the steady state is taken as the  $k$  value of the concrete. A minimum of three specimens was tested for each mix with two separate runs for each specimen. The mean value of six observations was considered the thermal conductivity of that particular mix.

### *Coefficient of Thermal Expansion*

The coefficient of thermal expansion (CTE) is defined as the change in unit length of a material in response to a degree of temperature change. The CTE of concrete is predominantly governed by the type of aggregate used in the concrete mix. The CTE of all four concrete mixes in this research were determined according to the AASHTO T 336-15 standard test method using equipment in the Iowa State University PCC Laboratory (see Figure 3.6).

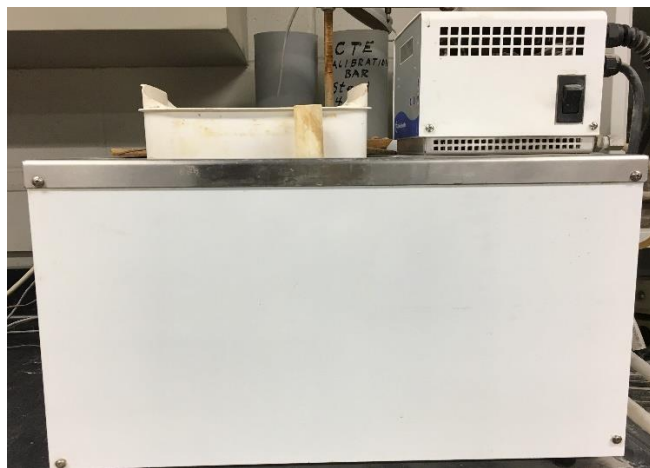


**Figure 3.6. Coefficient of thermal expansion test equipment**

The test method was used to determine the CTE of 4×7 in. cylindrical concrete specimens, which were maintained in a saturated condition, by measuring the length change of specimen over a temperature range of 10°C to 50°C. Grade 304 stainless steel with a known coefficient of thermal expansion value was used to calibrate the test apparatus and determine the correction factor ( $C_f$ ) before the actual test was performed. Steps used in the test were as follows:

1. After 28 days of curing, 1 in. is cut off from the top of each 4×8 in. cylindrical specimen and its length is measured to the nearest 0.004 in.
2. The specimen is placed in the support frame, making sure that the lower end of the specimen is firmly seated against the support buttons and that the linear variable differential transformer (LVDT) tip is seated against the upper end of the specimen.



3. The support frame and specimen, with the LVDT attached, is placed in the water bath, which is filled with tap water. The height of the water is kept constant throughout the test.
4. The temperature of the water bath is set to 10°C. When the bath reaches this temperature, it is allowed to remain at this temperature until thermal equilibrium of the specimen has been reached, as indicated by consistent readings of the LVDT. The LVDT and temperature sensor readings are recorded using a Campbell Scientific CR1000 data logger at one-minute intervals.
5. The temperature of the water bath is now set to 50°C and the same thermal equilibrium procedure is performed.
6. The temperature of the water bath is again decreased to 10°C and thermal equilibrium is allowed to be established.
7. The CTE value is the mean of the test results of two test segments.

The CTE value of one expansion or contraction test segment is calculated as follows:

$$CTE = \frac{\Delta L_a / \Delta L_o}{\Delta T} \quad (19)$$

$$\Delta L_a = \Delta L_m + \Delta L_f \quad (20)$$

$$\Delta L_f = C_f \times L_o \times \Delta T \quad (21)$$

Where  $\Delta L_a$  is the actual length change of specimen during the temperature change (mm),  $L_o$  is the measured length of the specimen at room temperature (mm),  $\Delta T$  is the measured temperature change, (°C),  $\Delta L_m$  is the measured length change of specimen during temperature change (mm),  $\Delta L_f$  is length change of the measuring apparatus during temperature change (mm), and  $C_f$  is the correction factor (microstrain/°C).

## 4. RESULTS AND DISCUSSION

### Properties of Fresh Concrete

Following the designed mix proportions as presented in the previous Table 3.1, all four concrete mixes were prepared per ASTM C192 using the revolving drum mixer in the PCC Laboratory at Iowa State University. Right after concrete was mixed, it was sampled following ASTM C172/C172M-10 and then tested for its fresh properties. Fresh properties including slump, air content, and unit weight were measured in accordance with ASTM C143/C143M (2015), ASTM C231/231M (2010), and ASTM C138/C138M-13 2013, respectively. The measured fresh properties of the four concrete mixes are shown in Table 4.1.

**Table 4.1. Properties of fresh concrete**

|                                 | <b>Mix 1</b>  | <b>Mix 2</b>   | <b>Mix 3</b>   | <b>Mix 4</b>         |
|---------------------------------|---------------|----------------|----------------|----------------------|
| <b>Property</b>                 | <b>I-20FA</b> | <b>IP-20FA</b> | <b>IS-20FA</b> | <b>I/II-20FA-30S</b> |
| Unit Weight, lb/ft <sup>3</sup> | 148.4         | 148.2          | 148            | 148.6                |
| Slump, in.                      | 3             | 2.5            | 2.5            | 2.5                  |
| Air Content, %                  | 5.5           | 6              | 6              | 6.5                  |

The unit weight of all concrete mixes was about 148 lb/ft<sup>3</sup>. The slump was maintained at 2.5–3 in. for all mixtures. The air content of the mixes was measured to be 5.5–6.5% as also shown in Table 4.1.

### Properties of Hardened Concrete

In accordance with the ASTM C192 (2016) standard practice, 4×8 in. cylindrical specimens were made and cured from fresh concrete. After approximately 24 hours, specimens were demolded and then moist-cured in a curing chamber at 74°F. The moist-cured samples were tested at 28 days for compressive strength, split tensile strength, and static modulus of elasticity as per the ASTM C39 (2016), ASTM C496 (2011), and ASTM C469/C469M (2014) standard test methods, respectively. The compressive strengths of the four concrete mixes were tested additionally after 1, 3, 7, and 14 days of moist-curing.

The chart in Figure 4.1 shows the development of the compressive strength for all four mixes.

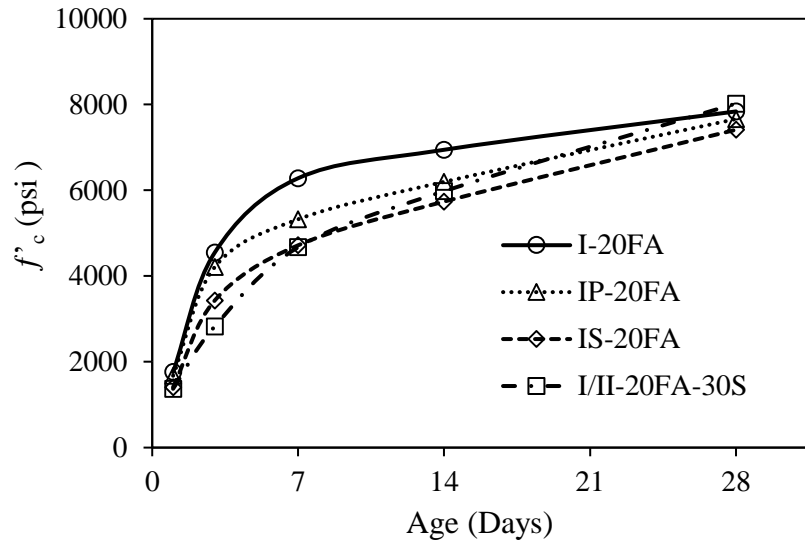


**Figure 4.1. Compressive strength development**

It can be observed from Figure 4.1 that Mix 4 (I/II-20FA-30S), containing the largest amount of SCMs, exhibits a slower strength gain at initial test ages (1 and 3 days) while the rate of strength gain increases at later ages (14 and 28 days) as compared to the other mixes containing smaller quantities of SCMs. The 28-day compressive strength of Mix 4 was the highest at 8,021 psi while for Mixes 1, 2, and 3, it was measured to be 7,839, 7,662, and 7,412 psi, respectively.

Other mechanical properties such as the split tensile strength and the static modulus of elasticity were also measured for all of the mixes. Table 4.2 shows the 28-day measured values of the split tensile strength and static modulus of elasticity.

**Table 4.2. Split tensile strength and E-modulus at 28 days**

| Property                               | I-20FA | IP-20FA | IS-20FA | I/II-20FA-30S |
|----------------------------------------|--------|---------|---------|---------------|
| Split Tensile Strength, psi            | 530    | 603     | 543     | 586           |
| Elastic Modulus ( $\times 10^6$ ), psi | 5.55   | 5.62    | 6.04    | 5.88          |

As shown in Table 4.2, the elastic modulus of all mixes was in the range 5.55–6.04  $\times 10^6$  psi. The split tensile strength was measured to be in the range 530–630 psi for all four mixes.

### *Maturity*

The Nurse-Saul method was used for developing the compressive strength-maturity relationship, as discussed in Chapter 3 under Tests and Methods. The datum temperature of 14°F was used for all of the mixes. Table 4.3 presents some of the initial data points as recorded by an iButton

temperature sensor (average of the two specimens) and later columns in the table show calculated values of the incremental and cumulative TTF.

**Table 4.3. Maturity calculations for Mix 1**

| <b>Time<br/>Interval,<br/>Minutes</b> | <b>Age,<br/>Hours</b> | <b>Avg<br/>Temperature<br/>(T<sub>a</sub>), °F</b> | <b>TTF<br/>Increment,<br/>°F-hr</b> | <b>TTF<br/>Cumulative,<br/>°F-hr</b> |
|---------------------------------------|-----------------------|----------------------------------------------------|-------------------------------------|--------------------------------------|
| 0                                     | 0                     |                                                    |                                     |                                      |
| 45                                    | 0.75                  | 58.33                                              | 33.24                               | 33.24                                |
| 90                                    | 1.5                   | 57.65                                              | 32.74                               | 65.98                                |
| 135                                   | 2.25                  | 57.43                                              | 32.57                               | 98.55                                |
| 180                                   | 3                     | 56.75                                              | 32.06                               | 130.61                               |
| 225                                   | 3.75                  | 56.75                                              | 32.06                               | 162.68                               |
| 270                                   | 4.5                   | 56.08                                              | 31.56                               | 194.23                               |
| 315                                   | 5.25                  | 55.85                                              | 31.39                               | 225.62                               |
| 360                                   | 6                     | 55.85                                              | 31.39                               | 257.01                               |
| 405                                   | 6.75                  | 55.40                                              | 31.05                               | 288.06                               |
| 450                                   | 7.5                   | 55.40                                              | 31.05                               | 319.11                               |
| 495                                   | 8.25                  | 55.18                                              | 30.88                               | 349.99                               |
| 540                                   | 9                     | 54.95                                              | 30.71                               | 380.70                               |
| 585                                   | 9.75                  | 54.95                                              | 30.71                               | 411.41                               |
| 630                                   | 10.5                  | 54.95                                              | 30.71                               | 442.13                               |
| 675                                   | 11.25                 | 54.95                                              | 30.71                               | 472.84                               |

TTF= time-temperature factor

The test for the compressive strength of all four mixes was performed at ages of 1, 3, 7, 14, and 28 days. The compressive strength was then plotted as a function of the calculated TTF. The compressive strength-maturity relationship for each mix was then developed by performing a regression analysis to determine a best-fit equation to the data. The best-fit equation for all mixes was found to be of the form where compressive strength is a linear function of the logarithm of the maturity index (in this case, TTF). Figure 4.2 shows the compressive strength – log (TTF) plot of all four mixes along with the best-fit curve and the best-fit equation.

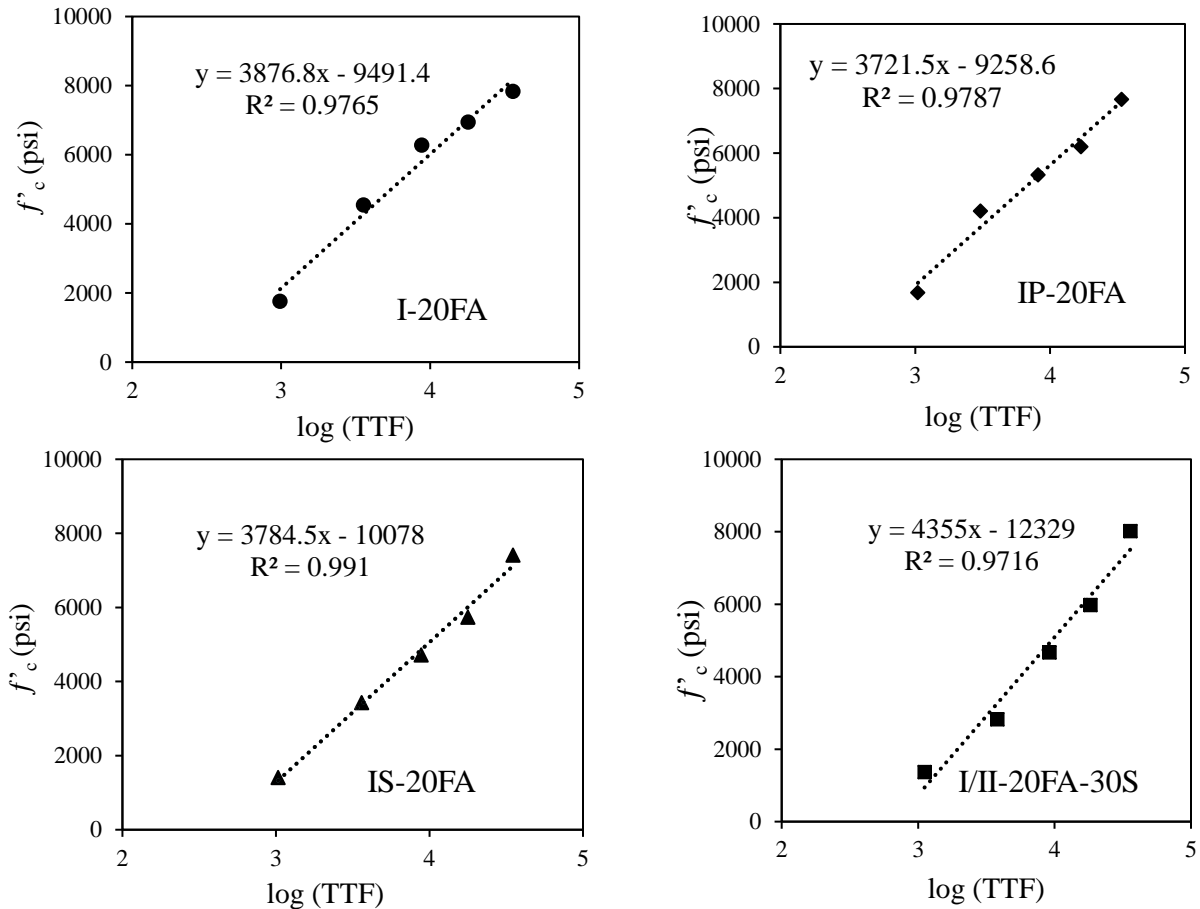


**Figure 4.2. Compressive strength – TTF best-fit curve**

The best-fit compressive strength-TTF equation for all of the mixes are of the form as shown previously in equation (2). ConcreteWorks allows the user to manually enter the coefficients  $a$  and  $b$  of equation (2). It can be observed from the equation that coefficient  $a$  is the slope of the curve while coefficient  $b$  is the y-intercept.

Table 4.4 summarizes the coefficients  $a$  and  $b$  of the best-fit equation of all four mixes.

**Table 4.4. Coefficients  $a$  and  $b$  of best-fit strength-maturity equation**

| Mix           | Coefficient $a$<br>(psi) | Coefficient $b$<br>(psi/°F/hr) |
|---------------|--------------------------|--------------------------------|
| I-20FA        | -9,491.4                 | 3,876.8                        |
| IP-20FA       | -9,258.6                 | 3,721.5                        |
| IS-20FA       | -10,078.0                | 3,784.5                        |
| I/II-20FA-30S | -12,329.0                | 4,355.0                        |

### *Isothermal Calorimetry*

Isothermal calorimetry was performed for all mixes to measure the heat of hydration and the rate of heat generation. As covered in Chapter 3 under Tests and Methods, the cement paste specimens prepared per the mix proportions for the four different concrete mixes, keeping the water-binder ratio as 0.43, were tested at constant temperatures of 10, 20, 30, and 40°C each using the isothermal calorimeter. To analyze the effect of the LRWR on the heat and process of hydration, two different pastes were tested corresponding to each mix—one containing the LRWR and the other without. The admixture dosage was kept the same as that used in concrete mixes.

Figures 4.3 through 4.7 show the charts for the rate of heat generation (mW/g) and cumulative heat (J/g) for all four mixes at 10, 20, 30, and 40°C.

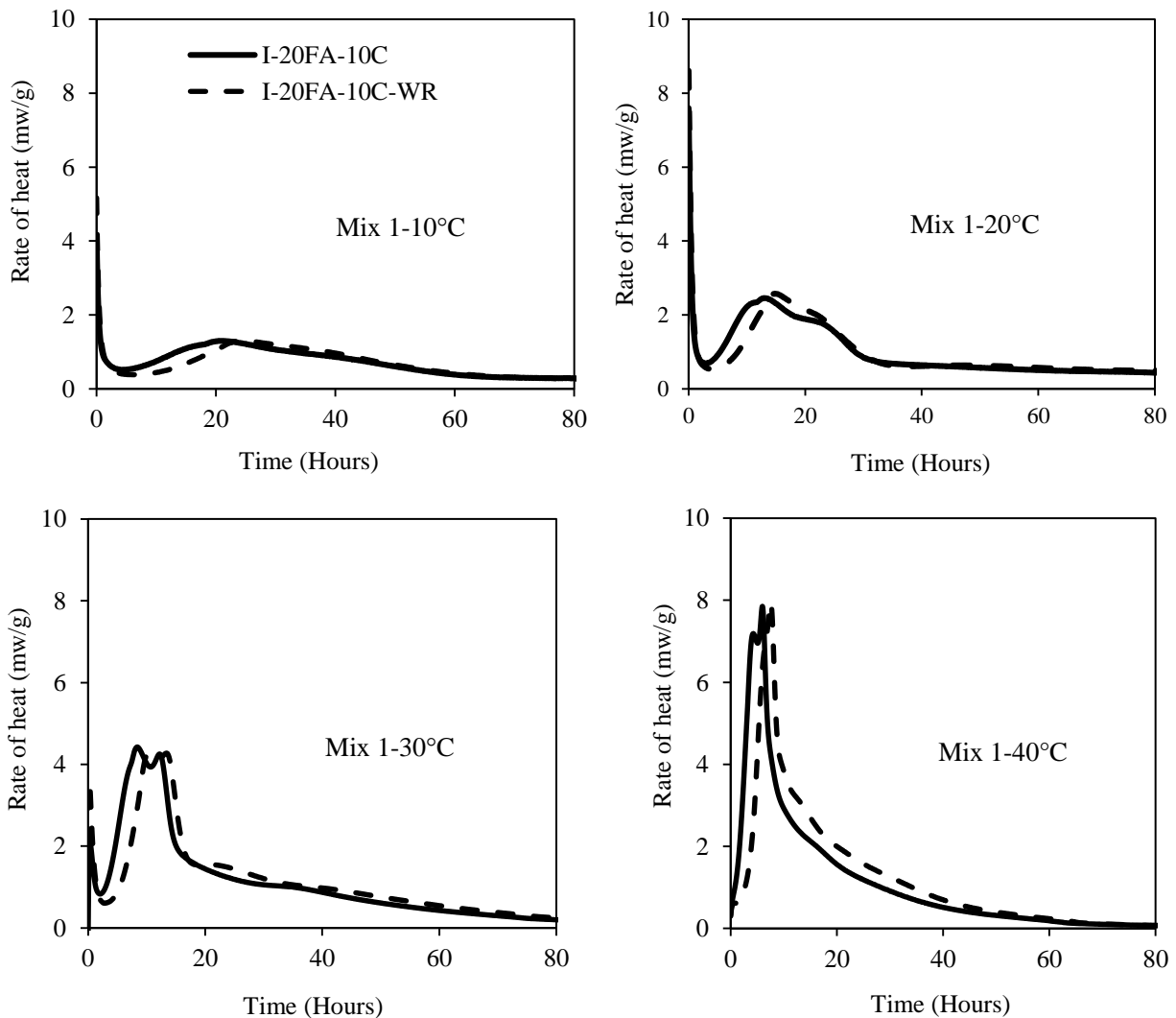


**Figure 4.3. Rate of heat generation (Mix 1)**

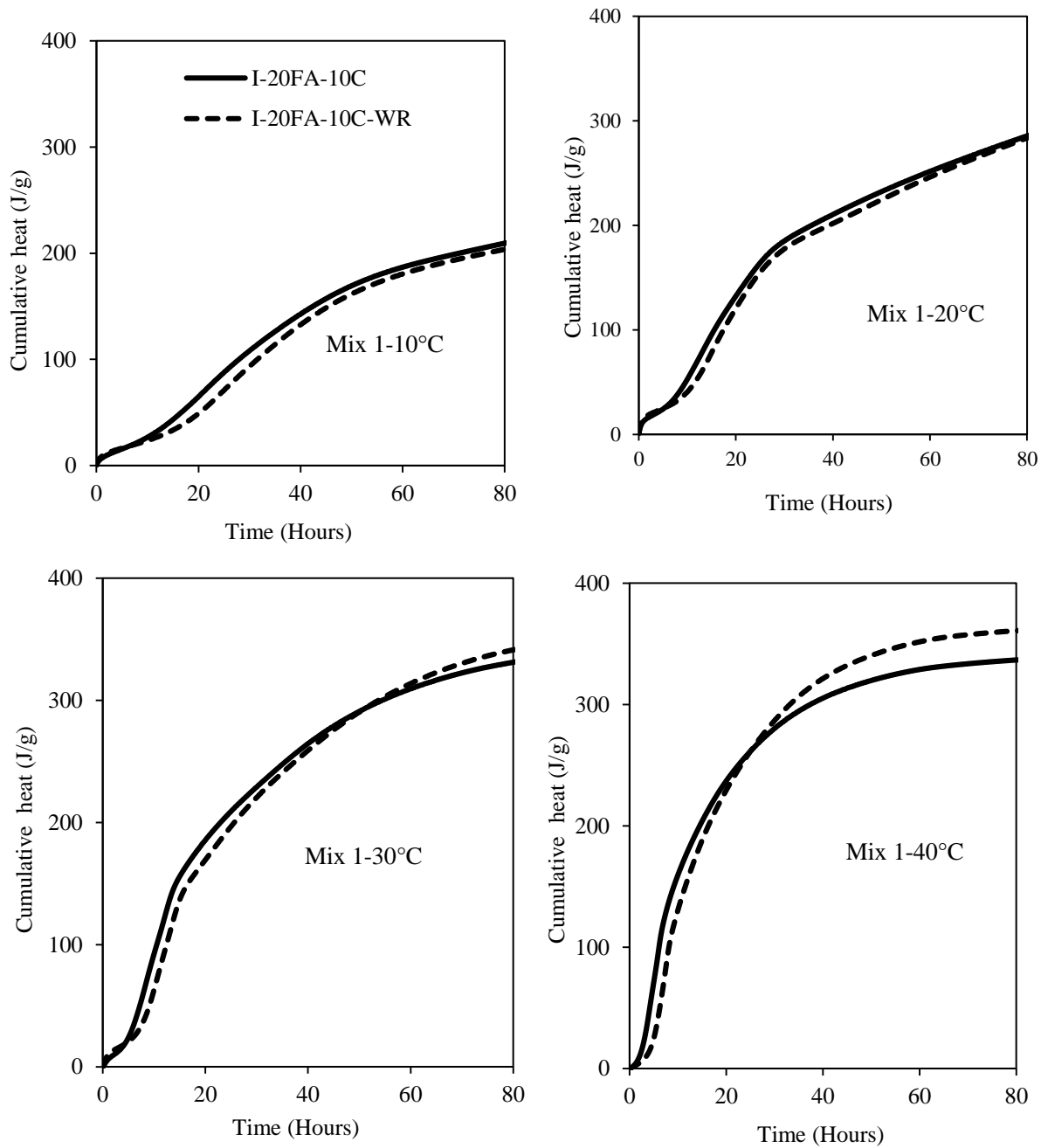


**Figure 4.4. Cumulative heat (Mix 1)**

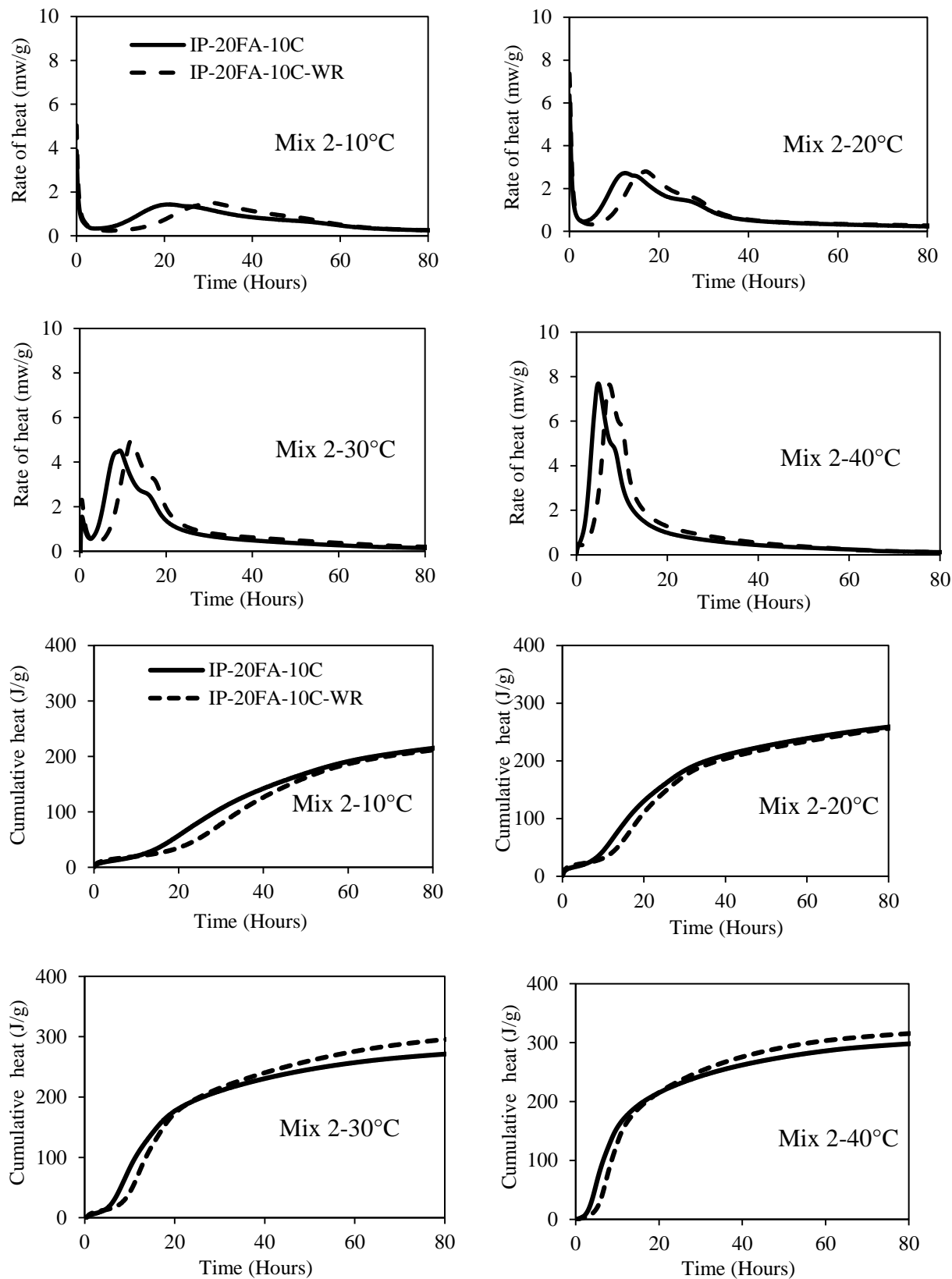


**Figure 4.5. Rate of heat and cumulative heat (Mix 2)**



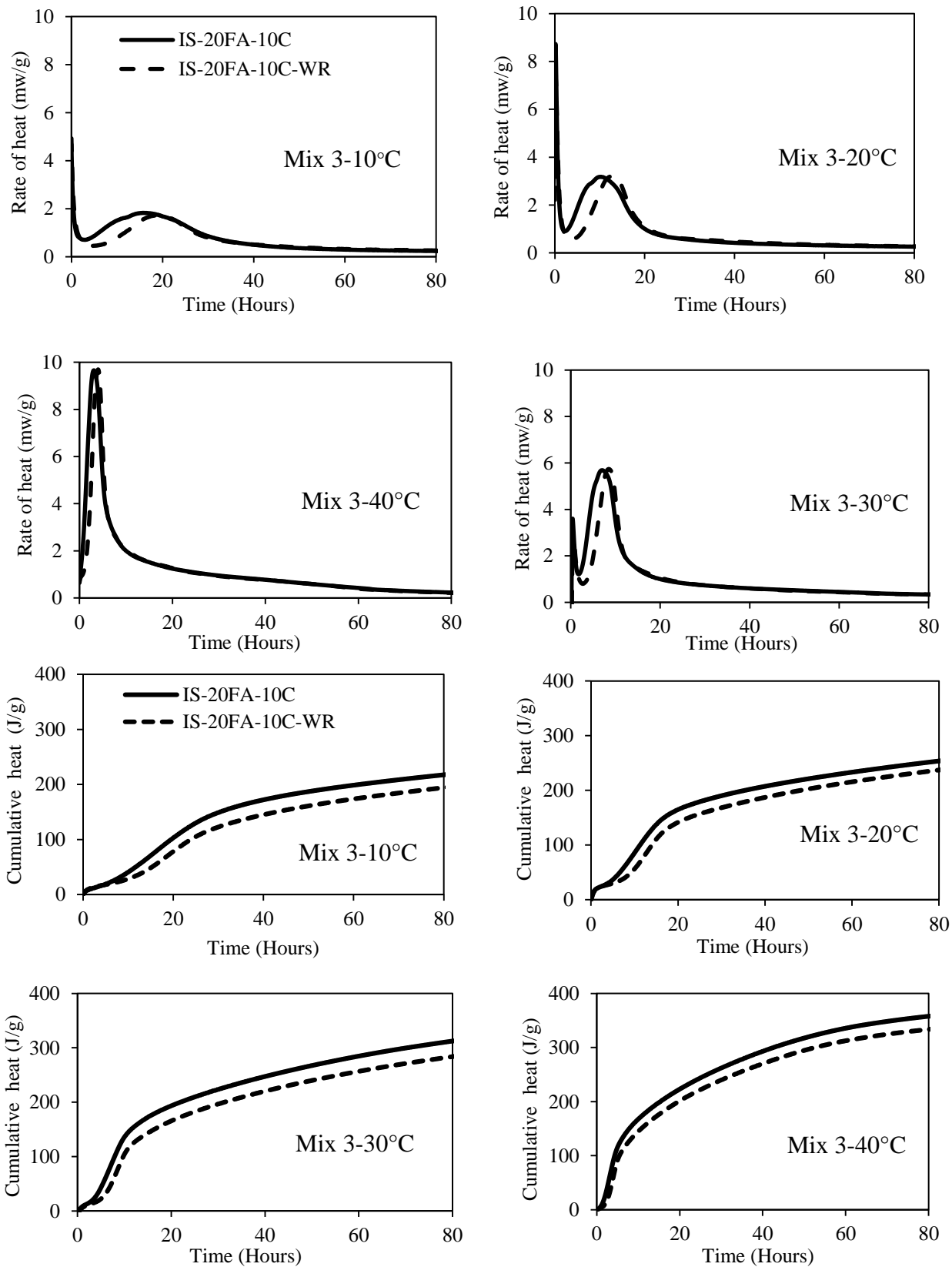


**Figure 4.6. Rate of heat and cumulative heat (Mix 3)**

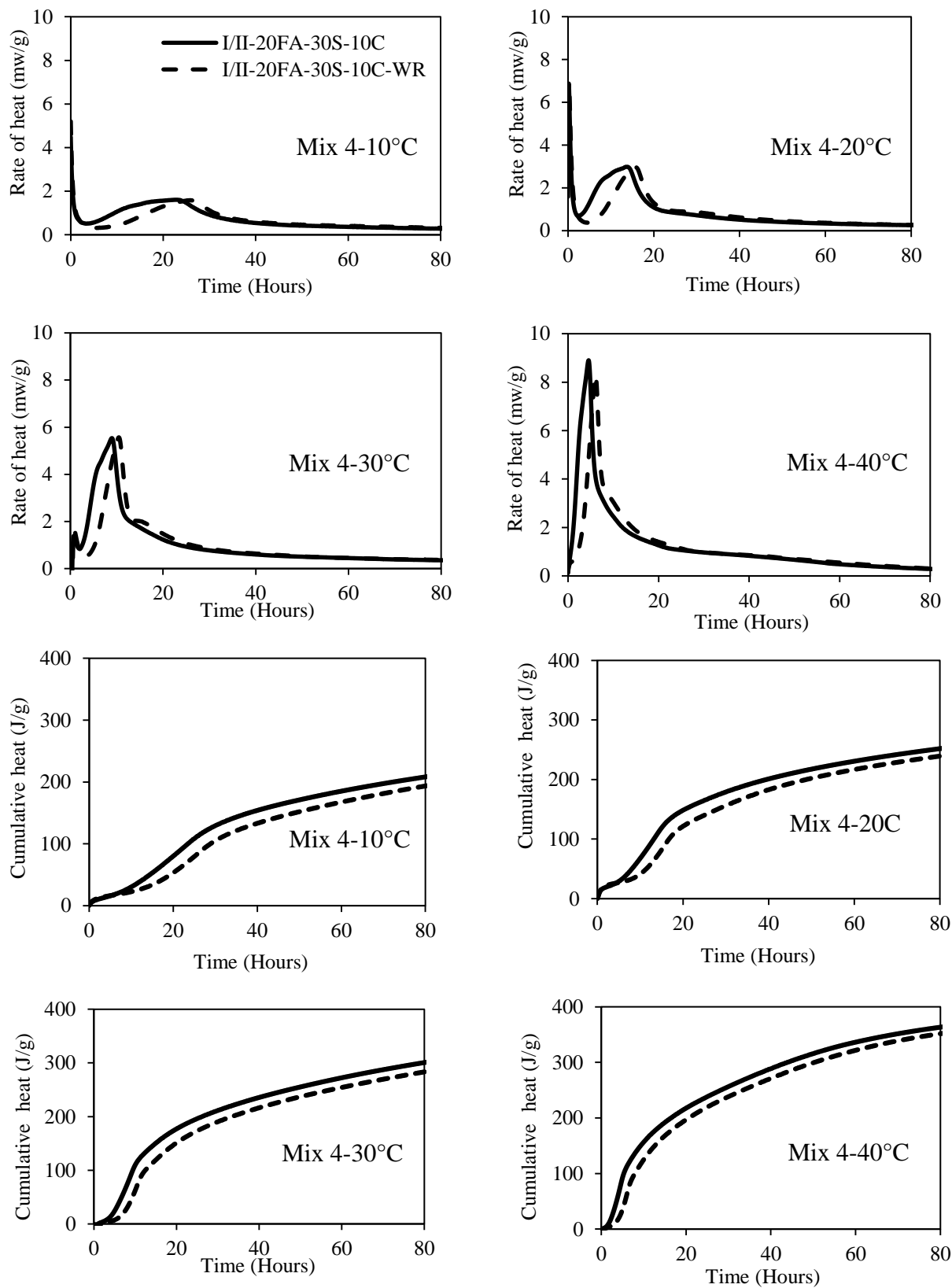


**Figure 4.7. Rate of heat and cumulative heat (Mix 4)**

Some of the observations from the isothermal calorimetry tests on all four mixes are as follows:

- Water reducers lead to a decrease in the rate of hydration as well as delays in hydration in all cases.
- The water reducer effect is more prevalent at a higher temperature than at lower temperatures.
- The second peak becomes more pronounced with an increase in temperature.
- The rate and degree of hydration increase with an increase in the testing temperature.
- The retarding effect of water reducers on the degree of hydration decreases with an increase in temperature.
- The acceleration period lasts longer at a lower temperature than at higher temperature.
- The differences in peaks across the samples are more prevalent at higher than at lower temperatures.
- At a higher degree of replacement of cement with SCMs (as in Mixes 2 and 3), while the hydration is delayed, the peak values are comparatively less affected by the water reducer.
- Mix 3 is effectively a ternary blend. While it shows a delay in hydration due to the water reducer, the peak rate of hydrations is almost similar.
- The first peak is almost invisible in Mix 3 and even less pronounced in Mix 4 as Mix 4 has an even higher level of replacement of 50%.

### Activation Energy

Using the chemical compositions of the cement as presented previously in Table 2.2, Bogue equations were followed to calculate approximate proportions of the four main minerals,  $C_3S$ ,  $C_2S$ ,  $C_3A$ , and  $C_4AF$ , in cement. The following equations were used to calculate the proportions of minerals.

$$C_3S = 4.0710CaO - 7.6024SiO_2 - 1.4297Fe_2O_3 - 6.7187Al_2O_3 \quad (22)$$

$$C_2S = 8.6024SiO_2 + 1.0785Fe_2O_3 + 5.0683Al_2O_3 - 3.0710CaO \quad (23)$$

$$C_3A = 2.6504Al_2O_3 - 1.6920Fe_2O_3 \quad (24)$$

$$C_4AF = 3.0432Fe_2O_3 \quad (25)$$

The Bogue equations are applicable only to portland cements with an  $Al_2O_3/Fe_2O_3$  (A/F ratio) of 0.64 or higher. All four types of cement had A/F ratios higher than 0.64 and, hence, these equations were used. Using the previous equations (4)–(6) and the proportion of minerals calculated from equations (22)–(25), total heat available for the hydration reaction was estimated for all four concrete mixes. The DOH of cementitious material at a specific time,  $t$ , is then determined by taking the ratio of heat evolved at time  $t$  to the estimated total amount of heat available ( $H_u$ ) as per the previous equation (4). The following observations were made regarding DOH:

- At a higher constant temperature, the degree of cement hydration is higher at a particular time.
- In Mixes 3 and 4, which contain GGBFS, the water reducer slightly decreases the degree of hydration at a given time and temperature.

Following the steps as mentioned in Chapter 3, four different  $\tau$  values (at 10, 20, 30, and 40°C) fitted to the cumulative isothermal heat of hydration curves were then plotted on an Arrhenius plot. The apparent activation energy ( $E_a$ ) was then calculated as the slope of a best-fit line to the four points on the Arrhenius plot multiplied by the natural gas constant,  $R$ . Figure 4.8 shows Arrhenius plots for the calculation of apparent activation energies of all mixes with the water reducer (WR).

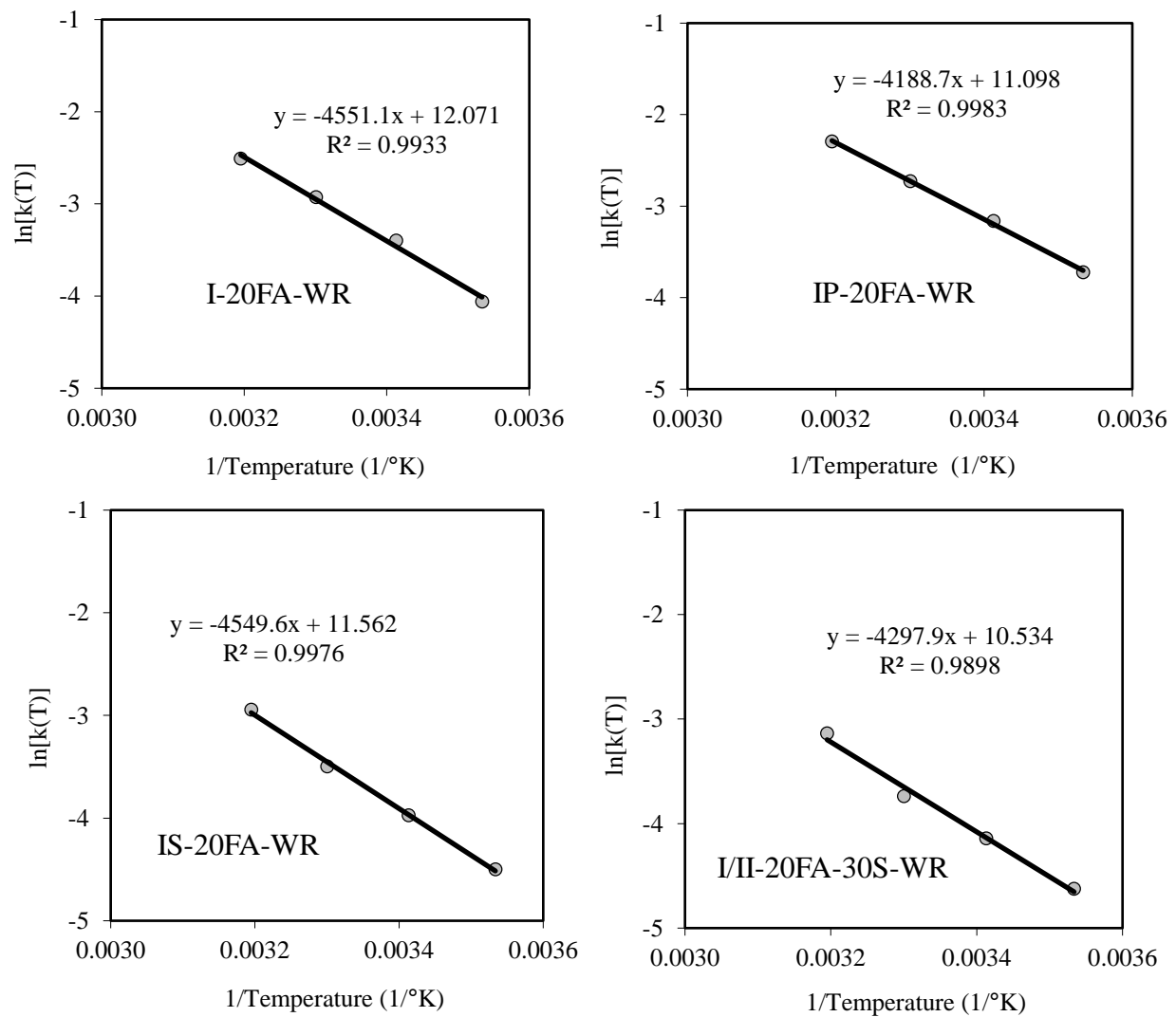


**Figure 4.8. Arrhenius plots for activation energy**

The fitted values of the hydration curve parameters,  $\alpha_u$ ,  $\beta$ , and  $\tau$  and the calculated values of the apparent activation energy ( $E_a$ ) are shown in Table 4.5.

**Table 4.5. Hydration curve parameters and  $E_a$  values of all mixes**

| Mixture          | Temp,<br>°C | $\alpha_u$ | $\beta$ | $\tau$ , hours | $R^2$ | Calculated<br>$E_a$ , J/mol |
|------------------|-------------|------------|---------|----------------|-------|-----------------------------|
| I-20FA           | 10          | 0.764      | 0.802   | 46.652         | 0.986 | 38,374                      |
|                  | 20          |            |         | 23.647         | 0.984 |                             |
|                  | 30          |            |         | 14.129         | 0.991 |                             |
|                  | 40          |            |         | 9.810          | 0.988 |                             |
| I-20FA-WR        | 10          | 0.842      | 0.795   | 58.012         | 0.975 | 37,840                      |
|                  | 20          |            |         | 29.872         | 0.955 |                             |
|                  | 30          |            |         | 18.636         | 0.993 |                             |
|                  | 40          |            |         | 12.301         | 0.985 |                             |
| IP-20FA          | 10          | 0.617      | 0.991   | 33.120         | 0.997 | 34,082                      |
|                  | 20          |            |         | 17.940         | 0.973 |                             |
|                  | 30          |            |         | 13.388         | 0.996 |                             |
|                  | 40          |            |         | 7.814          | 0.996 |                             |
| IP-20FA-WR       | 10          | 0.663      | 1.042   | 41.475         | 0.990 | 34,826                      |
|                  | 20          |            |         | 23.635         | 0.981 |                             |
|                  | 30          |            |         | 15.320         | 0.994 |                             |
|                  | 40          |            |         | 9.927          | 0.996 |                             |
| IS-20FA          | 10          | 1.222      | 0.391   | 85.896         | 0.983 | 38,634                      |
|                  | 20          |            |         | 53.876         | 0.909 |                             |
|                  | 30          |            |         | 30.059         | 0.991 |                             |
|                  | 40          |            |         | 18.118         | 0.994 |                             |
| IS-20FA-WR       | 10          | 1.114      | 0.433   | 89.830         | 0.988 | 37,828                      |
|                  | 20          |            |         | 53.063         | 0.972 |                             |
|                  | 30          |            |         | 33.012         | 0.992 |                             |
|                  | 40          |            |         | 18.960         | 0.994 |                             |
| I/II-20FA-30S    | 10          | 1.048      | 0.412   | 103.901        | 0.996 | 38,343                      |
|                  | 20          |            |         | 62.435         | 0.996 |                             |
|                  | 30          |            |         | 39.243         | 0.951 |                             |
|                  | 40          |            |         | 21.315         | 0.819 |                             |
| I/II-20FA-30S-WR | 10          | 0.981      | 0.480   | 101.728        | 0.991 | 35,734                      |
|                  | 20          |            |         | 62.885         | 0.983 |                             |
|                  | 30          |            |         | 41.948         | 0.992 |                             |
|                  | 40          |            |         | 23.016         | 0.993 |                             |

From the data presented in Table 4.5, it can be observed that the addition of the water reducer in a particular mix does the following:

- The ultimate degree of hydration,  $\alpha_u$ , increases for Mix 1 and 2, whereas it decreases in Mix 3 and 4.
- The hydration shape parameter,  $\beta$ , increases for all mixes except Mix 1.
- The hydration time parameter,  $\tau$ , increases at a particular temperature.

- The water reducer decreases the activation energy,  $E_a$ , for all mixes except Mix 2.
- $E_a$  increases clearly in a concrete mix containing slag (Mixes 3 and 4).

### Semi-Adiabatic Calorimetry

A semi-adiabatic drum calorimeter was fabricated in the PCC Laboratory (discussed in Chapter 3 under Tests and Methods) and it was calibrated before performing the test on the concrete specimens. De-ionized water was used for calibration. A regression analysis using the R-squared method with the Solver function in Excel was performed to match the modeled change in water temperature to the measured change in water temperature. The Solver function generated the best-fit calibration factors ( $C_{f1}$  and  $C_{f2}$ ) that were used to model the change in water temperature. 12×6 in. cylindrical specimens of all four fresh concrete mixes were tested in the semi-adiabatic calorimeter for 160 hours each and the temperature data were recorded at 15-minute intervals. Following the steps outlined in Chapter 3 under Tests and Methods, test data were used to determine the best-fit hydration parameters  $\alpha_u$ ,  $\beta$ , and  $\tau$ , as well as the true adiabatic temperature rise. Table 4.6 shows the best-fit hydration parameters.

**Table 4.6. Hydration parameters from semi-adiabatic calorimetry**

| Mixture       | $H_u$ , J/Kg | $E_a$ , J/mol | $\alpha_u$ | $\beta$ | $\tau$ , hours | $R^2$ |
|---------------|--------------|---------------|------------|---------|----------------|-------|
| I-20FA        | 501,400      | 37,840        | 0.678      | 0.820   | 20.360         | 0.975 |
| IP-20FA       | 490,032      | 34,826        | 0.643      | 0.841   | 18.120         | 0.993 |
| IS-20FA       | 468,077      | 37,828        | 0.937      | 0.522   | 33.300         | 0.986 |
| I/II-20FA-30S | 467,041      | 35,734        | 1.013      | 0.460   | 62.420         | 0.985 |

Figure 4.9 shows the measured the semi-adiabatic and calculated true adiabatic temperatures.

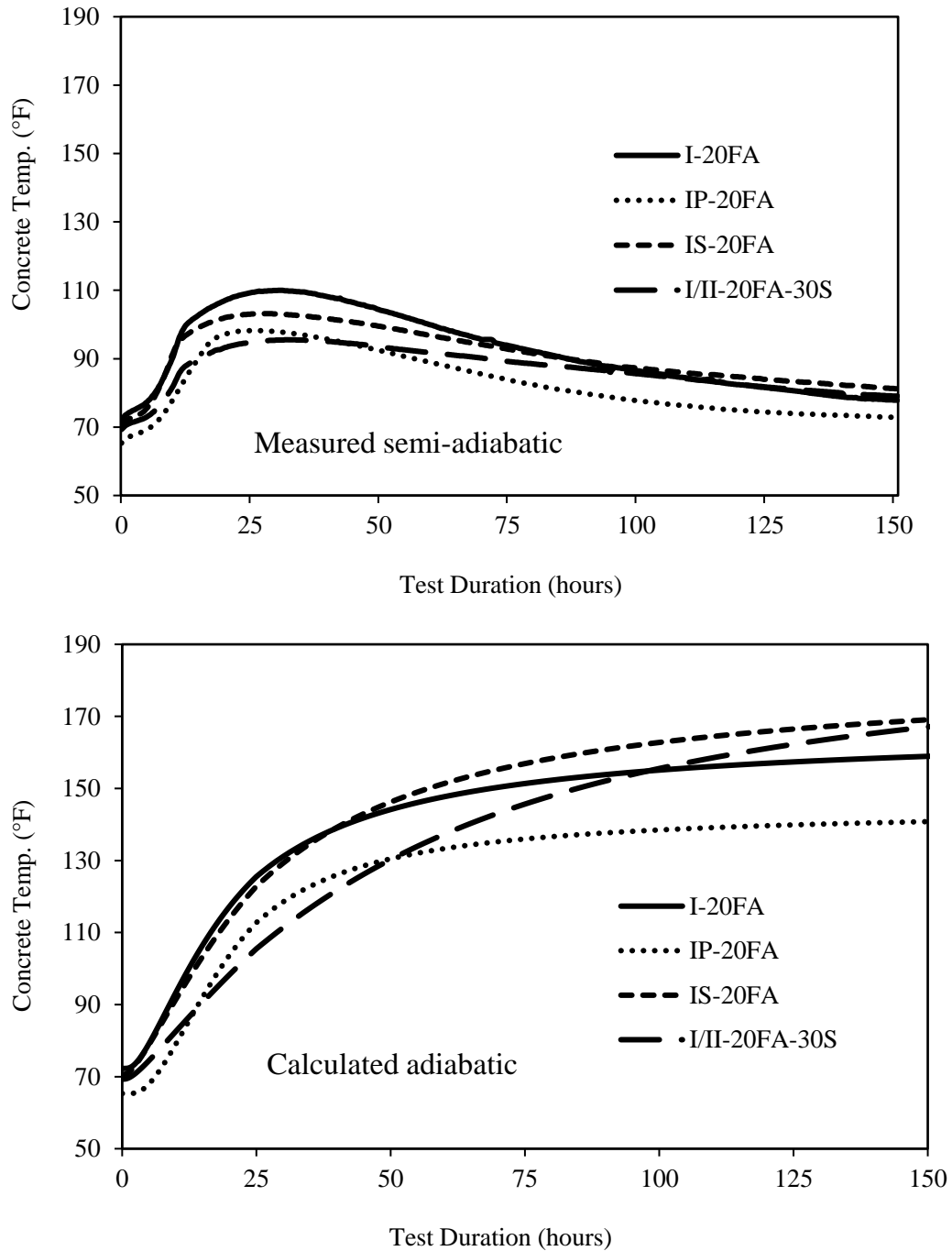


**Figure 4.9. Measured semi-adiabatic (top) and calculated adiabatic temperature (bottom)**

The following observations can be made from the semi-adiabatic tests:

- Mixes 3 and 4, containing slag, have a higher ultimate degree of hydration ( $\alpha_u$ ) and exhibit delayed hydration (larger  $\tau$ ) than those not containing slag, Mixes 1 and 2.

- Clearly, heat of hydration decreases with the addition of SCMs versus Class C fly ash and GGBFS.
- At 3 days, the adiabatic temperature (calculated from the measured semi-adiabatic temperature) rises up to 150, 132, 155, and 142°F for Mixes 1, 2, 3, and 4, respectively.

The best-fit hydration parameters, the ultimate heat of hydration ( $H_u$ ), and apparent activation energy ( $E_a$ ) are required as input in ConcreteWorks for temperature modeling of a particular concrete mix for the given boundary and environmental conditions.

### Thermal Conductivity

The test for thermal conductivity was performed as per the ASU cylindrical specimen method (Carlson et al. 2010) as outlined in Chapter 3 under Tests and Methods. Three 28-days moist cured specimens of each of the mixes were tested. Two separate runs were conducted for each specimen, thereby obtaining a total of six data points for each mix. Figure 4.10 shows the temperature development in the 0.5 in. diameter core and on the surface of one of the specimens of Mix 3 and Mix 4.

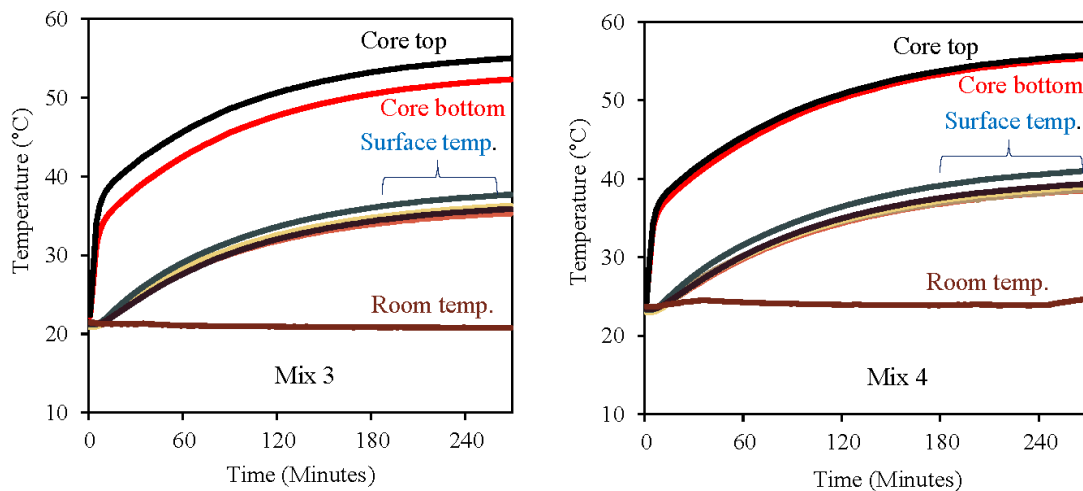


**Figure 4.10. Temperature development during thermal conductivity test**

It was observed from the experiments that the concrete specimens take approximately 2.5 to 3 hours to reach the steady state. The thermal conductivity value at the steady state is then considered as the thermal conductivity of that concrete mix. Thermal properties of concrete are predominantly dependent on the type of aggregate used in the concrete mix. Although the type of cementitious materials used was different for different mixes, the type of coarse aggregate used in all four mixes was limestone from the same source. Therefore, experimental values of thermal conductivity of the mixes were found to lie in a short range of 1.1–1.2 W/m-K.

Table 4.7 shows the mean and 95% confidence interval (CI) for the mean thermal conductivity of the concrete mixes.



**Table 4.7. 95% confidence interval for mean thermal conductivity**

| Mix           | Mean $k$ (W/m-K) | 95% CI for Mean $k$ (W/m-K) |
|---------------|------------------|-----------------------------|
| I-20FA        | 1.20             | (1.15–1.26)                 |
| IP-20FA       | 1.17             | (1.15–1.18)                 |
| IS-20FA       | 1.12             | (1.09–1.14)                 |
| I/II-20FA-30S | 1.10             | (1.06–1.14)                 |

The confidence interval signifies that if the test is performed several times, it can be believed that 95% of the thermal conductivity values would lie in this interval. The default value of thermal conductivity in ConcreteWorks is 2.6 W/m-K.

### Coefficient of Thermal Expansion

The coefficient of thermal expansion was determined using the AASHTO T 336-15 test method (discussed in Chapter 3 under Tests and Methods). Two 28-day moist-cured specimens of each of the mixes were used to perform the CTE test. Table 4.8 shows the measured CTE values of the mixes.

**Table 4.8. CTE values of concrete mixes**

| Property             | Mix 1 | Mix 2 | Mix 3 | Mix 4 |
|----------------------|-------|-------|-------|-------|
| CTE (microstrain/°C) | 8.03  | 8.16  | 9.08  | 7.19  |

As discussed in the last section, the thermal properties of concrete are predominantly dependent on the type of aggregate used in the concrete mix. In this research, limestone was used as coarse aggregate for all four mixes and, hence, the CTE value of all mixes were measured to be in a small range of 7.19–9.08 microstrain/°C.

## 5. FIELD INVESTIGATION

As part of Task 4, the construction of Pier 4 of I-35 NB to the US 30 WB (Ramp H) bridge in Ames, Iowa was analyzed and the process was documented. Figure 5.1 shows the location designated as DESIGN NO. 616.

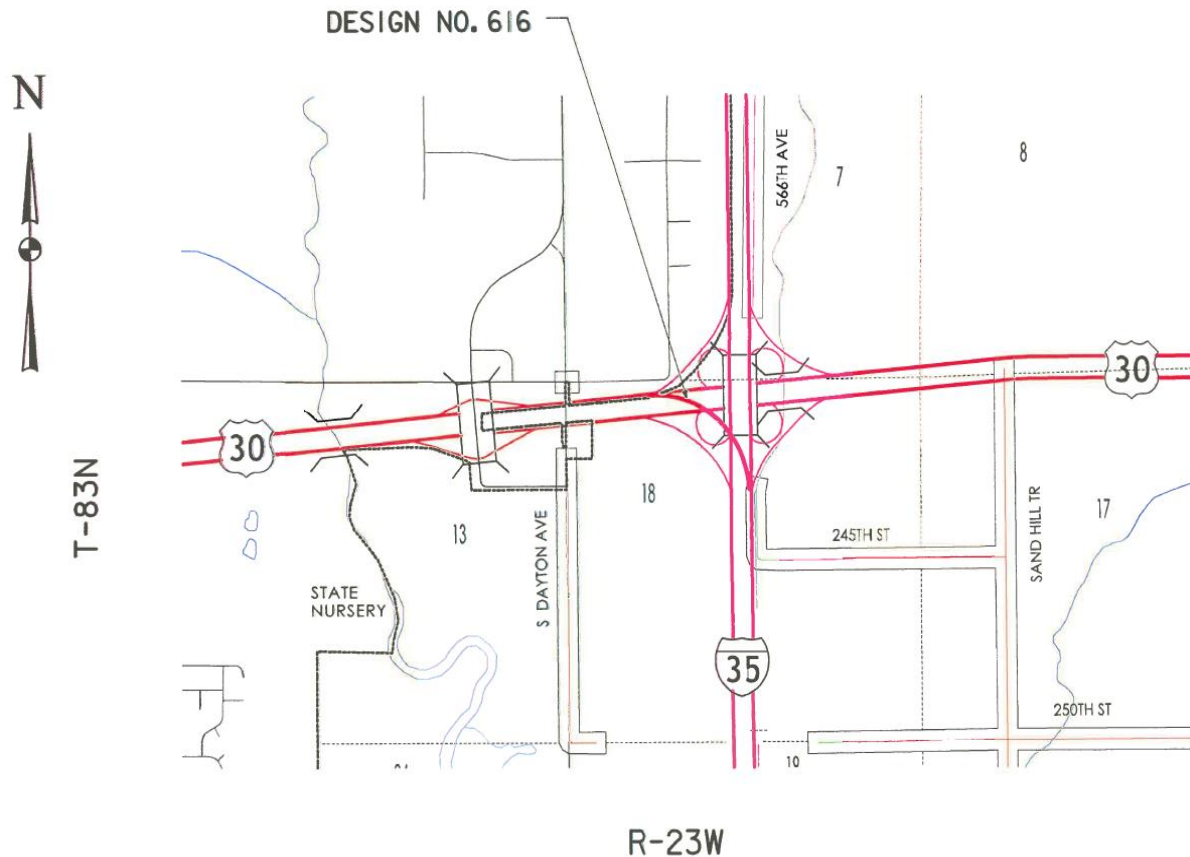


**Figure 5.1. Location of the I-35 to US 30 Bridge**

The I-35 NB to US 30 WB (Ramp H) bridge is a seven-span continuous welded girder bridge constructed on six piers with a total length of 1,690 ft and a width of 36 ft extending from Station 8517+07 to Station 8533+97.

All of the piers have a rectangular cross section except one, the footing of Pier 3, which has a cross section of a rectangle cut on the two opposite corners. The footing of Pier 4 (Footing #4) was selected as the focus of the field investigation in this project as it is the largest of all of the footings; the stem and column were not investigated. Figure 5.2 shows the location of all six bridge piers.

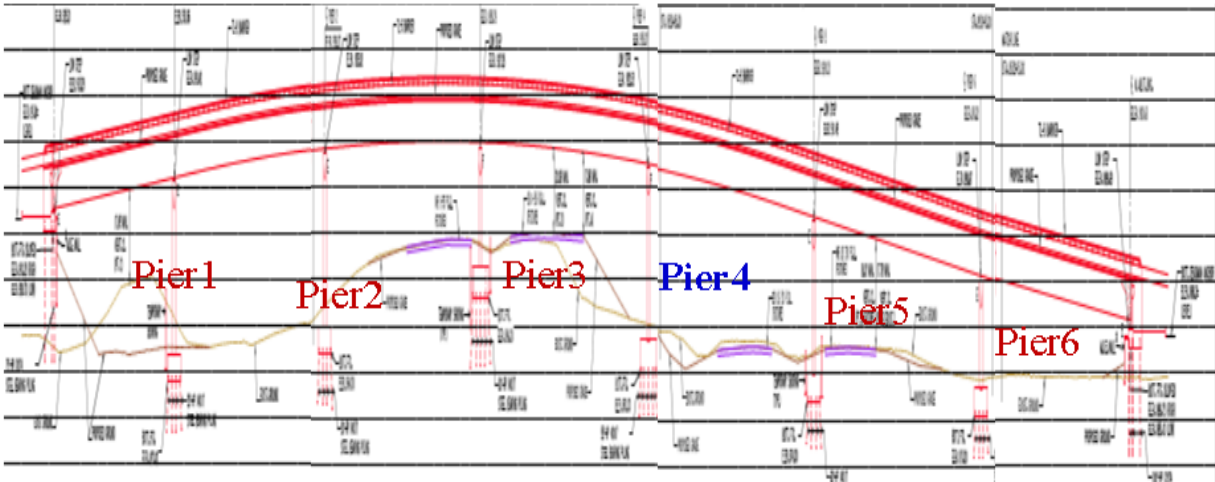


**Figure 5.2. Locations of all six piers**

The dimensions and layout of the corresponding footings of all six piers are shown in Figure 5.3.

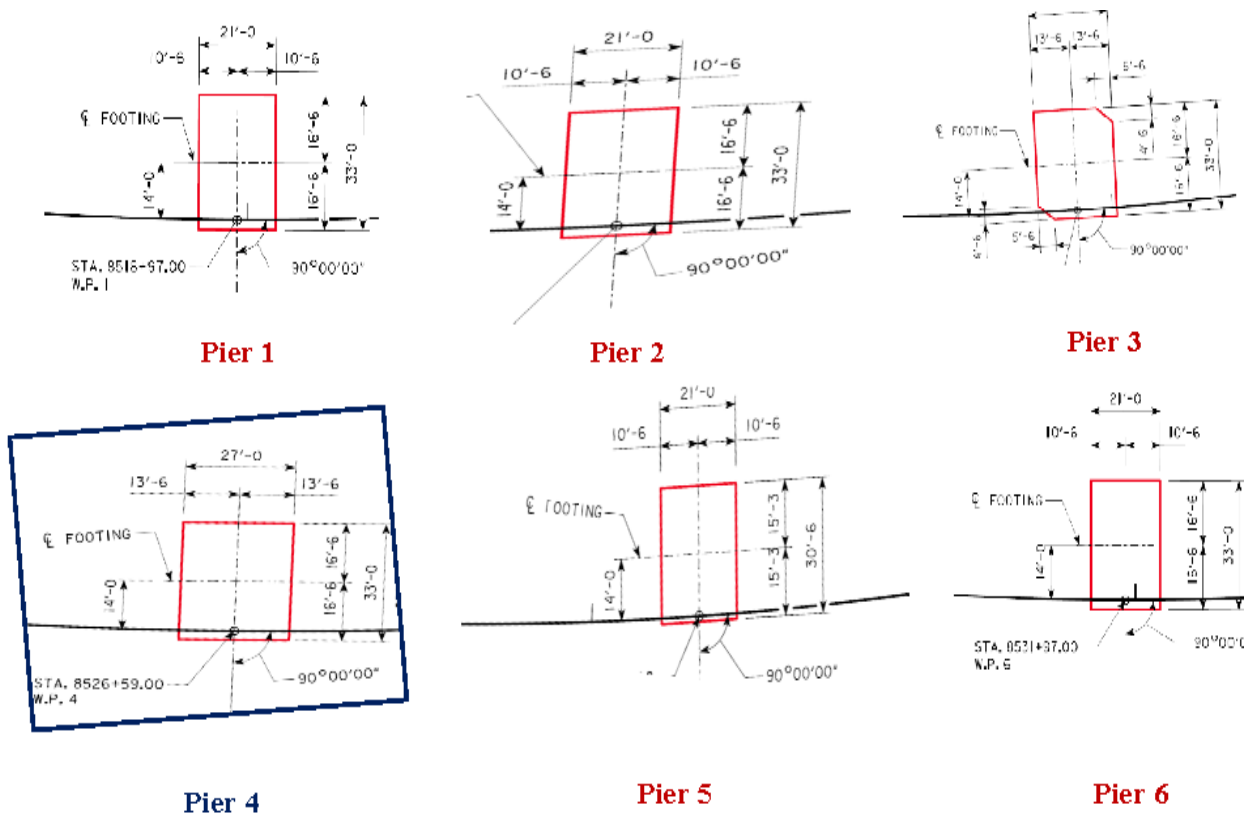


**Figure 5.3. Dimensions of all six piers**

As proposed by the TAC members, the investigation of the Pier 4 footing was carried out in three phases: prior, during, and after placement of concrete. The following sections of this chapter present the phase-wise investigation of the Pier 4 footing.

## Investigation before Placement of Concrete

### *Subsurface Profile*

The bridge site is located in an area of Iowa that has been formed by extensive Wisconsin Age glacial activity. During the very initial stage of project finalization, a soil investigation at the job site was carried out by HDR, Inc. The primary geologic strata encountered in this investigation included the following.

- Topsoil
- Existing fill soils
- Cohesive alluvium
- Alluvial Sand
- Glacial till
- Bedrock

The subsurface profile around Pier 4 of the bridge site is presented in Figure 5.4.

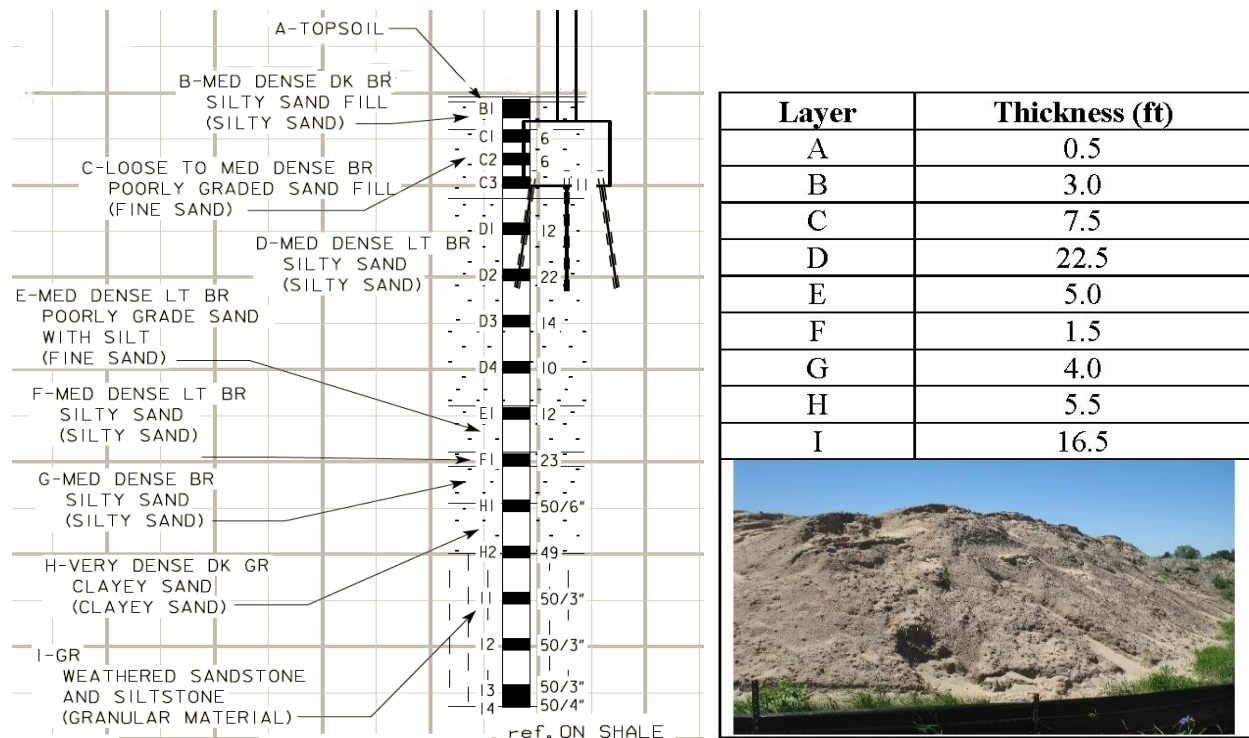


**Figure 5.4. Subsurface profile of Pier 4 job site (left), Thickness of layers (top right), and Excavated soil (bottom right)**

The table in the figure shows the thicknesses of the different layers encountered in the soil investigation.

Topsoil depths ranged from 5 to 8 in. along the project alignment. Alluvial sands were generally encountered below the cohesive alluvium or fill and were found to consist of brown and gray silty sand (SM), poorly graded sand (SP), clayey sand (SC) and poorly graded sand with silt (SP-SM).

Bedrock was encountered at depths ranging from 34 to 83 ft, corresponding to approximate elevations of 800 to 850 ft. The bedrock units appeared to include siltstone, sandstone, and shale, based on examination of split-barrel samples, with varying degrees of weathering.

#### *Footing Subbase and Support*

The load transfer mechanism for Footing 4 was 30 HP 14×117 steel bearing H-piles driven 55 ft below the ground surface, and the steel reinforcement footing cage was placed over these piles.

Based on the outcomes of the soil investigation, a layer of crushed limestone aggregate was placed on the subbase to provide a firm and dry casting surface. Figure 5.5 shows the driven H-piles and the crushed rock casting surface.

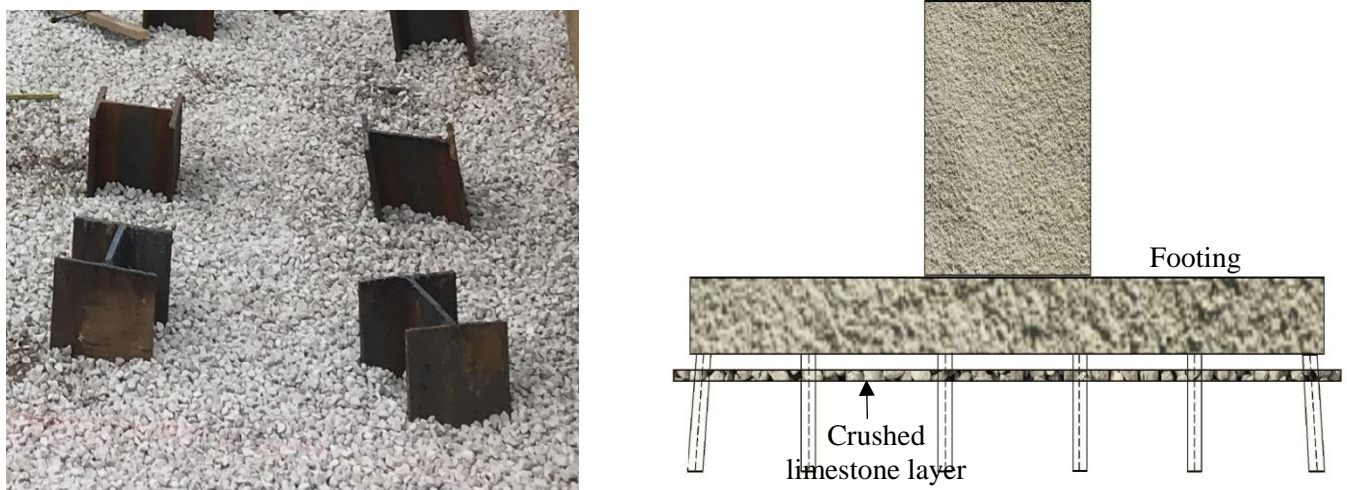


**Figure 5.5. Limestone subbase with steel bearing H-piles (left) and front elevation of footing with subbase (right)**

#### *Footing Formwork Material*

In central Iowa, wood and steel formwork materials are usually used to form footing placements. The choice of formwork material depends on the nature of construction as well as the availability and cost of the material. Wood formwork was used in the construction of the Pier 4 footing as shown in Figure 5.6.



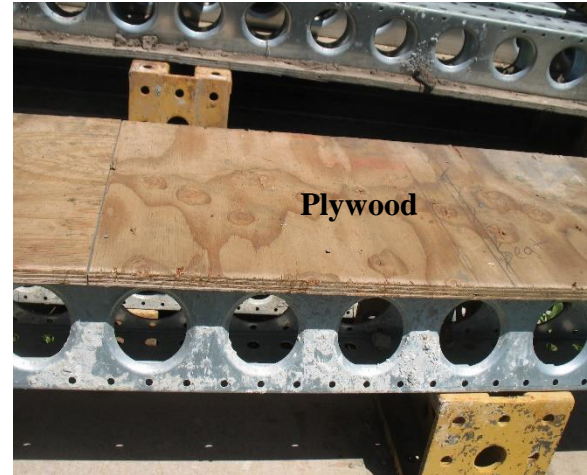


**Figure 5.6. Formwork used in Pier 4 footing**

This formwork consisted of plywood attached to galvanized cold-rolled steel supporting members with nails. These in turn were supported by vertical cold-rolled steel members with longer cross-sections.

#### *Installation of Sensors*

To monitor the thermal development of the concrete placement for the footing, seven sets of intelliRock temperature sensors were installed. Each set included a primary temperature sensor and a backup temperature sensor. The location of each set of sensors is shown in Figure 5.7 and described after the figure.

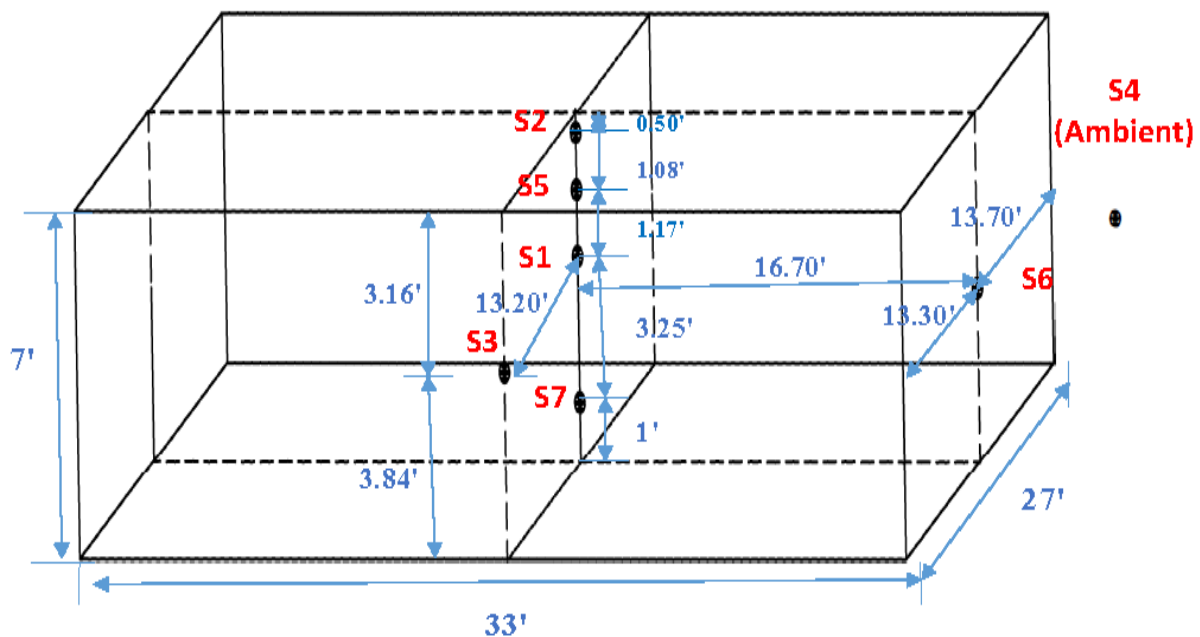


**Figure 5.7. Locations of temperature sensors installed in Pier 4 footing**

**Temp Sensor 1** – At the center of the concrete footing and installed 2.25 ft below the top temperature Sensor 2 (as measured)

**Temp Sensor 2** – In the middle of the length and width, near the top and lateral surfaces of the footing, and installed 3 ft below the top-most reinforcing steel bar, 16 ft from the east face and 16.7 ft from the west face reinforcing steel bar (as measured)

**Temp Sensor 3** – In the middle of the length and height, near the long lateral surface of the footing, and installed at 2.9 ft from the top-most reinforcing steel bar and 2.5 ft from the bottom-most reinforcing steel bar, 16 ft from the east face and 16.7 ft from the west face reinforcing steel bar (as measured)

**Temp Sensor 4** – Ambient air temperature, installed outside the north face formwork (as measured)

**Temp Sensor 5** – 1.08 ft below temp Sensor 2, to monitor the temperature change along the vertical direction (as measured)

**Temp Sensor 6** – In the middle of the height and width, near the short lateral surface of the footing, to monitor temperature in another cross section, and installed 3 ft from the top-most reinforcing steel bar and 2.5 ft from the bottom-most reinforcing steel bar, 13.3 ft from the north face and 13.66 ft from the south face (as measured)

**Temp Sensor 7** – In the center, near the bottom surface of the footing, to investigate the effect of the subgrade temperature, and installed 1 ft from the bottom subgrade and 5.50 ft from the top temp Sensor 2 (as measured)

After the footing reinforcement cage and the stem reinforcement cage were placed on top of the steel bearing piles, the sensors were installed at their intended locations. After installation, exact locations of the sensors were measured as shown in Figure 5.8.

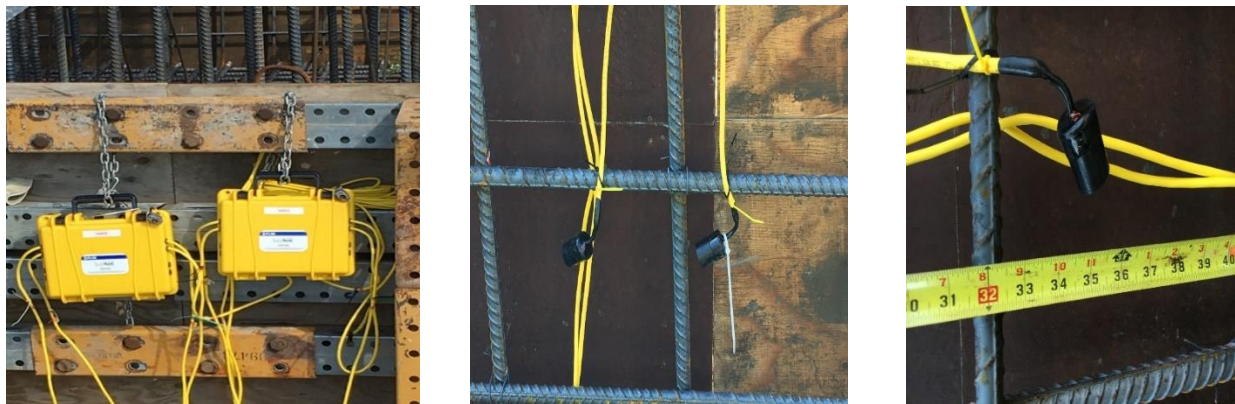


**Figure 5.8. Data loggers (left), primary and backup sensors (center), and measurement of sensor locations (right)**

The temperature data were recorded in 1-hour intervals and, as per the thermal control plan (TCP), the data were monitored remotely as well at 4-hour intervals for a period of 10 days from the day of concrete placement. The main sensor and backup sensors were marked with different colors, and different identification codes were assigned to them.

### *Thermal Control Plan*

According to the Iowa DOT Developmental Specifications for Mass Concrete-Control of Heat of Hydration (DS-15032 Effective Date October 20, 2015), the following limits apply to mass concrete placements:

- The concrete temperature at time of placement shall be between 40°F and 70°F.
- The maximum concrete temperature shall not exceed 160°F.
- The differential temperature between the centroid and a point 2 to 4 in. inside the surface along the shortest line from the centroid to the nearest surface or top surface of the element shall not exceed the limits of Table 5.1.
- Thermal control of each mass placement shall be maintained until the temperature of the interior is within 50°F of the average outside air temperature (determined by averaging the daily high and low temperatures over the preceding seven calendar days).

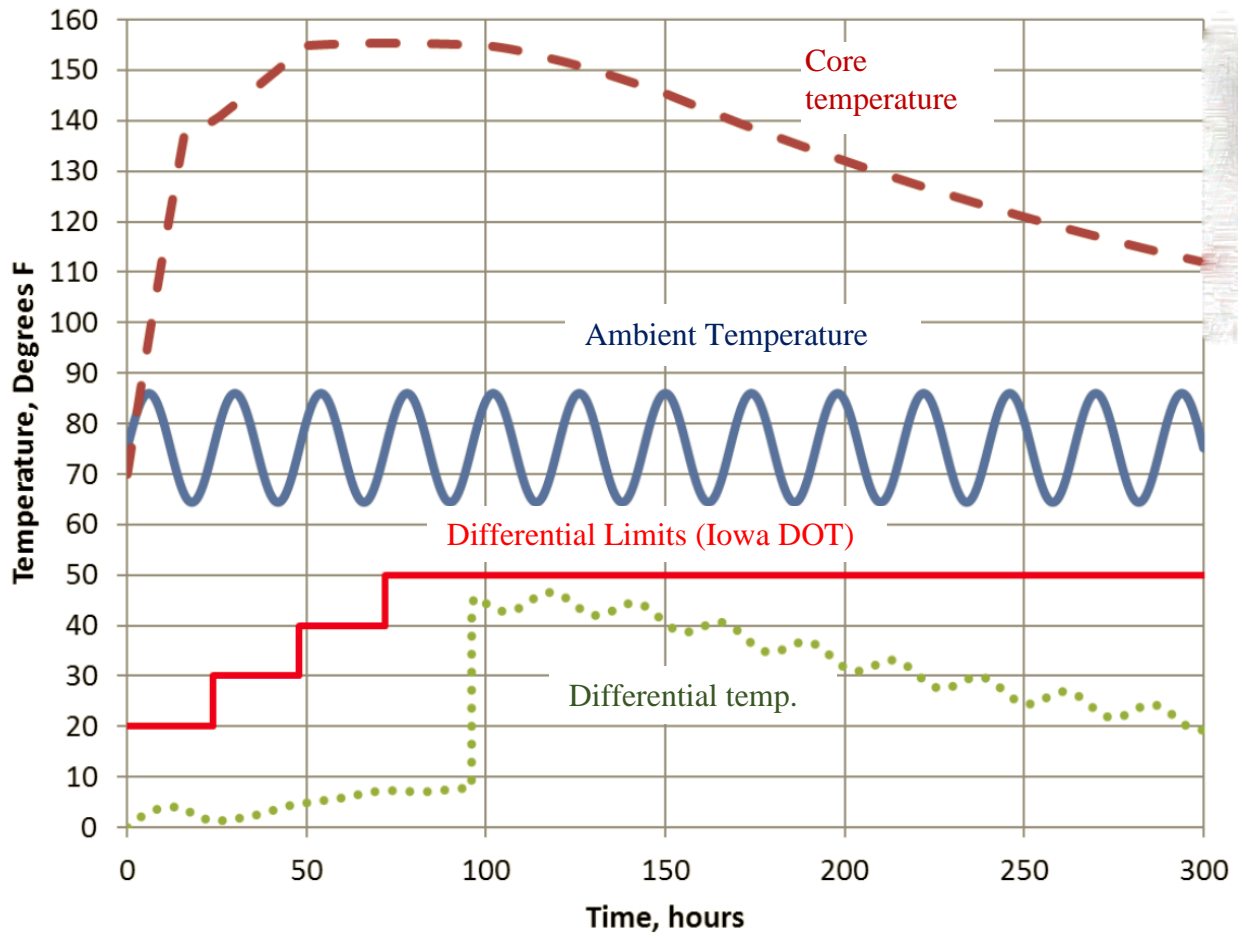
**Table 5.1. Iowa DOT maximum temperature differential limits**

| <b>Time<br/>(hours)</b> | <b>Maximum Temperature<br/>Differential (°F)</b> |
|-------------------------|--------------------------------------------------|
| 0–24                    | 20                                               |
| 24–48                   | 30                                               |
| 48–72                   | 40                                               |
| >72                     | 50                                               |

Beton Consulting Engineers, LLC (BCE) prepared the TCP for the Pier 4 footing. Their thermal model assumed the critical dimension of the member as 7 ft and the concrete temperature as it enters the formwork was assumed to be 70°F. The temperature development in the footing was predicted considering the average ambient temperature of 75°F as estimated by Accuweather for the month of June and July 2017.

The TCP suggested that the footing must be wrapped in insulating blankets for a minimum of 96 hours after concrete placement to keep the temperature differential under the specified limits. According to their thermal analysis, the maximum concrete temperature at the core was expected to reach approximately 155°F at approximately 50 hours after placement. As depicted in Figure 5.9, the temperature differential was predicted to reach its maximum of approximately 46°F at approximately 96 hours after the insulating blankets were removed.





Beton Consulting Engineers 2017

**Figure 5.9. Predicted maximum temperature at the core, ambient temperature, and temperature differential compared to Iowa DOT specified limits**

## Investigation during Placement of Concrete

### *Construction Process*

Given that weather conditions such as ambient temperature, relative humidity, and wind speed greatly affect the temperature development in mass concrete members, actual monitoring in real time is necessary to ensure that the maximum temperature and temperature differential are within specified limits. The concrete was placed on a day when the expected maximum temperature was 85°F. The weather conditions on the day of placement were recorded using a portable weather station installed at the job site.

The concrete mix supplied by Manatts Ready Mix Plant, Ames was placed using a pump mounted on a truck, and the concrete was compacted using needle vibrators at each individual placement layer (Figure 5.10).



**Figure 5.10. Pouring concrete using pump (left) and compaction using vibrator (right)**

Table 5.2 shows the mass concrete mixture proportion (C-4WR-F20) used for the Pier 4 footing.

**Table 5.2. Concrete mix proportion**

| Mixture Constituents        | Quantity(lb/yd <sup>3</sup> ) |
|-----------------------------|-------------------------------|
| Total Cementitious Content  | 593                           |
| Type I/II Cement            | 474                           |
| Class C Fly Ash             | 119                           |
| Fine Aggregate              | 1,500                         |
| Coarse Aggregate            | 1,517                         |
| Water                       | 255                           |
| Entrained Air (%)           | 6.0                           |
| Water-to-Cementitious Ratio | 0.43                          |

#### *Tests for Fresh Properties of Concrete*

On the day of the concrete placement for the Pier 4 footing, the research team first sent one 6×12 in. cylindrical specimen of the fresh concrete mix to the PCC laboratory for the semi-adiabatic calorimetry test. Approximately 40 minutes of time elapsed from when the concrete was collected from the mixing truck to the time it was placed into the semi-adiabatic calorimeter in the lab. The data recording was started as soon as the concrete was placed into the calorimeter.

The research team also tested the concrete mix for its fresh properties on the job site itself. Relevant ASTM International, Inc. standards were followed for measuring slump, air content, unit weight, and temperature of the fresh concrete. The measured values are shown in Table 5.3.

**Table 5.3. Fresh properties of Pier 4 footing concrete**

| <b>Fresh Property</b>             | <b>Measured Value</b> |
|-----------------------------------|-----------------------|
| Slump (in.)                       | 2.75                  |
| Air Content (%)                   | 7.5                   |
| Unit Weight (lb/ft <sup>3</sup> ) | 149.12                |
| Temperature (°F)                  | 63.6                  |

#### *Measured Weather Conditions*

Weather conditions such as ambient temperature and relative humidity have an important impact on the temperature development in a mass concrete member as well as on the hydration process of cementitious materials. It was important to monitor the weather conditions on the day of the placement of the concrete. For this purpose, a portable weather station was installed at the job site for recording the temperature, relative humidity, and wind speed. Figure 5.11 shows the installed weather station.



**Figure 5.11. Weather station at job site**

#### *Casting of Specimens at Job Site*

As planned, 40 cylindrical specimens of the field concrete mix were made at the job site by the team. The specimens were cast so that the following tests could be performed in the laboratory at various ages:

- Compressive strength – maturity tests
- Split tensile strength
- Elastic modulus
- Thermal conductivity
- Coefficient of thermal expansion

The cast specimens were left in the field to cure without demolding them; thus, the specimens experienced the same conditions as the footing placement. Figure 5.12 shows casting and curing the specimens in the field.



**Figure 5.12. Casting cylindrical specimens (left) and curing specimens in field conditions at the job site (right)**

iButton temperature sensors were inserted in two specimens to record the temperature development of the concrete, which was required for the compressive strength-maturity relationship. The tests for compressive strength were performed on the field-cured specimens at 1, 3, 7, 14, and 28 days. All other tests were performed in the PCC Laboratory on the 28-day-cured specimens.

### *Insulation*

To control the maximum temperature difference of the footing concrete placement, as per the TCP, the footing was insulated after concrete placement. The exterior of the formwork and the top face of the placement were wrapped with a black insulating blanket with a specified R value rating of 5 (Figure 5.13).



**Figure 5.13. Insulation blanket over formwork**

A 2 in. insulation blanket was also put on the bottom face formwork by the contractor.

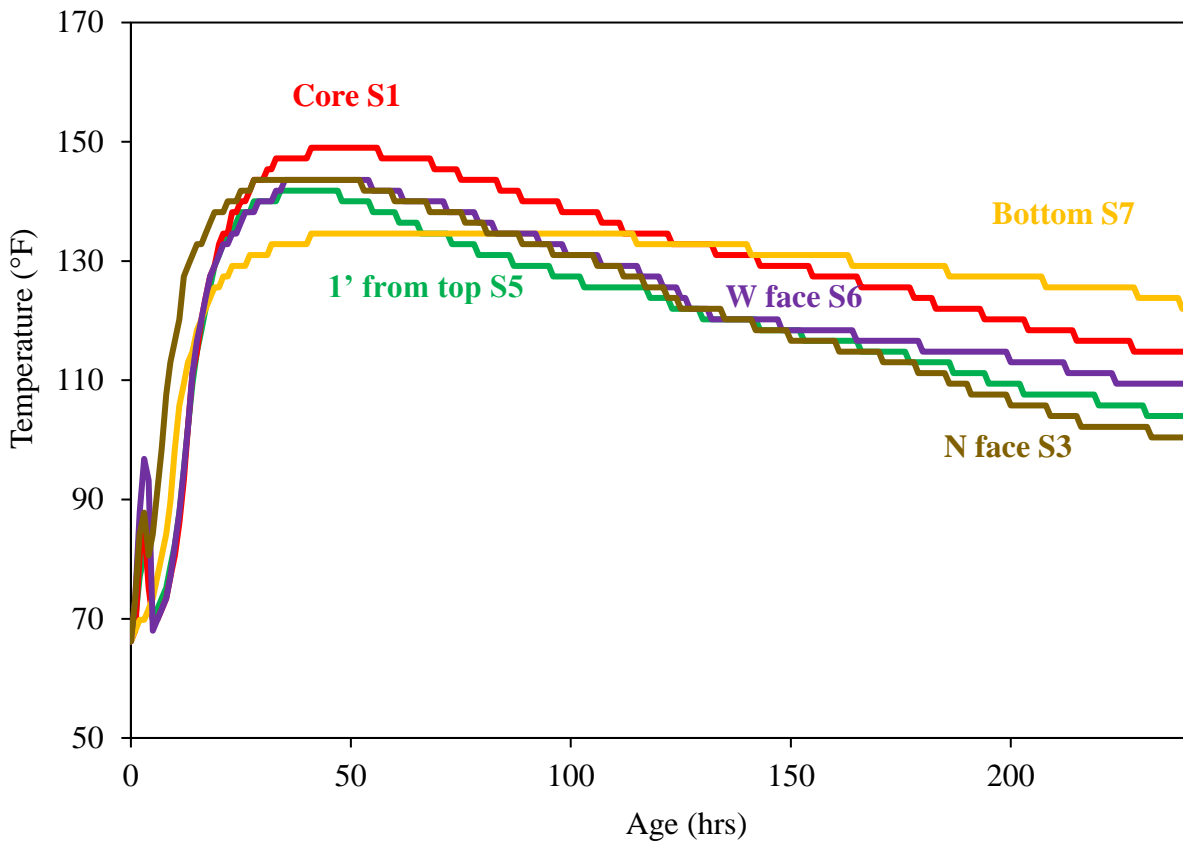
### *Collection of Materials for Laboratory Tests*

On the same day, specimens were cast and tests for fresh concrete properties were conducted at the job site. Then, materials required for casting one cubic yard of concrete in the laboratory were collected. As per the mix design used for the field concrete mix, the concrete constituent materials of cement, fly ash, aggregates, and chemical admixtures were collected from the Manatts Ready Mix Plant in Ames. The materials were the same as those used for the field concrete mix. Later, these materials were used in the laboratory to perform isothermal and semi-adiabatic calorimetry tests.

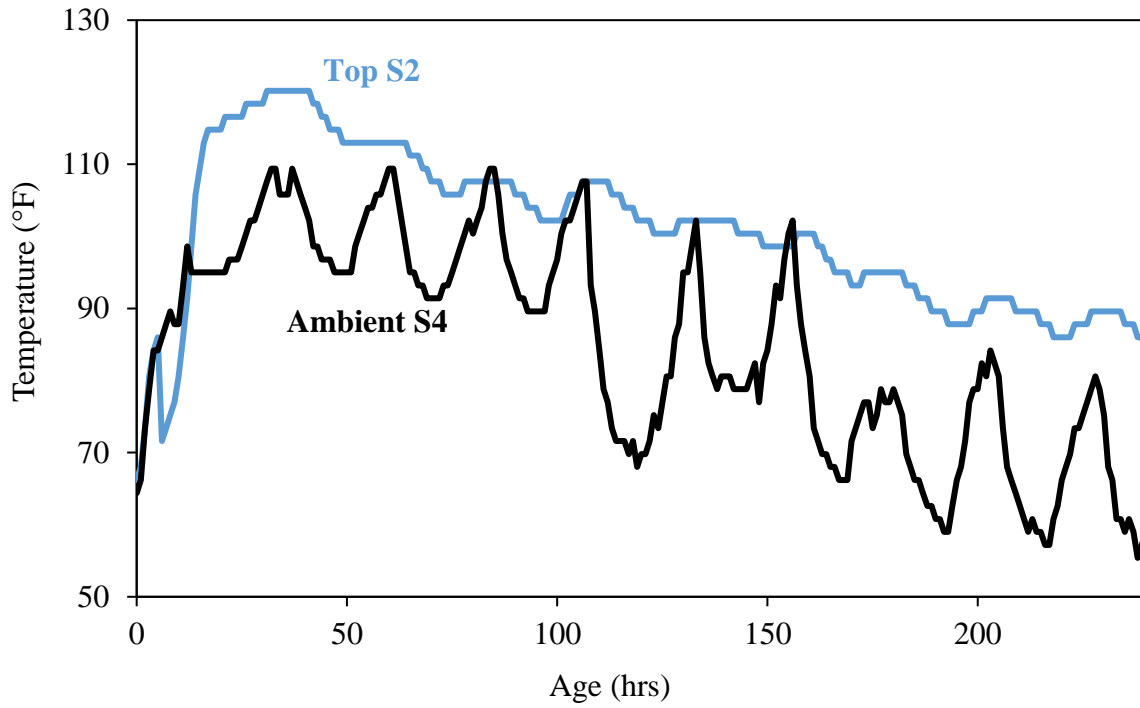
### **Investigation after Placement of Concrete**

#### *Monitoring of Sensors*

Immediately after placement of the concrete, the seven installed temperature sensors started logging the data, which was monitored remotely. After every 4-hour interval, the sensor data were sent via e-mail to the research team and analyzed. Figure 5.14 shows the plot of the temperature data of all of the sensors with time, while Figure 5.15 presents the differential temperatures along with the Iowa DOT limits for the differential temperature in early-age mass concrete.



Temperature data of core, bottom, side, and additional top sensors



Temperature data of top and air sensors

**Figure 5.14. Recorded temperature data of all sensors**

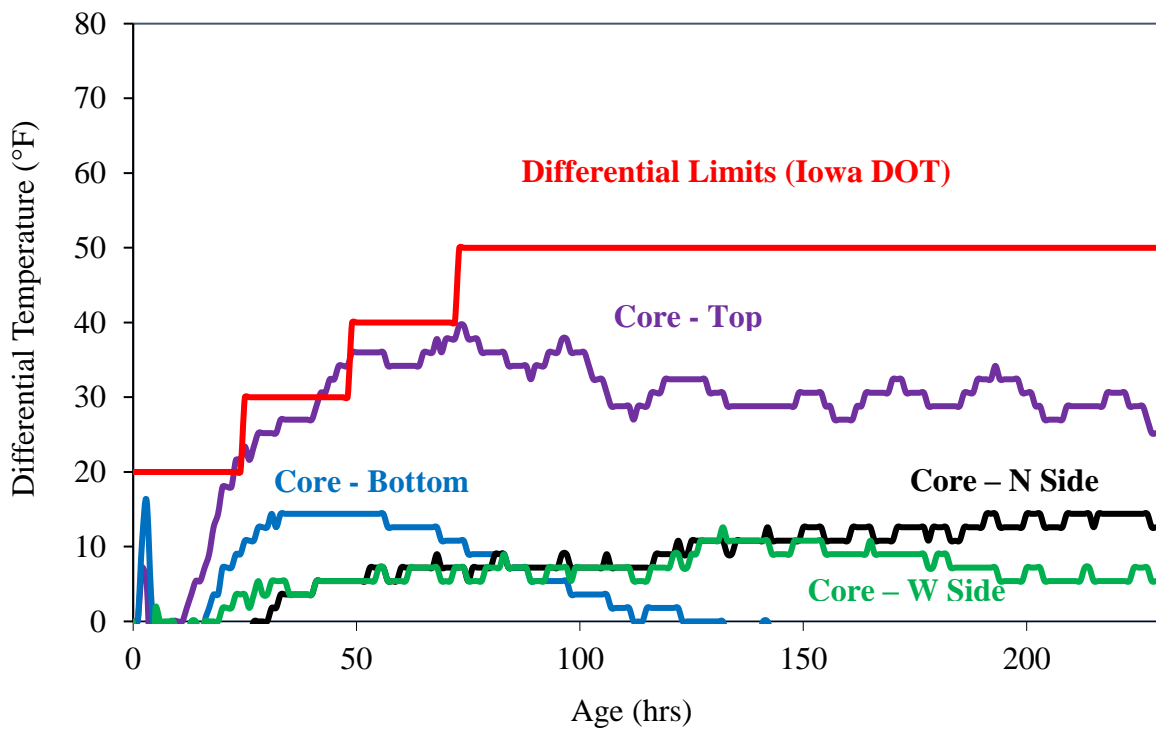


**Figure 5.15. Differential temperature in concrete footing with age**

Ten days after concrete placement, when all the formwork and insulation blankets were removed, the temperature logging was also stopped. Subsequently, the collected temperature data of 10 days at 1-hour intervals was analyzed collectively. As mentioned previously in this chapter under Thermal Control Plan, the Iowa DOT specifications and guidelines and the TCP provided by Beton Consulting Engineers were followed closely to determine the time of removal of the formwork and insulation.

After analyzing the data, the following observations were made by the research team:

- The concrete temperature at the time of placement was 66.2°F, which was within the specified limits of 40°F and 70°F.
- The maximum concrete temperature of 149°F was recorded at the core (Sensor 1) after 40.35 hours of concrete placement (Figure 5.14), as opposed to the predicted maximum value of 155°F. The specification requires the concrete temperature to be less than 160°F.
- As evident from the differential temperature plot in Figure 5.15, the differential temperature between the core and the north face as well as the west face sensors was found to be well within the specified limits. The differential temperature between the core and top sensors were observed to cross the specified limit only for a short duration from 44 to 48 hours. Barring this, the differential temperature was within the specified limits as presented previously in Table 5.1. As opposed to the predicted maximum temperature differential of 46°F, the maximum value was observed to be 39.6°F at 73.5 hours.

From the plot in Figure 5.14, the following observations can also be made:

- Of all the locations where sensors were installed, the temperature was the highest in the core (Sensor S1), and it reached a maximum of 149°F.
- The maximum value of the temperature recorded at the top (S2) was 120°F.
- There was no significant difference in the recorded temperature in the centers of the north side and west side faces (S3 and S6).

Table 5.4 summarizes the measured and predicted temperature values.

**Table 5.4. Comparison of measured and predicted temperature**

| Property                         | Measured            | Predicted                |
|----------------------------------|---------------------|--------------------------|
| Maximum Concrete Temperature     | 149°F @ 40.35 hours | 155°F @ approx. 50 hours |
| Maximum Temperature Differential | 39.6°F @ 73.5 hours | 46°F @ approx. 96 hours  |



### *Weather Conditions*

The temperature, relative humidity, and wind speed were recorded using a portable weather station on the day of the concrete placement. The weather fluctuations for 14 days after concrete placement until the formwork and insulation were removed were monitored from available online resources. The weather history database came from a weather station installed very near to the job site in Ames by the Weather Underground (<https://www.wunderground.com/>), and it was used to monitor the environmental conditions for the analysis period. The following data were monitored each day:

- Maximum and minimum temperature
- Maximum and minimum relative humidity
- Maximum wind speed
- Rain and/or thunderstorm

The monitored conditions are presented in Table 5.5, while Figure 5.16 shows the plots for the variation of temperature and relative humidity.

**Table 5.5. Weather conditions at Pier 4 site**

| Date      | Day | Temperature (°F) |     | Relative Humidity (%) |     | Max Wind Speed (mph) | Event        |
|-----------|-----|------------------|-----|-----------------------|-----|----------------------|--------------|
|           |     | Max              | Min | Max                   | Min |                      |              |
| 6/16/2017 | 0   | 87               | 64  | 93                    | 55  | 16                   | Rain         |
| 6/17/2017 | 1   | 83               | 64  | 100                   | 58  | 28                   |              |
| 6/18/2017 | 2   | 79               | 57  | 93                    | 43  | 24                   |              |
| 6/19/2017 | 3   | 81               | 57  | 93                    | 36  | 21                   |              |
| 6/20/2017 | 4   | 90               | 54  | 100                   | 24  | 24                   | Thunderstorm |
| 6/21/2017 | 5   | 87               | 61  | 93                    | 55  | 26                   |              |
| 6/22/2017 | 6   | 87               | 70  | 93                    | 51  | 26                   |              |
| 6/23/2017 | 7   | 76               | 59  | 100                   | 46  | 25                   |              |
| 6/24/2017 | 8   | 78               | 53  | 86                    | 24  | 28                   | Rain         |
| 6/25/2017 | 9   | 74               | 49  | 83                    | 33  | 25                   |              |
| 6/26/2017 | 10  | 74               | 48  | 100                   | 35  | 17                   |              |
| 6/27/2017 | 11  | 77               | 45  | 100                   | 41  | 20                   |              |
| 6/28/2017 | 12  | 84               | 65  | 93                    | 65  | 30                   |              |
| 6/29/2017 | 13  | 83               | 63  | 100                   | 58  | 26                   |              |

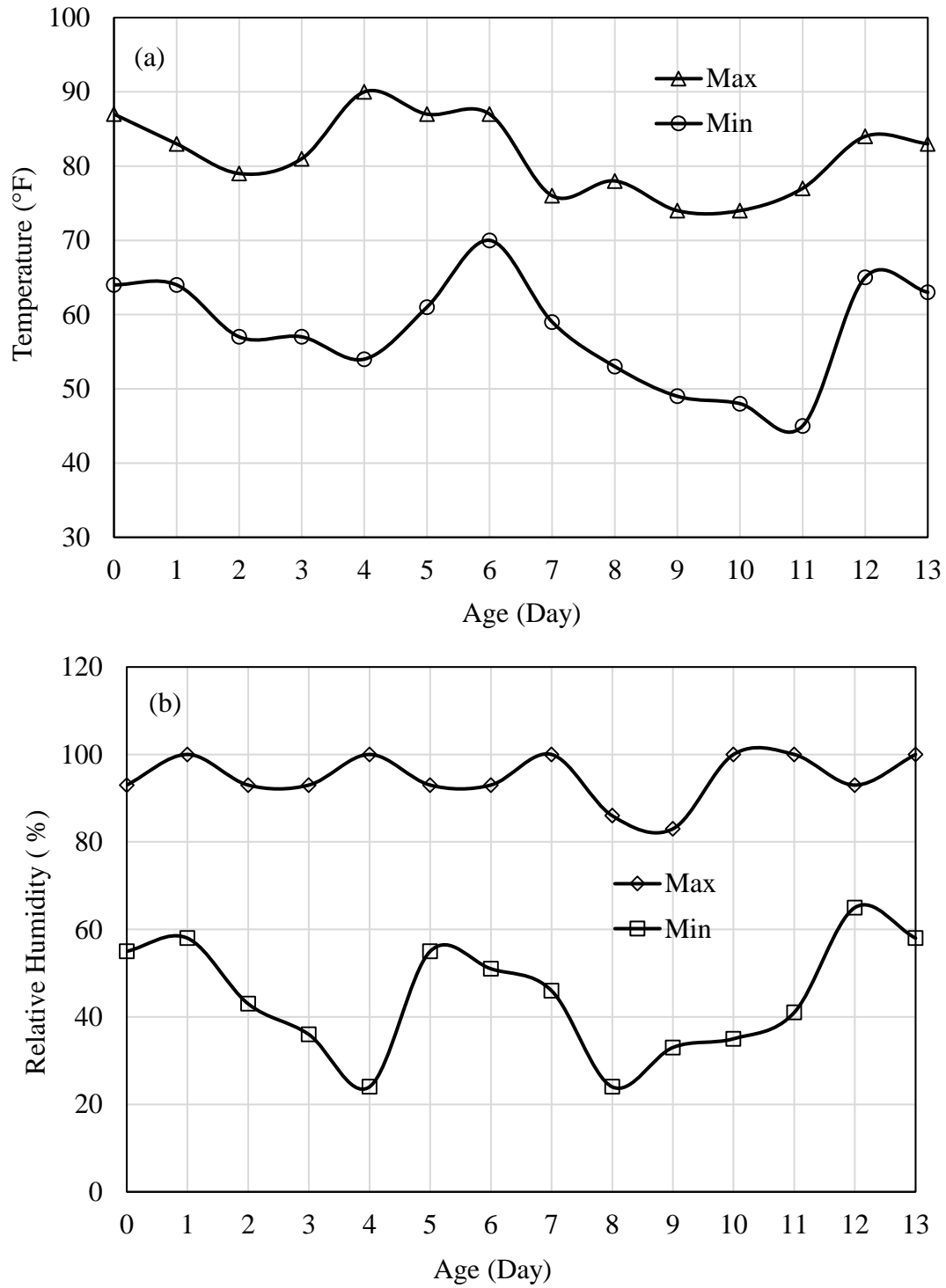


**Figure 5.16. Temperature (top) and relative humidity (bottom) variations with age**

### *Formwork and Insulation Removal*

The decision regarding when to remove the insulation blankets and formwork should be made based on the monitoring of temperature development in the mass concrete member. As discussed in the last section, the maximum temperature and the differential temperature were within specified limits. Therefore, the formwork was removed five days after placement of the concrete from three faces of the footing (all except the north side face since the temperature sensor data loggers were installed there). After formwork removal on the fifth day, the placement was again wrapped with the insulating blankets. Ten days after placement, the remaining formwork on the north side face was removed and the blankets from all of the faces including the top face was also removed. After visually observing the exposed concrete surface, no explicit cracks were visible on the surface. Two days after formwork and insulation removal, the concrete footing was backfilled using the excavated soil. Figure 5.17 shows the formwork and insulation removal from the footing.



**Figure 5.17. Insulation and formwork removal stage: Day 0 Insulation blanket (top left), Day 5. Formwork removed from three sides (top right), Day 10 Exposed concrete surface (bottom left), and Day 12 Footing backfilled with soil (bottom right)**

### *Laboratory Testing of Field-Cast Specimens*

As mentioned previously, on the day of concrete placement, concrete specimens were made and later cured in the field. Various tests were performed in the PCC Laboratory on these specimens. The following sections present the results of these tests.

#### Concrete Constituent Material Properties

The concrete mix contained cementitious materials, aggregates, water, and chemical admixtures. The cement and fly ash were analyzed using x-ray fluorescence (XRF) for their chemical and physical properties. The properties of coarse and fine aggregates like specific gravity, absorption, dry rodded unit weight (DRUW), fineness modulus (FM), etc. were tested in the laboratory. Table 5.6 shows the chemical composition of the cement and fly ash, and Table 5.7 presents the properties of the aggregate.

**Table 5.6. Cement and fly ash properties**

| <b>Material</b>     | <b>SiO<sub>2</sub></b> | <b>Al<sub>2</sub>O<sub>3</sub></b> | <b>Fe<sub>2</sub>O<sub>3</sub></b> | <b>CaO</b> | <b>MgO</b> | <b>SO<sub>3</sub></b> | <b>Na<sub>2</sub>O</b> | <b>K<sub>2</sub>O</b> | <b>Others</b> | <b>Ignition Loss</b> |
|---------------------|------------------------|------------------------------------|------------------------------------|------------|------------|-----------------------|------------------------|-----------------------|---------------|----------------------|
| Type I/II Cement, % | 20.44                  | 5.11                               | 3.27                               | 60.95      | 3.59       | 3.03                  | 0.18                   | 0.61                  | 1.52          | 1.96                 |
| Class C Fly Ash, %  | 33.76                  | 15.23                              | 6.3                                | 31.17      | 4.98       | 2.25                  | 1.35                   | 0.6                   | 4.93          | 0.57                 |

**Table 5.7. Aggregate properties**

| <b>Material</b>  | <b>Specific Gravity</b> | <b>Absorption, %</b> | <b>DRUW, lb/ft<sup>3</sup></b> | <b>Fineness Modulus</b> |
|------------------|-------------------------|----------------------|--------------------------------|-------------------------|
| Coarse Aggregate | 2.68                    | 0.82                 | 100.44                         | -                       |
| Fine Aggregate   | 2.65                    | 0.98                 | -                              | 2.85                    |

#### Compressive Strength – Maturity Relationship

The Nurse-Saul method was used for developing the compressive strength-maturity relationship. The datum temperature of -10°C was used. The test for compressive strength was conducted at 1, 3, 7, 14, and 28 days. The compressive strength was then plotted as a function of the calculated TTF. The compressive strength-maturity relationship for each mix was then developed by performing regression analysis to determine a best-fit equation to the data. The best-fit equation was found to be of the form where compressive strength is a linear function of the logarithm of the maturity index (in this case TTF). Figure 5.18 (left) shows the development of compressive strength with age while Figure 5.18 (right) shows the compressive strength – TTF plot along with the best-fit curve and the best-fit equation.

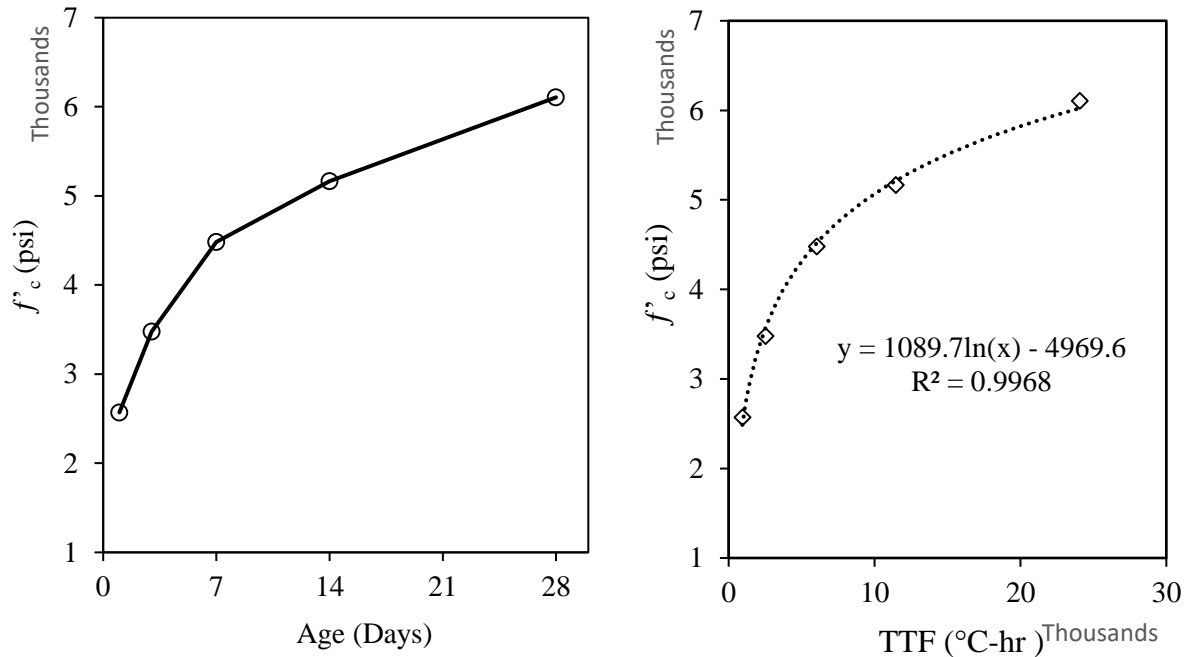


**Figure 5.18. Compressive strength development (left) and compressive strength-TTF curve (right)**

### Mechanical Properties

The tests for other mechanical properties of hardened concrete such as splitting tensile strength and elastic modulus of elasticity were performed on the 28-day cured specimens in the PCC Laboratory. The tests were performed as per relevant ASTM standards C496/496M and C469/469M. The mean split tensile strength was measured to be 521 psi while the mean elastic modulus of elasticity was  $6.4 \times 10^6$  psi. The values of the split tensile strength and elastic modulus of the four concrete mixes tested in the laboratory earlier were in the range of 530–603 psi and  $5.55 \times 10^6$ – $6 \times 10^6$  psi, respectively.

### Thermal Properties

The same test methods were followed to test the thermal properties of the field concrete mix as for the four concrete mixes tested in the laboratory earlier. The thermal conductivity test was performed as per the ASU cylindrical specimen method and the mean value was found to be 1.1 W/m-K with a 95% confidence interval of (1.04, 1.16) for the mean thermal conductivity. The thermal conductivity of the four concrete mixes tested in the laboratory earlier were in the range 1.1–1.2 W/m-K. Figure 5.19 shows the variation of temperature in the core and at the surface of the 4×6 in. cylindrical specimen during the test.

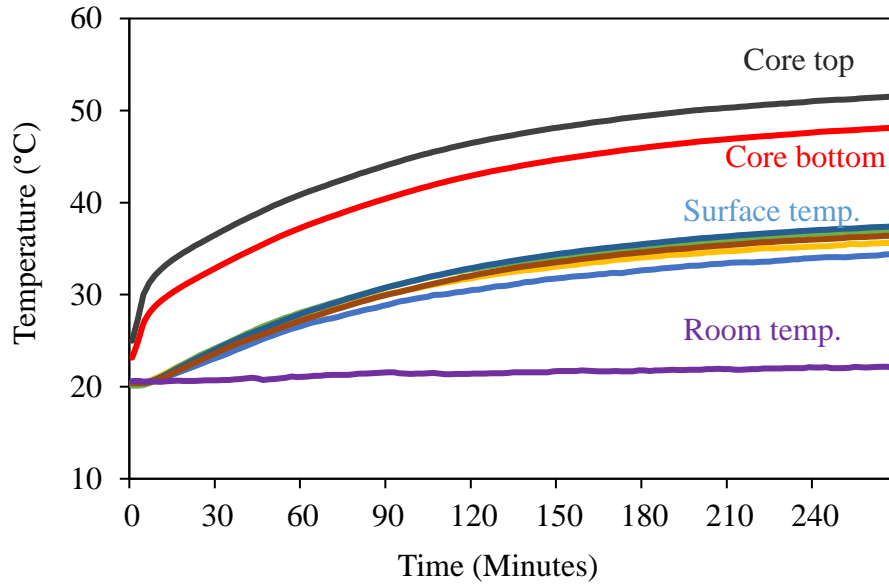


**Figure 5.19. Variation of temperature in thermal conductivity test**

The AASHTO TP 60-00 (2007) method was followed to test the coefficient of thermal expansion (CTE) of the field concrete mix. The mean CTE value was 7.06 microstrain/°C. The CTE values of the four concrete mixes tested in the laboratory earlier were in the range 7.19–9.07 microstrain/°C.

#### Isothermal Calorimetry

The cement paste specimens prepared as per the mix proportion of the field concrete mix, were tested at constant temperatures of 10, 20, 30, and 40°C, each, using the isothermal calorimeter. Figure 5.20 shows the rate of heat generation (mW/g) for the field mix tested using isothermal calorimetry.

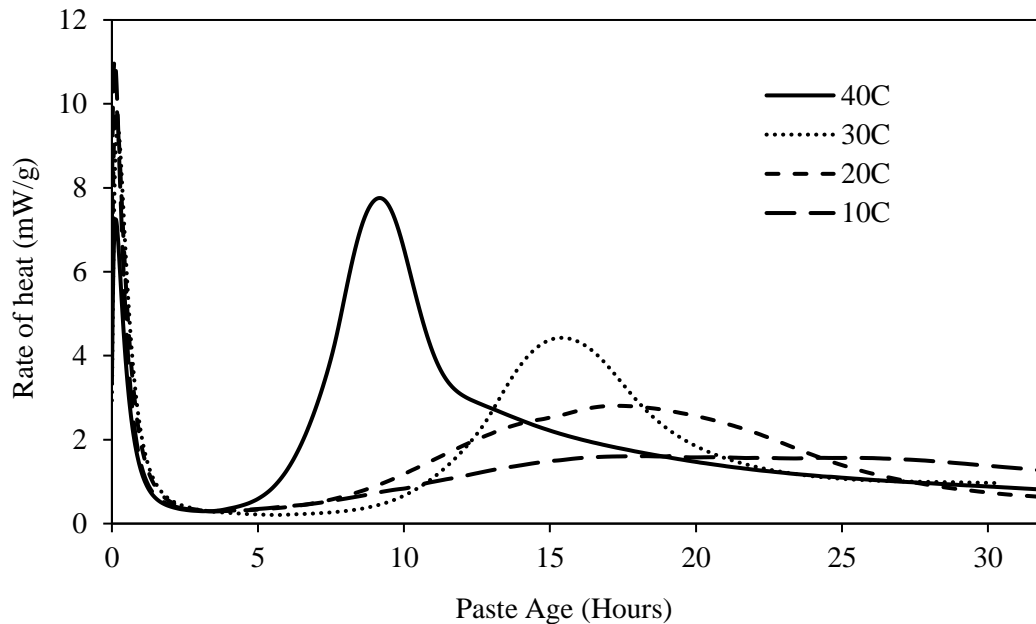


**Figure 5.20. Rate of heat generation at different temperatures**

The chemical composition of cement as presented in Table 5.6 was used to first calculate the Bogue values of  $C_3S$ ,  $C_2S$ ,  $C_3A$ , and  $C_4AF$ , and, then, the empirical relationships were applied to estimate the total heat available for the reaction. The hydration curve parameters and the apparent activation energy were then calculated according to the modified ASTM C1074 procedure as outlined in New Model for Estimating Apparent Activation Energy of Cementitious Systems by Riding et al 2011. The ultimate heat, curve parameters, and calculated apparent activation energy values are shown in Table 5.8.

**Table 5.8.  $H_u$ , Curve parameters and activation energy from isothermal calorimetry**

| Mixture                  | $H_u$ , J/Kg | Temp,<br>°C | $\alpha_u$ | $\beta$ | $\tau$ , hours | $R^2$ | Calculated<br>$E_a$ , J/mol |
|--------------------------|--------------|-------------|------------|---------|----------------|-------|-----------------------------|
| Field Mix<br>(I/II-20FA) | 4,72,296     | 10          | 0.990      | 0.862   | 45.620         | 0.992 | 32,643                      |
|                          |              | 20          |            |         | 29.122         | 0.853 |                             |
|                          |              | 30          |            |         | 28.394         | 0.996 |                             |
|                          |              | 40          |            |         | 10.362         | 0.829 |                             |

#### Semi-Adiabatic Calorimetry

The fresh concrete specimen collected from the job site on the day of the concrete placement for the Pier 4 footing was sent to the PCC Laboratory for the semi-adiabatic calorimetry test. However, since a substantial amount of time passed during this transit, the initial heat generation and consequent temperature change could not be recorded. Therefore, it was suggested by the research team to repeat the test in the laboratory. The test was performed again in the laboratory by mixing concrete using the materials collected from the ready-mix plant. The test data were

used to determine the best-fit hydration parameters,  $\alpha_u$ ,  $\beta$ , and  $\tau$ , as well as the true adiabatic temperature rise. Table 5.9 shows the best-fit hydration parameters.

**Table 5. 9. Hydration parameters from semi-adiabatic calorimetry**

| Mixture                  | $H_u$ , J/Kg | $E_a$ , J/mol | $\alpha_u$ | $\beta$ | $\tau$ , hrs | $R^2$ |
|--------------------------|--------------|---------------|------------|---------|--------------|-------|
| Field Mix<br>(I/II-20FA) | 472,296      | 32,643        | 0.748      | 0.840   | 20.006       | 0.994 |

Figure 5.21 shows the measured semi-adiabatic and calculated true adiabatic temperature from the field as well as the laboratory specimens of the field concrete mix.

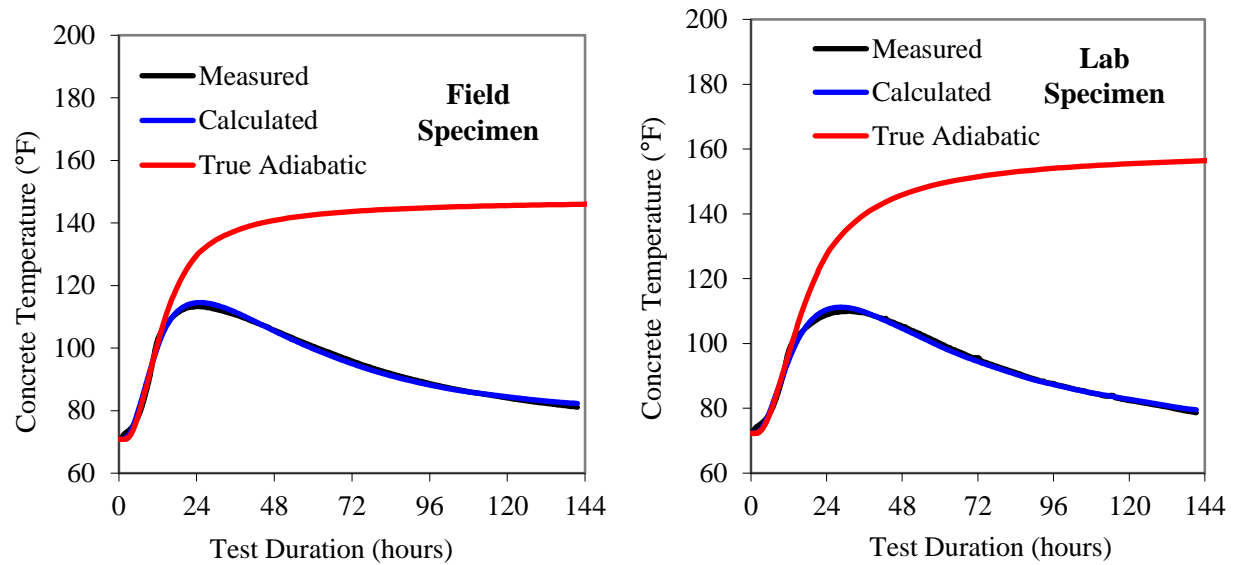


**Figure 5.21. Measured semi-adiabatic and calculated true adiabatic temperature for field specimen (left) and laboratory specimen (right)**

It can be deduced from the plots that the adiabatic temperature rise of the concrete mix is lower for the field specimen as compared to that of the specimen prepared in the laboratory. The maximum adiabatic temperature rise was found to be closer to the measured one in the laboratory mixed specimen.



## 6. CONCRETEWORKS MODIFICATIONS

ConcreteWorks version 2.1.0 was reviewed in Task 1 and a few parameters were identified that were required to be modified. Based on the results from the laboratory tests on four concrete mixes and from the observations made during the field investigation, several other modifications were also recommended by the research team. Modifications were made accordingly in the program and are discussed in the sections that follow. Relevant screenshots from the software are also presented.

### Modifications in Input

The modifications made in the input are as follows:

1. As identified during the initial review, the earlier version of the software had an upper limit of 14 days for the thermal analysis duration. The analysis duration in the new version was increased to 30 days as shown in the Figure 6.1.

**General Inputs**

Units  
☐ Metric ☒ English

Chloride Units Percent of Concrete

Project Time and Date  
Placement Time 7 am  
Placement Date

June 2017

| Sun | Mon | Tue | Wed | Thu | Fri | Sat |
|-----|-----|-----|-----|-----|-----|-----|
| 28  | 29  | 30  | 31  | 1   | 2   | 3   |
| 4   | 5   | 6   | 7   | 8   | 9   | 10  |
| 11  | 12  | 13  | 14  | 15  | 16  | 17  |
| 18  | 19  | 20  | 21  | 22  | 23  | 24  |
| 25  | 26  | 27  | 28  | 29  | 30  | 1   |
| 2   | 3   | 4   | 5   | 6   | 7   | 8   |

Today: 8/15/2018

Analysis Setup  
Temperature Analysis Duration (days) 30  
Life Cycle Analysis Duration (Years) 20

**Figure 6.1. Analysis duration increased to 30 days**

The software provides the user with an option to increase the duration even further than 30 days if required.

2. Only four cities in Iowa—Des Moines, Waterloo, Mason City, and Sioux City—were available to select for the project location in the earlier version. As the new modified version is expected to be used in mass concrete construction projects throughout Iowa, weather data of four additional major cities were included. The cities added were Ames, Cedar Rapids, Davenport, and Burlington. The screenshot from the new version is shown in Figure 6.2.

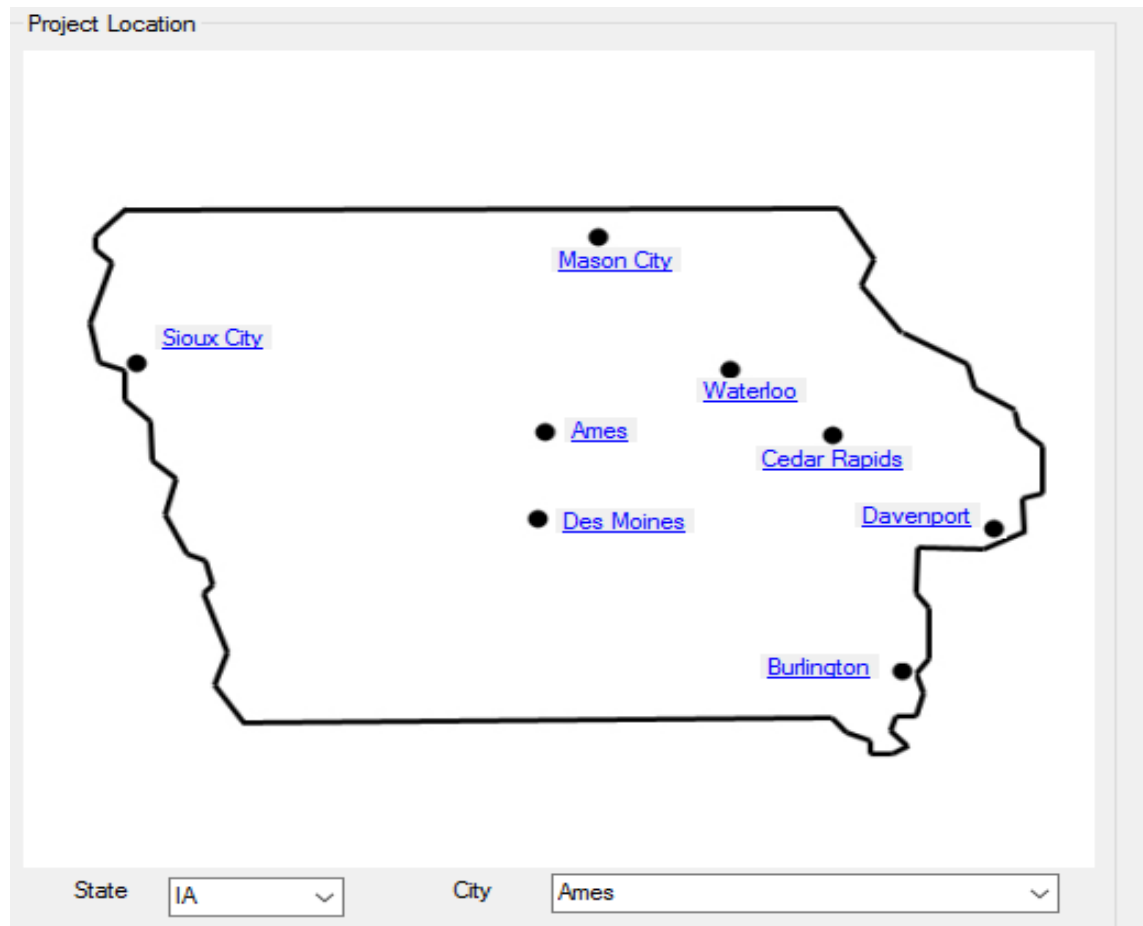


**Figure 6.2. Four new Iowa cities incorporated into ConcreteWorks**

Thirty years of climate data from the Modern-Era Retrospective analysis for Research and Applications (MERRA) climate data for Mechanistic-Empirical Pavement Design Guide (MEPDG) inputs, which were developed by the Federal Highway Administration (FHWA), were used for inclusion into ConcreteWorks. When the software is used at project locations other than the eight Iowa cities, the climate data can be entered manually.

- The earlier ConcreteWorks version had the option of only two-dimensional (2D) and three-dimensional (3D) analysis for rectangular footings. The one-dimensional analysis option was also included in the new version, as shown in the Figure 6.3.

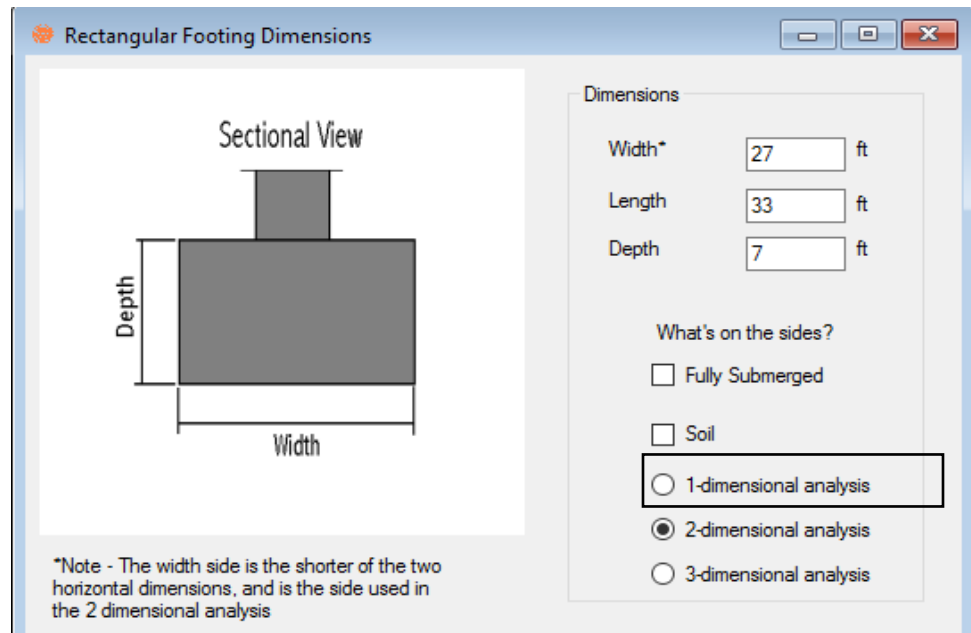


**Figure 6.3. One-dimensional analysis added to ConcreteWorks**

- Based on the results of the tests conducted on four commonly used concrete mixes in Iowa, the default values of the material properties were changed in the new version of the software. These properties included cement chemical/physical properties, hydration calculation properties, and thermal properties, as shown in Figure 6.4 and Figure 6.5.

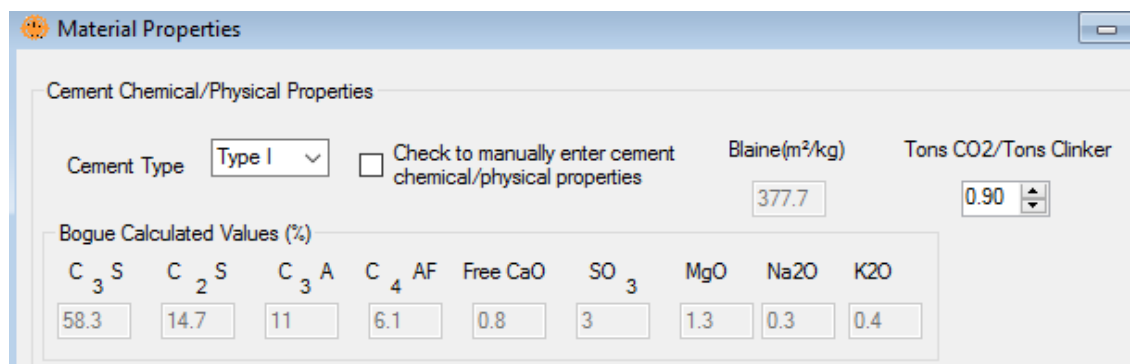
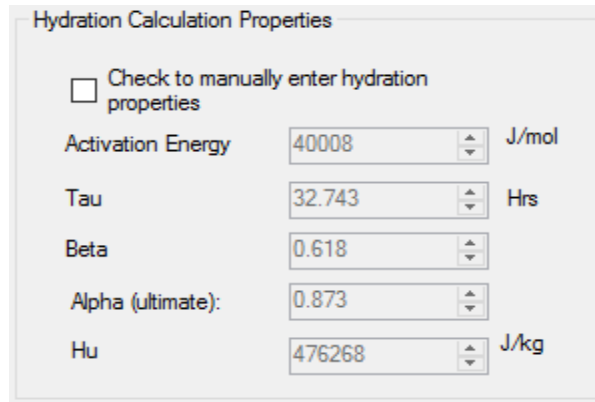


**Figure 6.4. Default cement chemical/physical properties in new ConcreteWorks**



Hydration Calculation Properties

☐ Check to manually enter hydration properties

Activation Energy: 40008 J/mol

Tau: 32.743 Hrs

Beta: 0.618

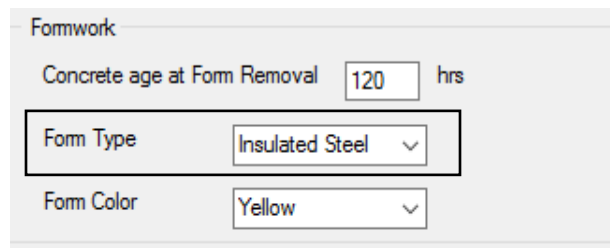
Alpha (ultimate): 0.873

Hu: 476268 J/kg

**Figure 6.5. Default hydration parameters in new ConcreteWorks**

The software also has the option to manually enter the material properties. The default values of concrete thermal conductivity and combined aggregate specific heat were not changed. Although thermal conductivity of all concrete mixes was measured, the values obtained were less than (in the range of 1.1–1.2 W/m-K) the default value in the earlier version (2.7 W/m-K). The thermal analysis of the field project using the earlier ConcreteWorks version had shown that the analysis performed using the default value of thermal conductivity results in temperature profiles closer to that measured at the job site than using the laboratory-measured value of thermal conductivity. Therefore, it was decided by the research team to keep the thermal conductivity value the same as that in the earlier version.

5. During one of the quarterly team meetings, it was pointed out by the TAC that the earlier version of ConcreteWorks had the option of selecting only wood or steel as the type of formwork used in the rectangular concrete footing. In some projects, nowadays, insulated steel formwork is also used to insulate the footing. Therefore, this was also added as one of the form types in the new modified version, as shown in the Figure 6.6.



Formwork

Concrete age at Form Removal: 120 hrs

Form Type: Insulated Steel

Form Color: Yellow

**Figure 6.6. Insulated steel formwork added to new ConcreteWorks**

6. For modeling the heat dissipation and development in a mass concrete member, the boundary conditions and insulation R-value are also required. R-value is the ratio of the thickness of the insulation and its thermal conductivity. The earlier version of ConcreteWorks had the option of entering the R-value of only the insulation blanket. As the insulated steel formwork option was added, its R-value was also required to be added. Hence, the new version has a default form insulation R-value (as shown in Figure 6.7).

| Insulation R-Value                                               |      |                           |
|------------------------------------------------------------------|------|---------------------------|
| Blanket R-Value<br>(Thickness / Thermal<br>Conductivity)         | 0.50 | hr-ft <sup>2</sup> °F/BTU |
| Form Insulation R-Value<br>(Thickness / Thermal<br>Conductivity) | 2.91 | hr-ft <sup>2</sup> °F/BTU |

**Figure 6.7. Insulated formwork R-value**

A value different from the default can also be entered manually by the user.

- The measured temperature data from the I-35 NB to US 30 WB bridge footing investigation was analyzed and compared to the thermal analysis results from the earlier ConcreteWorks version. One of the very important outcomes of this comparison was the requirement for a model to be incorporated in ConcreteWorks to predict the initial temperature of the soil beneath the footing. As the bottom face of the mass concrete member (i.e., the footing) is not covered by an insulating blanket or formwork, the temperature of soil beneath the footing affects the heat development and dissipation within the footing. The earlier ConcreteWorks version required the user to enter the soil temperature, which was a constant value. A new model that calculates the initial soil temperature profile based on weather data was included in the modified version of ConcreteWorks. This model is the one proposed by Barber (1957) in his work on the calculation of maximum pavement temperatures from weather reports. The mathematical equations used in the model are as follows.

$$T(z) = T_m + T_v \cdot \left( \frac{H \cdot \exp(-z \cdot C)}{\sqrt{(H+C)^2 + C^2}} \right) \cdot \sin \left( 0.262 \cdot t - z \cdot C - \arctan \frac{C}{H+C} \right)$$

$$T_m = 0.5 \cdot T_A + (0.0498 \cdot L) \quad \text{for } T \geq T_A$$

$$T_m = 0.5 \cdot T_A + 0.278 \cdot (0.0498 \cdot L) \quad \text{for } T < T_A$$

$$T_v = 0.5 \cdot T_R + 1.67 \cdot (0.0498 \cdot L) \quad \text{for } T \geq T_A$$

$$T_v = 0.5 \cdot T_R \quad \text{for } T < T_A$$

$$H = \left( \frac{4.1 + 1.13 \cdot w^{0.75}}{k} \right) \quad C = \left( \frac{k}{c_p \cdot \rho} \right)$$

Where,  $T(z)$ =soil temperature (°C) at depth  $z(m)$ ,  $T_A$ =mean air temperature (°C),  $L$ =solar radiation ( $W/m^2$ ),  $T_R$ =maximum daily temperature minus the minimum daily temperature (°C),  $w$ =wind speed (m/s),  $k$ =soil thermal conductivity ( $W/m^2$ ),  $C$ =soil thermal diffusivity calculated ( $m^2/s$ ),  $c_p$ =soil specific heat ( $J/kg/°C$ ),  $\rho$ =soil density ( $kg/m^3$ ), and  $t$ =time from the beginning of the temperature cycle (hours).

Figure 6.8 shows how the new soil temperature model is incorporated in ConcreteWorks.

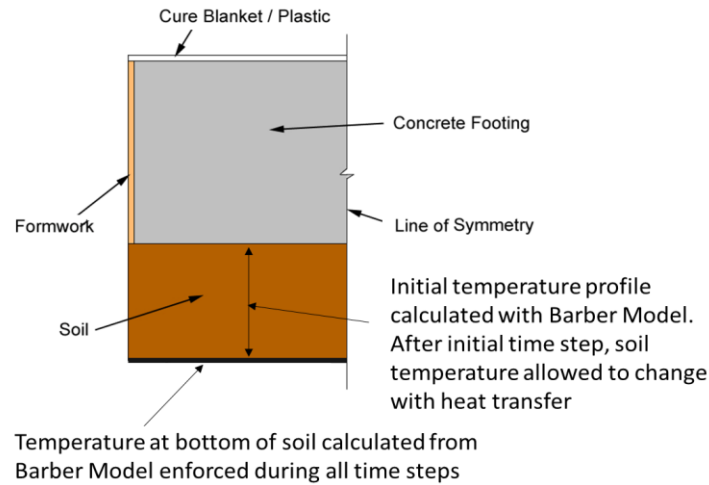


**Figure 6.8. New soil temperature calculation model incorporated into ConcreteWorks**

Using the Barber model, the initial temperature profile is calculated considering the weather data of the project location. After the initial time step, soil temperature is then allowed to change with heat transfer at all time steps. The thermal analysis of the I-35 NB to US 30 WB bridge footing that was performed using the new modified version of ConcreteWorks (presented in Chapter 7) showed results better than the one that was performed without the soil temperature model.

## Modifications in Output

The modifications made in the ConcreteWorks output are as follows.

1. The initial version of ConcreteWorks was developed for use by the Texas DOT (TxDOT) and, hence, the TxDOT mass concrete specifications were used to compare the outputs. Since the new version is going to be used in Iowa, the Iowa DOT mass concrete specifications were added in the modified version of the software. This newly added feature is shown in Figure 6.9 and Figure 6.10.

| Parameter                                 | Value    | Units              |
|-------------------------------------------|----------|--------------------|
| <b>Results</b>                            |          |                    |
| Iowa 2018 Specifications Used             |          |                    |
| Iowa DOT temperature limits               | exceeded |                    |
| Max Temperature                           | 140      | °F                 |
| Original Concrete Materials CO2 emissions | 271      | lb/yd <sup>3</sup> |

**Figure 6.9. Iowa DOT mass concrete temperature differential limits shown in the output**

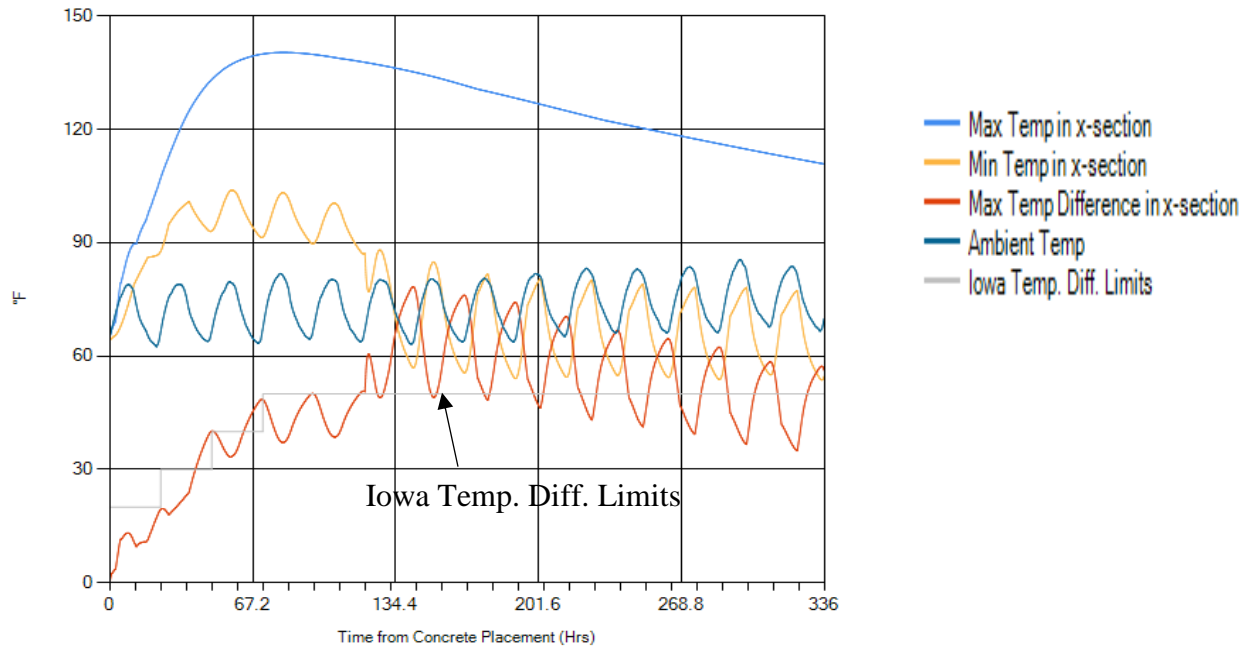


**Figure 6.10. Iowa DOT mass concrete temperature differential limits incorporated into new ConcreteWorks**

Using the Barber model, the initial temperature profile is calculated considering the weather data from the project location. After the initial time step, soil temperature is then allowed to change with heat transfer at all time steps. The thermal analysis of the I-35 NB to US 30 WB bridge footing that was performed using the new modified version of ConcreteWorks (presented in Chapter 7) showed results better than the one that was performed without the soil temperature model.

2. In the initial phase of this project (Task 1), it was observed that in order to analyze the temperature profile at points within the concrete member where thermocouples are installed, these points had to be selected on the sectional view in ConcreteWorks. Accurate locations of thermocouples could not be entered in the earlier version, as shown in Figure 6.11.

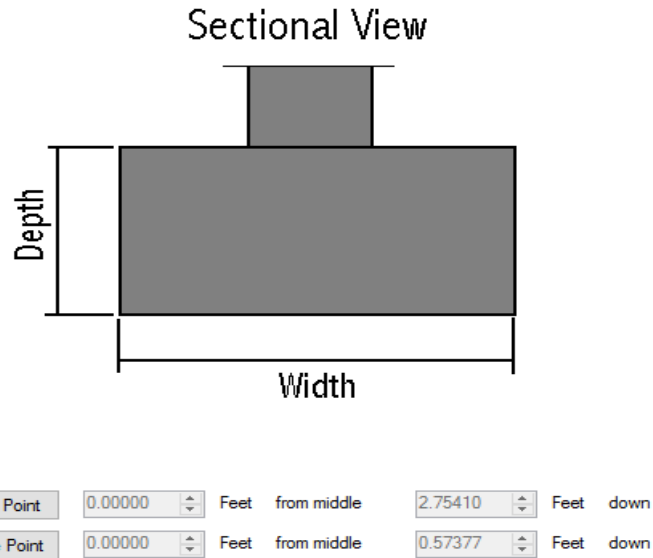


**Figure 6.11. Thermocouple locations in the old ConcreteWorks**

The modified version of the software gives the user the option of two methods for specifying the position for thermocouple point selection. The user can either click on the location on the computer screen or manually enter the location coordinates of the thermocouples. The new feature is shown in Figure 6.12.

Point Selection Method

☐ Click on Position ☒ Enter Position

**Figure 6.12. Thermocouple locations picked by exact position in new ConcreteWorks**

Getting the exact temperature profile of thermocouple points could be very helpful in comparing the maximum temperature and temperature differential predictions with those of measured ones.



## 7. THERMAL ANALYSIS USING CONCRETEWORKS AND 4C

As discussed in Chapter 6, the ConcreteWorks software was modified based on the test results obtained from laboratory and field mixes. Since the measured data from the I-35 NB to US 30 WB bridge footing investigation were available, the earlier and new modified versions of ConcreteWorks, as well as from 4C-Temp&Stress, were then used to conduct the thermal analysis. For comparison purposes, the input values in 4C were also kept the same as those in the modified ConcreteWorks. This chapter presents the results from the analysis of the field and laboratory mixes using all three programs.

### Analysis of the Field Mix

The mass concrete member shape, mix proportions, material properties, environmental, and construction parameters from the I-35 NB to US 30 WB bridge footing investigation were input into the three programs—old ConcreteWorks, new ConcreteWorks, and 4C—and the outputs were analyzed and compared. Figure 7.1 presents a screenshot of the input values for the analysis of the field mix from the modified ConcreteWorks.

The following sub-sections discuss the various output parameters including maximum temperature, differential temperature, cracking probability, etc. These parameters are also compared to their corresponding field-measured values.

#### *Maximum Temperature*

The maximum in-place temperature reached inside a mass concrete member can affect the long-term performance of a structure (Riding et al. 2006). The conditions at the core of a mass concrete member (a rectangular footing in this case) can be almost fully adiabatic for a few days. The heat generated, due to the exothermic hydration reaction of cementitious materials and water, is not dissipated easily. It is due to this reason that the temperature at the core of the member is found to be maximum. Figure 7.2 shows the maximum temperature output from the three programs. Also shown is the measured maximum temperature in the rectangular footing for the same set of the member, boundary, environmental, and construction conditions. Table 7.1 presents the comparison of the predicted values of maximum temperature and the time to reach maximum temperature with those of field-measured values.

**Table 7.1. Comparison of measured and predicted concrete temperature for field mix**

| <b>Property</b>             | <b>Max Concrete Temperature (°F)</b> | <b>Time to reach Max Temperature (hrs)</b> |
|-----------------------------|--------------------------------------|--------------------------------------------|
| Field Measured              | 149.00                               | 50                                         |
| ConcreteWorks Predicted-Old | 152.91                               | 46                                         |
| ConcreteWorks Predicted-New | 149.16                               | 52                                         |
| 4C Predicted                | 150.46                               | 65                                         |

Input Check

Parameter

Value

Units

General Inputs

Project Location

Unit System

Chloride Units

Life Cycle Analysis Duration

Analysis Duration

Concrete placement time

Concrete placement date

Member Inputs

Shape Choice

Member width

Member length

Member depth

Type of Analysis

Mixture Proportions

Cement Content

C Fly Ash Content

Water Content

Coarse Aggregate Content

Fine Aggregate Content

Air Content

Chemical Admixture ASTM C494

Material Properties

Cement Type

Cement Chemistry Values

Hydration Parameter Values

Coarse Agg. type

Fine Agg. type

Coarse Agg. type

Des Moines

English

Percent of Concrete

20

14

8

6/16/2017

Rect. footing

27

33

7

2-d

474

119

255

1522

1500

7.5

Type A, NRWR

I/II

Default

Default

Limestone

Siliceous River Sand

Limestone

Years

days

am

ft

ft

ft

lb/yd<sup>3</sup>

lb/yd<sup>3</sup>

lb/yd<sup>3</sup>

lb/yd<sup>3</sup>

lb/yd<sup>3</sup>

%

Parameter

Value

Units

Environment Inputs Summary

Ave. Daily Max Temp.

Ave. Daily Min Temp.

Ave. Max Daily Solar Radiation

Ave. Max Daily Wind Speed

Ave. Max Relative Humidity

Ave. Min Relative Humidity

Construction Inputs

Concrete Fresh Temperature

Blanket R-Value

Forms are stripped after

Form Color

Form Type

Side Cure Method

Delay between stripping and curing

Soil temperature

Footing Subbase

Time of top cure blanket placement

Footing top cure method used

Footing top cure method used

Corrosion Inputs

Steel Type

Steel Cover

Dref

81.5

58

731.1

24.1

95.1

45

67.5

0.5

120

Natural Wood

Wood

Black Plastic

1

80

Limestone

5

Wet blanket

Black Plastic

Black Steel

2

1

°F

°F

W/m<sup>2</sup>

m/s

%

%

°F

°F

hrs

Wood

Black Plastic

hrs

°F

hrs

Black Steel

x 10<sup>-4</sup>

Default values are indicated by green

Questionable input values are indicated by red

Back

Calculate Temperatures

Figure 7.1. Input data in the new ConcreteWorks (field mix)

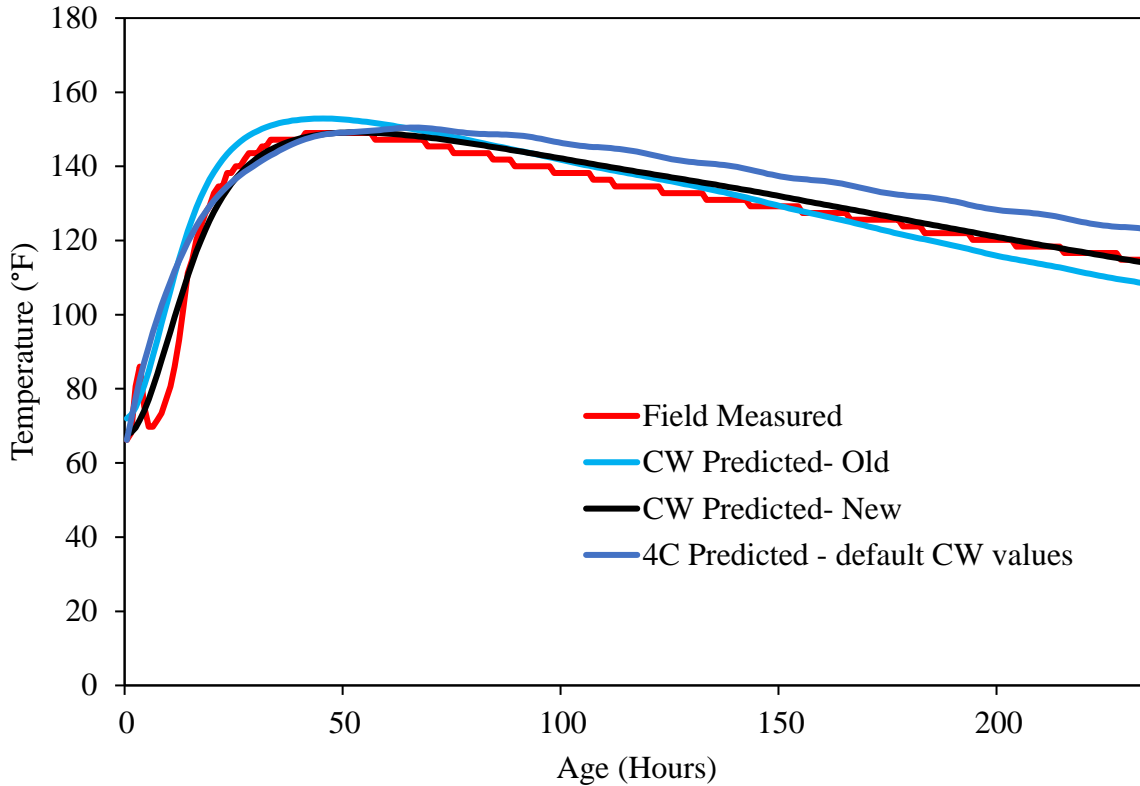


**Figure 7.2. Maximum temperature comparisons for field mix**

From Figure 7.2 and the values shown in Table 7.1, the following observations can be made:

1. The maximum temperature predicted by the new modified version of ConcreteWorks (149.16°F) is the closest of all three to the field-measured value (149°F). As the default values of material properties in the new ConcreteWorks were all set according to the measured values, the complete temperature development profile of the rectangular footing, including the maximum temperature, is very well predicted by the new ConcreteWorks version.
2. To plan the control of thermal cracking in advance of the start of the construction of a mass concrete member, it is very helpful if the time to reach the maximum temperature is known in addition to the maximum temperature. As observed from the output results, the new ConcreteWorks prediction of the time to reach the maximum temperature (52 hours) is also close to that of the field-measured value (50 hours).
3. The 4C predicted values of both the maximum temperature and the time to reach the maximum temperature (150.46°F and 65 hours) are more than the corresponding measured values, although still close. Also, as can be seen in Figure 7.2, the rate of cooling after reaching the peak as predicted by 4C is less than ConcreteWorks predicted as well as the measured rate of cooling. This can be due to the fact that, unlike ConcreteWorks, the 4C software does not have the option to enter specific material properties of a concrete mix such

as the type of mineral admixture used, the chemical/physical properties of cementitious materials, etc.

#### *Temperature at Thermocouple Locations*

Seven sets of intelliRock temperature sensors were installed in the rectangular footing before the concrete placement (as discussed in Chapter 5). The sensors were installed to monitor the temperature development at seven designated locations on the footing and take relevant measures for its thermal crack control. The locations analyzed within the rectangular footing were core, top, 1 ft from the top, bottom, north face, and south face. The seventh sensor was placed outside the footing to measure the ambient temperature.

Usually, in rectangular footings, which qualify as mass concrete, only three locations are critical from the perspective of thermal cracking. These locations are core, top, and the center of the face at the smallest distance from the core of the member. For the purpose of refining the prediction model in ConcreteWorks, the temperatures at additional locations such as 1 ft from the top, bottom, and the center of the face at the largest distance from the core were also analyzed.

One of the most important features in ConcreteWorks is that it provides the user with an option to get the temperature development profile of any point within the mass concrete member. The finite element mesh in 4C can also be used to analyze the same. The three computer programs were used to obtain the temperature profile at all of the locations where the sensors were installed and the outputs were then compared with the measured values. The comparison charts of the temperature profiles at all sensor locations are shown in Figure 7.3.

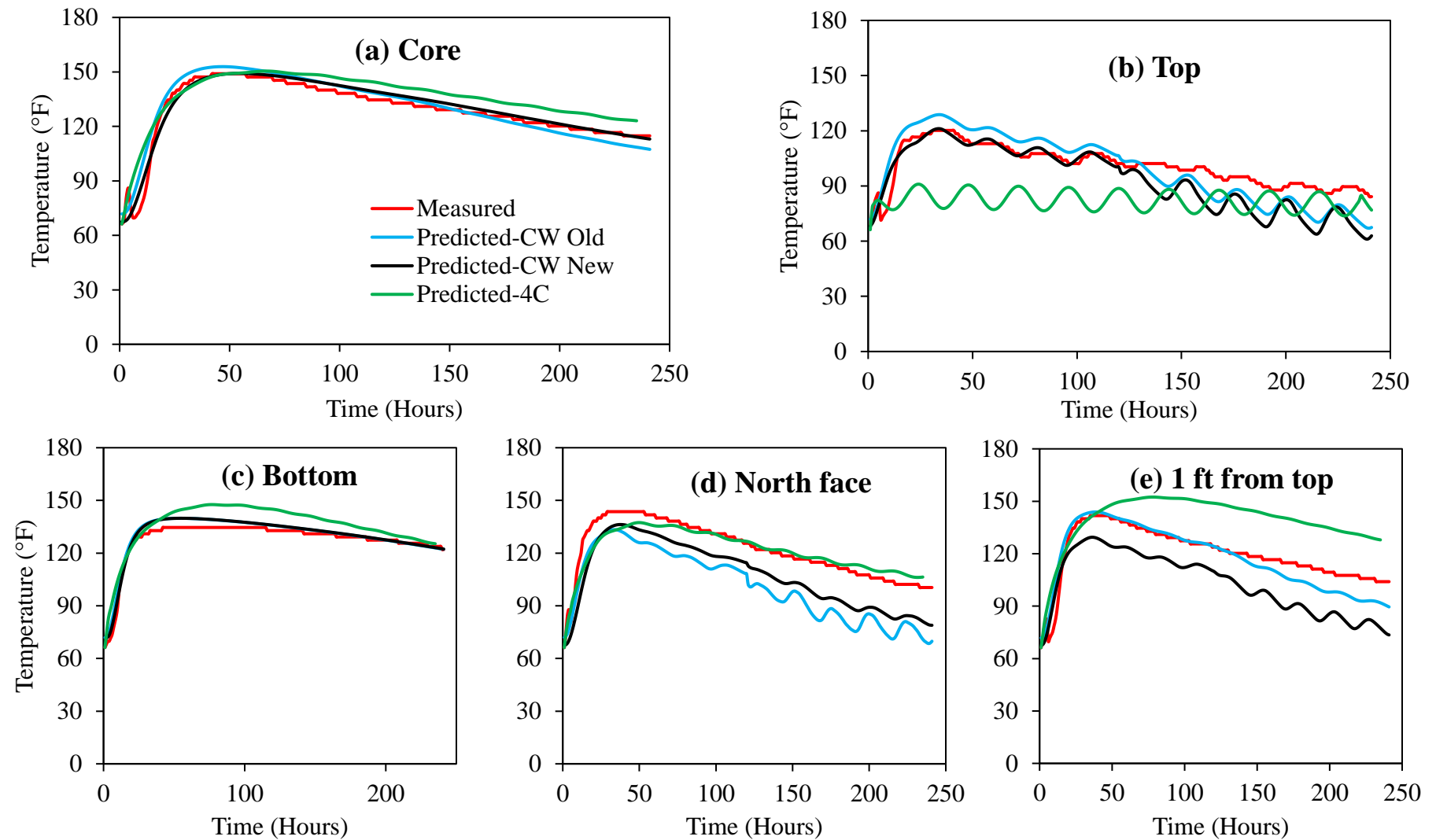


**Figure 7.3. Temperature profiles at installed thermocouple locations (field mix)**

The maximum temperature at all locations of the sensors as predicted by ConcreteWorks and 4C as well as the measured values are presented in Table 7.2.

**Table 7.2. Comparison of maximum temperature at thermocouple locations for field mix**

| Sensor Location | Maximum Temperature, °F |                                    |                                    |                  |
|-----------------|-------------------------|------------------------------------|------------------------------------|------------------|
|                 | Measured                | Predicted-<br>ConcreteWorks<br>Old | Predicted-<br>ConcreteWorks<br>New | Predicted-<br>4C |
| Core            | 149.0                   | 152.9                              | 149.2                              | 150.5            |
| Top             | 120.2                   | 128.8                              | 121.2                              | 91.0             |
| Bottom          | 134.6                   | 139.8                              | 139.8                              | 147.6            |
| North Side      | 143.6                   | 133.3                              | 136.3                              | 137.4            |
| 1 ft from Top   | 141.8                   | 143.9                              | 129.4                              | 152.4            |

Observations from the output are as follows:

1. All three programs predict the temperature in the core to be the highest. Old and new ConcreteWorks predictions are similar and closest to the measured value. The rate of cooling predicted by 4C is lower. The values of the measured and predicted maximum temperature in the core were all presented in Table 7.1 in the previous section.
2. The maximum temperature at the top of the footing predicted by 4C is lower than the actual value, whereas the ConcreteWorks predictions of the same parameter are quite close to the actual value.
3. The temperature profile at the bottom of the footing as predicted by 4C is much higher than the measured one. The ConcreteWorks predictions of the same parameter are quite close to the measured temperature profile. From the data shown in Table 7.2, the maximum temperature at the bottom predicted by 4C is 147.6°F, whereas that predicted by ConcreteWorks is 139.8°F.
4. The temperature profile at the center of the face at the shortest distance from the core, i.e., the north side, is shown in Figure 7.3(d). The measured maximum temperature at this face is 143.6°F, whereas that predicted by ConcreteWorks as well as 4C are lower than this. The complete profile predicted by 4C is more similar to the measured profile.
5. The maximum temperature at 1 ft from the top was measured to be 141.8°F. The temperature profile predicted by 4C at this point is much higher than the measured one. However, the ConcreteWorks simulates the profile at this location reasonably well as show in Figure 7.3(e).

### *Differential Temperature*

Large temperature differences in a mass concrete member can be very detrimental from the perspective of thermal cracking/shock. The maximum temperature difference causes a volume change due to expansion/contraction when the member is restrained by adjacent parts of the mass foundation, which might result in cracking (Riding et al. 2006). It is for these reasons that almost all DOTs, including the Iowa DOT, have restrictions on the maximum temperature differential that a mass concrete member can experience during early age.

It is very helpful in developing a TCP if the temperature differentials between the critical points within a mass concrete member can be predicted in advance. The computer programs discussed here predict the maximum temperature difference as one of the outputs and also the differential between two points could be predicted and analyzed.

As part of this study, the temperature differentials between the core of the rectangular footing and other thermocouple locations such as top, bottom, north side, and 1 ft from the top were calculated and analyzed. The differential temperature charts are shown in Figure 7.4.

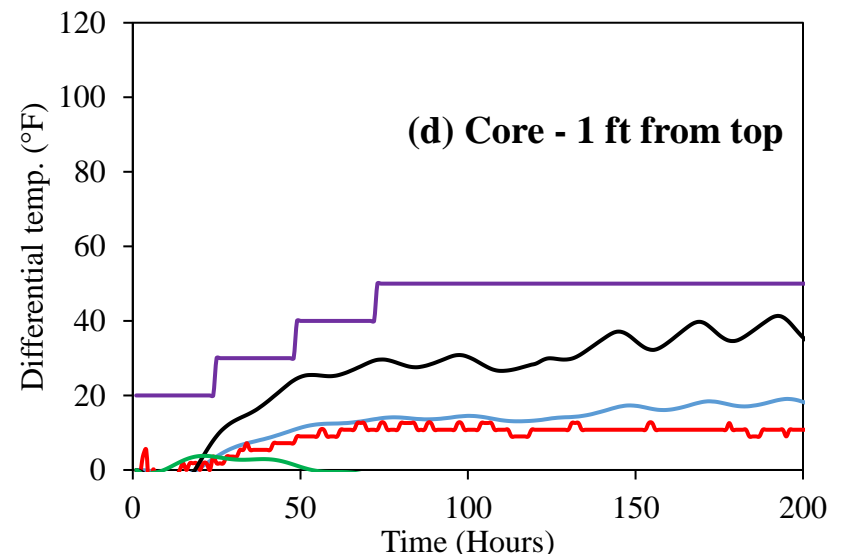
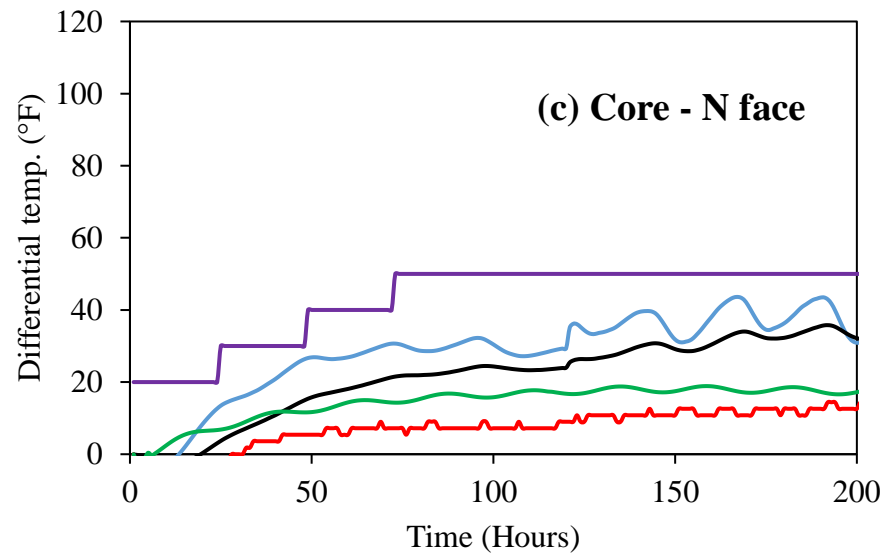
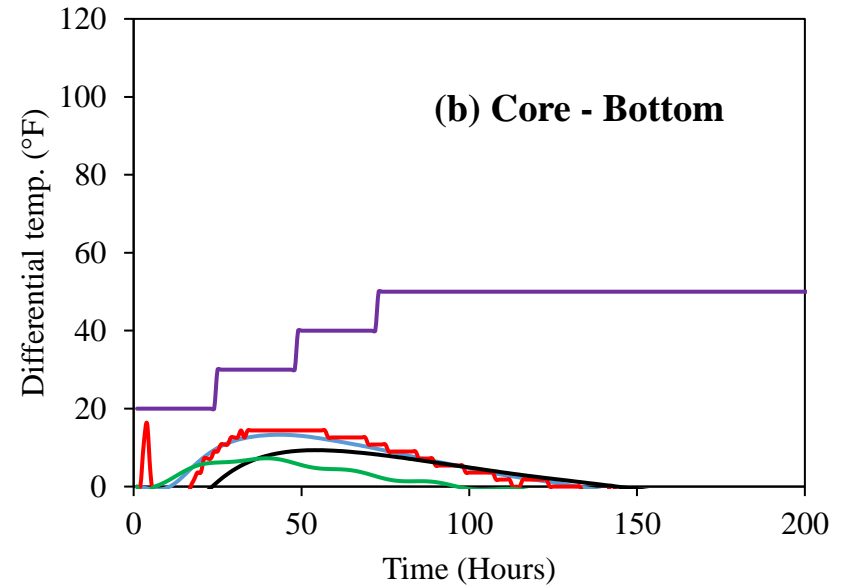
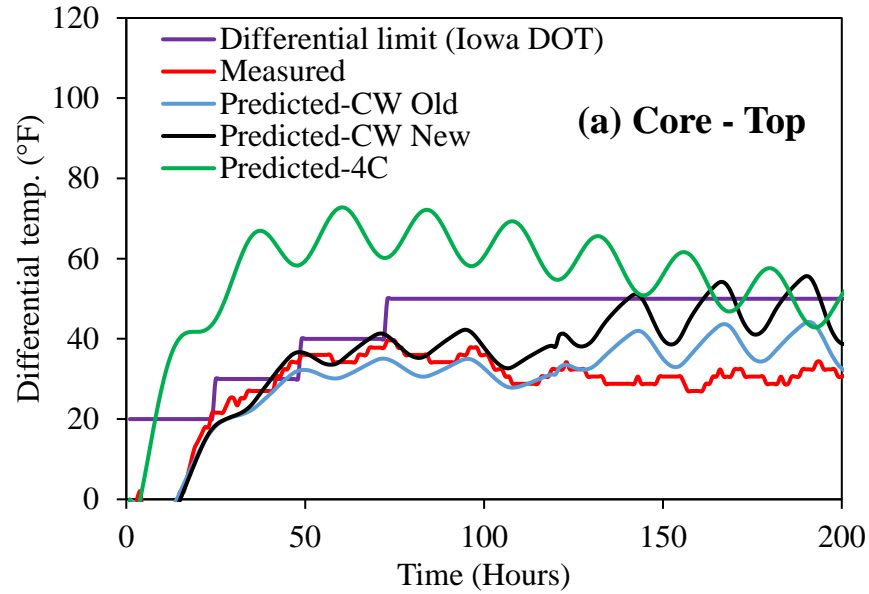


**Figure 7.4. Differential temperature analysis (field mix)**



The time series for maximum temperature differential specified by the Iowa DOT are also plotted in these charts. The specification states that the differential temperature between the centroid and a point 2 to 4 in. inside the surface along the shortest line from the centroid to the nearest surface or top surface of the element shall not exceed 20°F in the first 24 hours, 30°F between 24–48 hours, 40°F between 48–72 hours, and 50°F after that. The observations from these charts are as follows:

1. The measured temperature difference, between the core and top of the footing, is within the Iowa DOT limits for most of the early-age period as shown in Figure 7.4(a). The 4C predictions of this parameter are very high, probably because the temperature predicted by 4C at the top is lower than that of the measured values. The new ConcreteWorks prediction of the core and top differential temperature profile is very similar to the measured profile. Since this is the most critical differential location, its prediction as close as possible to the actual value will be helpful in developing a TCP.
2. The profile of the temperature difference between the core and bottom sensors is shown in Figure 7.4(b). The ConcreteWorks predictions are a bit lower than the measured values but are all within the specification limits.
3. The temperature difference between the core and the center of the face at the shortest distance from the core (the north face) is also very critical for thermal cracking. The measured temperature difference for the field project was very well within the specification limits as shown in Figure 7.4(c). Prediction by all three programs is higher than the measured values and also within the limits. Considering a factor of safety for important projects, predictions on a bit higher side could be acceptable.
4. As discussed earlier, the temperature at a location 1 ft from the top was also analyzed. The differential temperature between the core and this point is shown in Figure 7.4(d). The 4C predictions of this parameter are lower than the actual value. However, the ConcreteWorks profile of temperature difference is higher than the actual value.

### *Maturity*

ConcreteWorks has the option of choosing one of the methods amongst Nurse-Saul and equivalent age for computing the maturity index. The user can select either of the two. However, due to its simplicity, the Nurse-Saul method is frequently used for construction projects in Iowa and, for this reason, as well as for this research, this method was used. The coefficients  $a$  and  $b$  of the best-fit strength-maturity equation were used as input to the ConcreteWorks program. Figure 7.5 shows the comparison of the measured and ConcreteWorks predicted values for maturity presented in terms of a TTF against the age of the concrete.

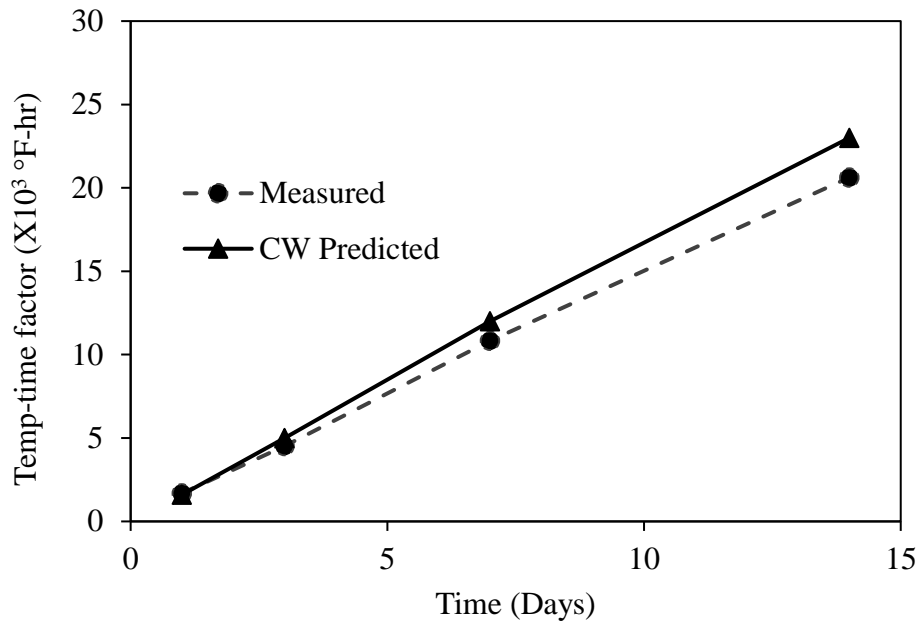


**Figure 7.5. Maturity comparisons for field mix**

As shown in Figure 7.5, the ConcreteWorks predicted TTF value with age is a bit higher than the measured value, which is acceptable from the perspective of a factor of safety. Therefore, it can be inferred that the new ConcreteWorks performs well in maturity calculations.

### *Compressive Strength*

The compressive strength development model is essential in ConcreteWorks because it is used to calculate the elastic modulus and tensile strength development, which are used consequently to calculate the cracking probability. One of the outputs of ConcreteWorks is also the compressive strength development of the mass concrete member being analyzed. For the I-35 NB to US 30 WB project, cylinders were cast during the concrete pour of the footing, and their compressive strengths were measured at various ages. The measured and ConcreteWorks predicted values are shown in Figure 7.6.

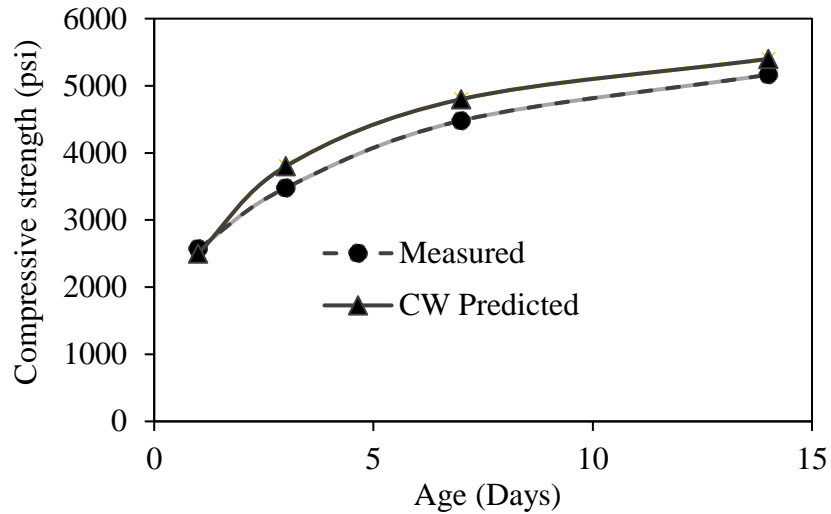
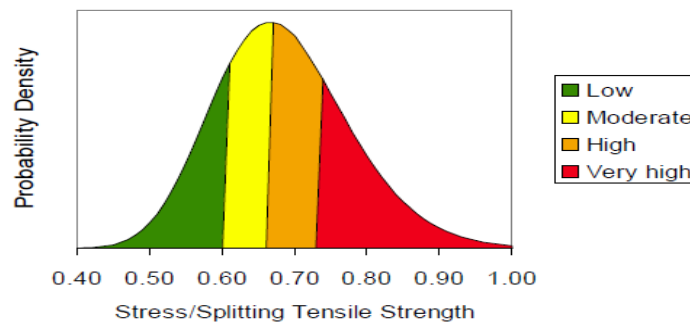


**Figure 7.6. Compressive strength comparisons for field mix**

Similar to the maturity predictions by ConcreteWorks, the compressive strength predictions are also a bit higher than the measured values, which are acceptable from the perspective of factor of safety.

#### *Cracking Probability*

One of outputs in ConcreteWorks is cracking probability/potential. The cracking potential classification of a mass concrete member is based on the calculated tensile stress-to-tensile strength ratio. The concrete tensile stress-to-tensile strength ratio calculated in the software is assigned a cracking probability classification using the probability density shown in Figure 7.7.



Riding et al. 2014

**Figure 7.7. Probability density for cracking probability classification in ConcreteWorks**

A lognormal distribution is assumed to model the relationship between the stress-to-strength ratio and the probability of cracking. A 25% or lower cracking probability is assumed to be low, a 25 to 50% cracking probability is assumed to be moderate, a 50 to 75% is assumed to be high, and higher than 75% cracking probability is assumed to be a very high (Riding et al. 2017).

The cracking probability of the I-35 NB to US 30 WB bridge rectangular footing as predicted by ConcreteWorks is shown in Figure 7.8.

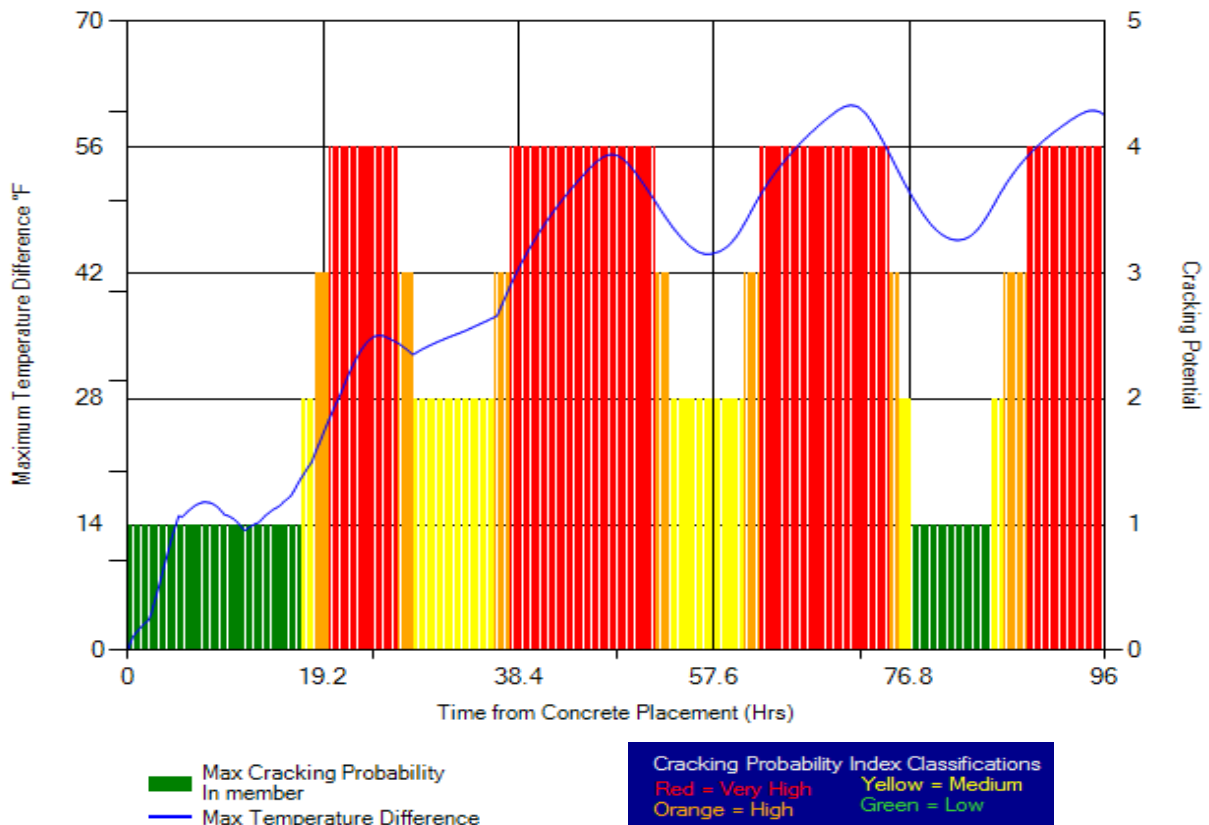


**Figure 7.8. Cracking probability prediction for field mix**

The blue line in Figure 7.8 shows the maximum temperature difference in the footing between any two points. Blocks of red, orange, yellow, and green present the relative cracking potential of the concrete member (footing in this case). As evident, the cracking probability in the first 24 hours is predicted to be low. However, ConcreteWorks predicts a very high cracking probability at 20–30 and 38–50 hours after concrete placement. It is important to point out here that a high or very high cracking risk classification does not mean that the structural member will crack or vice-versa. It only indicates that the probability of cracking is higher than if the concrete cracking risk classification is low, medium, or high.

### Analysis of Laboratory Mixes

Four concrete mixes commonly used in mass concrete construction in Iowa were tested for their various properties as presented in Chapter 4. These results were later used to modify the ConcreteWorks program. The old and new ConcreteWorks, as well as 4C, were then used to analyze the performance of these four mixes under the conditions of the I-35 NB to US 30 WB bridge footing construction. All of the inputs in ConcreteWorks and 4C, such as general, shape,

construction, and environmental inputs, were kept the same as those used in the analysis of the field mix. Figure 7.9 shows the input values for one of the mixes (Mix 1).

Input Check

Parameter

Value

Units

**General Inputs**

Project Location

Des Moines

Unit System

English

Chloride Units

Percent of Concrete

Life Cycle Analysis Duration

20

Years

Analysis Duration

14

days

Concrete placement time

8

am

Concrete placement date

6/16/2017

**Member Inputs**

Shape Choice

Rect. footing

Member width

27

ft

Member length

33

ft

Member depth

7

ft

Type of Analysis

2-d

**Mixture Proportions**

Cement Content

474

lb/yd<sup>3</sup>

C Fly Ash Content

119

lb/yd<sup>3</sup>

Water Content

255

lb/yd<sup>3</sup>

Coarse Aggregate Content

1532

lb/yd<sup>3</sup>

Fine Aggregate Content

1518

lb/yd<sup>3</sup>

Air Content

5.5

%

Chemical Admixture

Mid-Range WR

**Material Properties**

Cement Type

I

Cement Chemistry Values

Default

Hydration Parameter Values

Default

Coarse Agg. type

Limestone

Fine Agg. type

Siliceous River Sand

Coarse Agg. type

Limestone

Parameter

Value

Units

**Environment Inputs Summary**

Ave. Daily Max Temp.

81.5

°F

Ave. Daily Min Temp.

58

°F

Ave. Max Daily Solar Radiation

731.1

W/m<sup>2</sup>

Ave. Max Daily Wind Speed

24.1

m/s

Ave. Max Relative Humidity

95.1

%

Ave. Min Relative Humidity

45

%

**Construction Inputs**

Concrete Fresh Temperature

67.5

°F

Blanket R-Value

0.5

°F

Forms are stripped after

120

hrs

Form Color

Natural Wood

Form Type

Wood

Side Cure Method

Black Plastic

Delay between stripping and curing

1

hrs

Soil temperature

80

°F

Footing Subbase

Limestone

Time of top cure blanket placement

5

hrs

Footing top cure method used

Wet blanket

Footing top cure method used

Black Plastic

**Corrosion Inputs**

Steel Type

316 Stainless Steel

Steel Cover

2

Dref

101.3

x 10<sup>-4</sup>

Default values are indicated by green

Questionable input values are indicated by red

Back

Calculate Temperatures

Figure 7.9. ConcreteWorks input for Mix I-20

90

The analysis results are discussed separately for all four mixes in the following sub-sections.

#### *Mix 1 (I-20FA)*

The mix proportion for Mix 1 was presented previously in Table 3.1, along with that of other mixes. The cementitious materials used in the mix were Type I cement and 20 % Class C fly ash. Figure 7.10 shows the temperature profile predicted by the three programs at the core of the footing if Mix 1 is used.

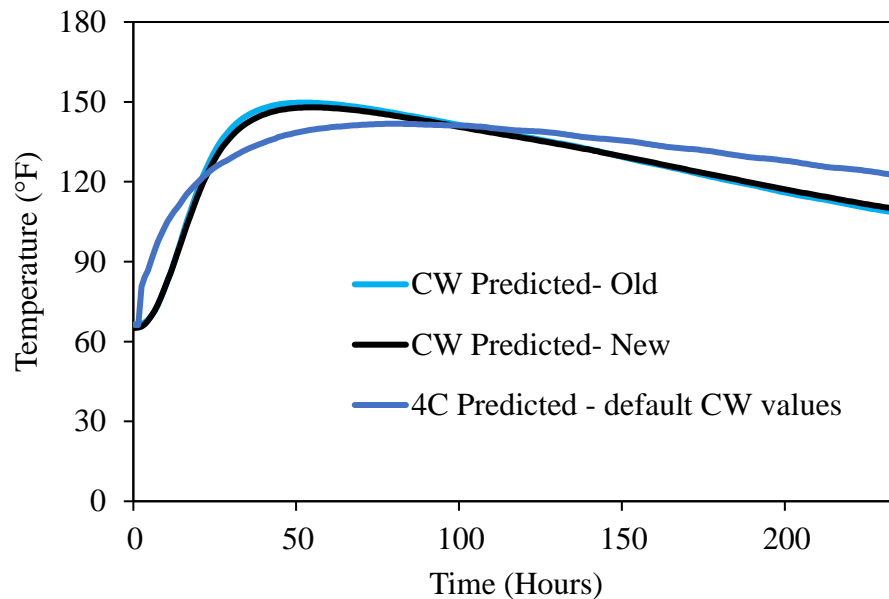


**Figure 7.10. Temperature at the core of footing (Mix 1)**

The temperature at the top and the north face and the temperature differentials are presented in Figure 7.11.

The maximum temperature predicted for Mix 1 are 149.7, 148, and 142°F by old ConcreteWorks, new ConcreteWorks, and 4C, respectively. From the charts presented in Figure 7.11, it can be observed that the ConcreteWorks predictions of maximum temperature at the top and north face of the footing are higher than that predicted by 4C. The ConcreteWorks predicted temperature differential between the core and the top are within the specified limits; however, that by 4C exceeds the limit. On the other hand, the prediction of the differential between the core and north face are all within the limits.

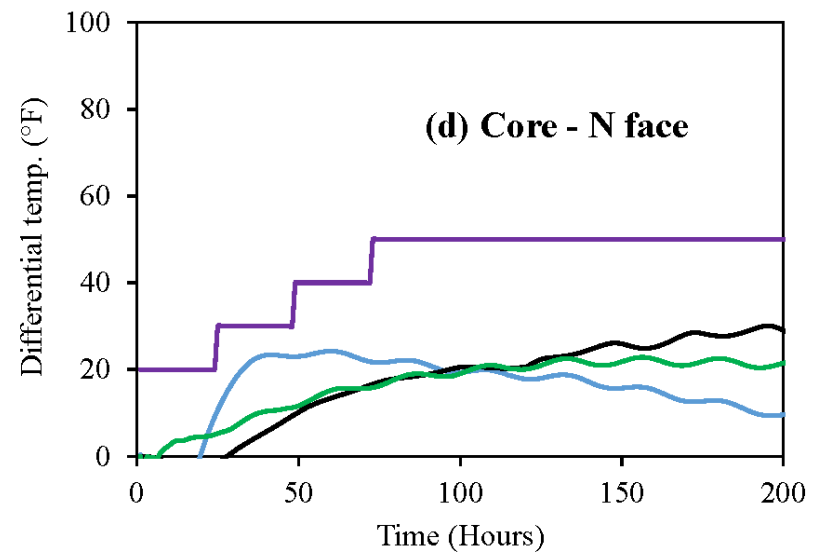
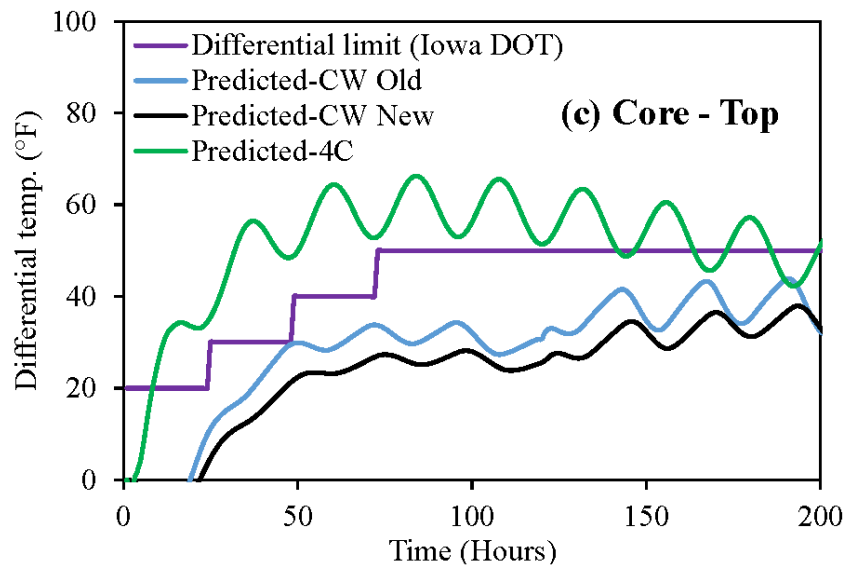
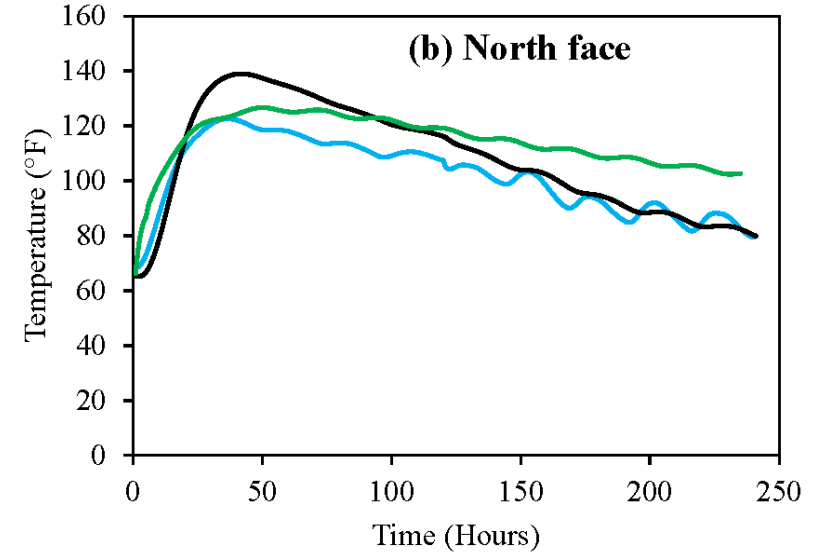
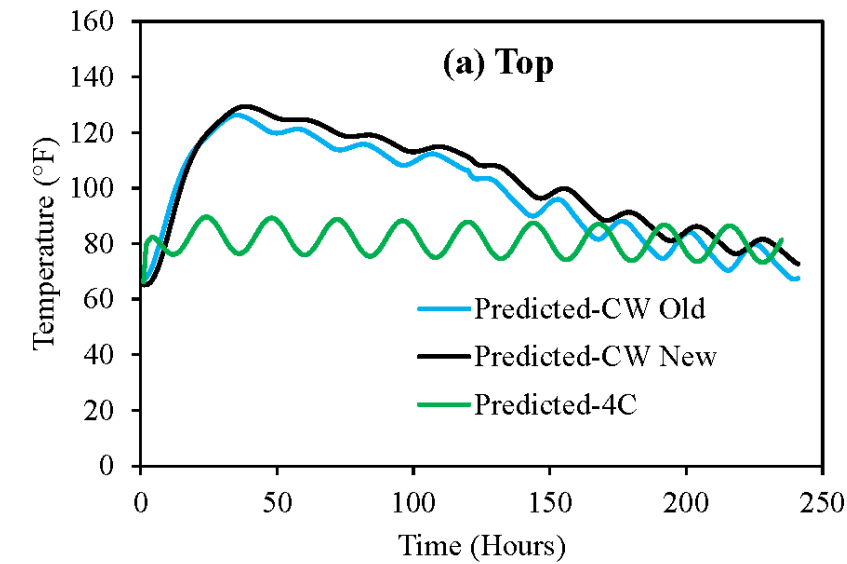


**Figure 7.11. Differential temperature comparisons for Mix 1**



The ConcreteWorks predicted cracking probability of the footing for Mix 1 is shown in Figure 7.12.

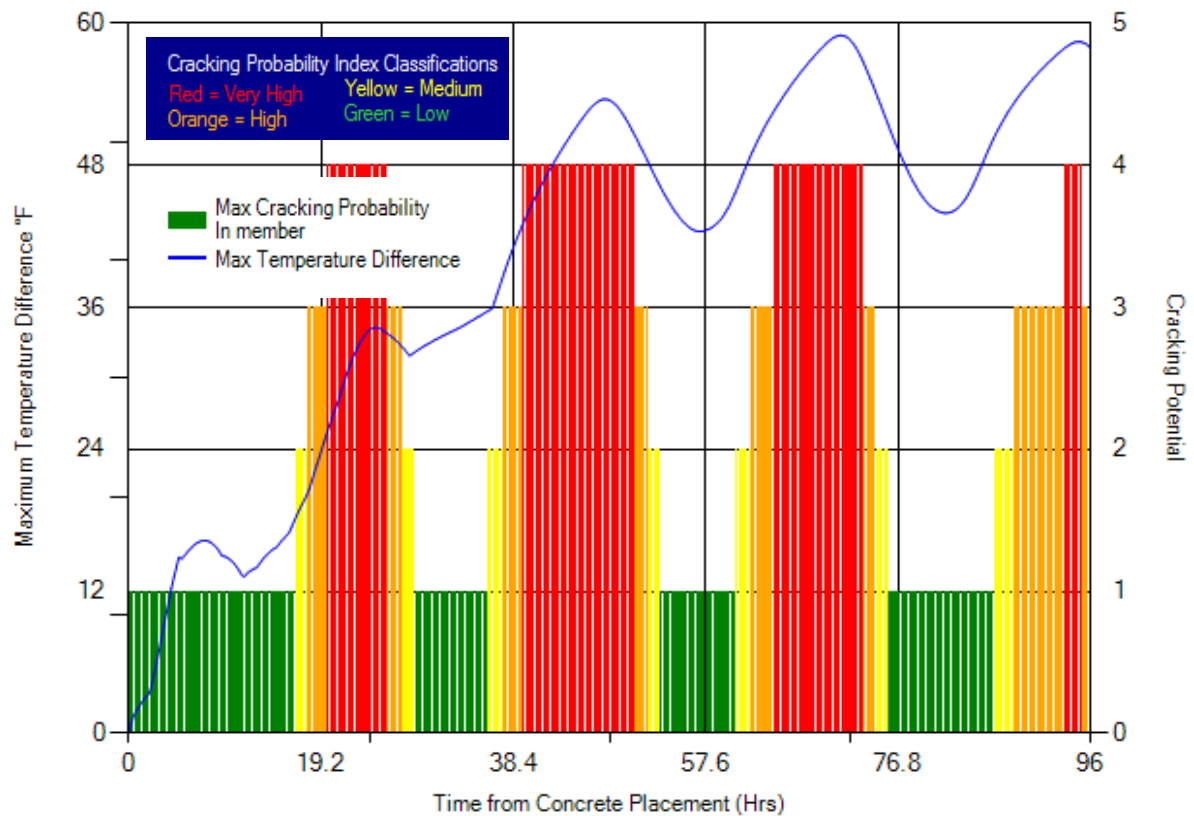


**Figure 7.12. Cracking probability prediction for Mix 1**

Similar to the ConcreteWorks predictions for the field mix, the cracking probability is predicted to be low in the first 20 hours, whereas it is very high at approximately 20–30 and 38–50 hours after the placement of concrete.

#### *Mix 2 (IP-20FA)*

The cementitious materials used in Mix 2 were Type IP (25) cement containing 25% Class F fly ash and 20% Class C fly ash added to the concrete mix. The maximum temperature profile at the core of the bridge footing as predicted by ConcreteWorks and 4C is presented in Figure 7.13.

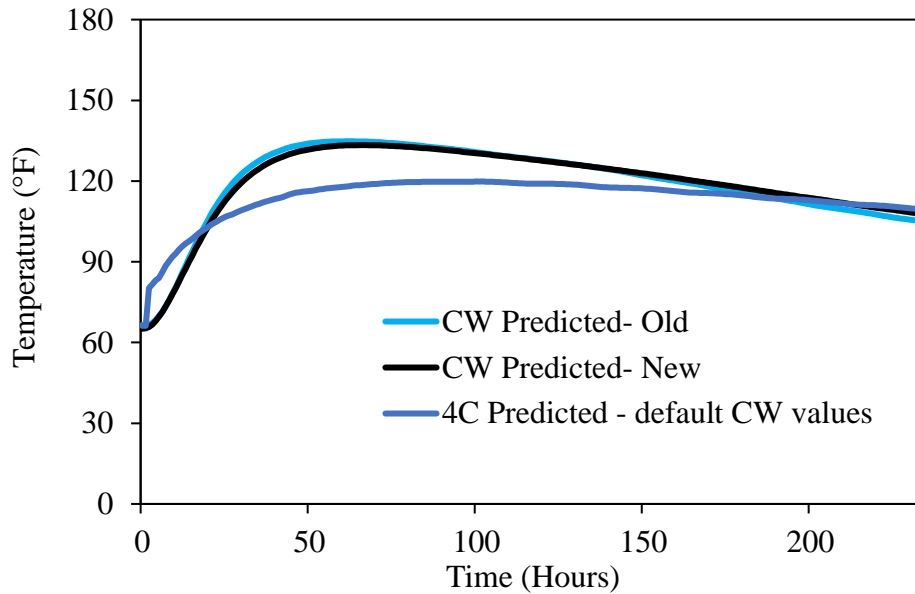


**Figure 7.13. Temperature at the core of footing (Mix 2)**

The maximum temperature predicted for Mix 2 was 134.8, 133.4, and 120°F by old ConcreteWorks, new ConcreteWorks, and 4C, respectively.

The temperature profile at other thermocouple locations, such as the top and north face, as well as their temperature differentials at the core of the footing, are shown in Figure 7.14.

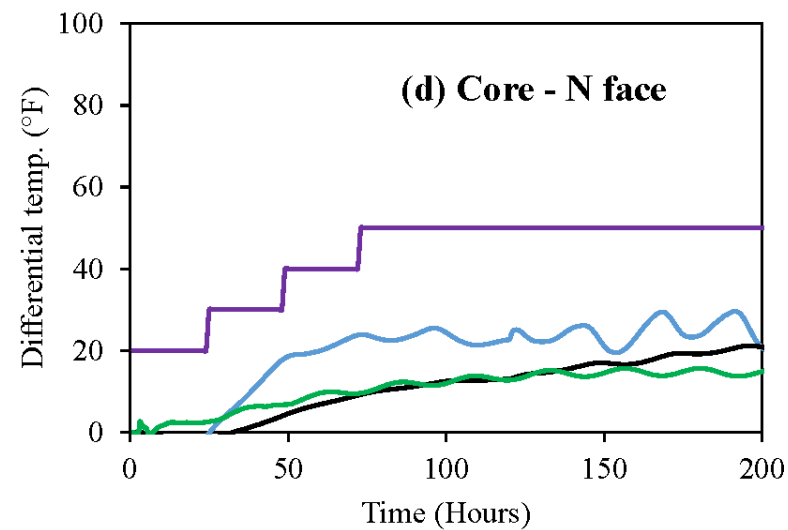
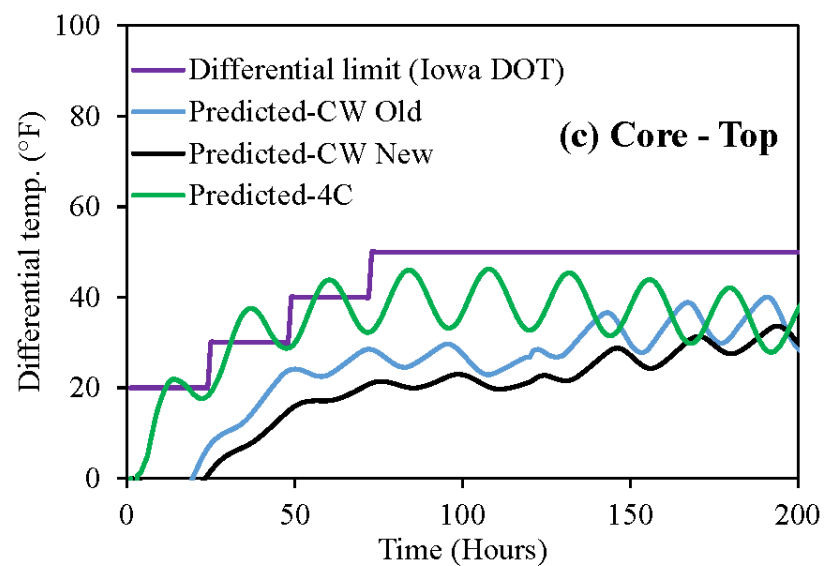
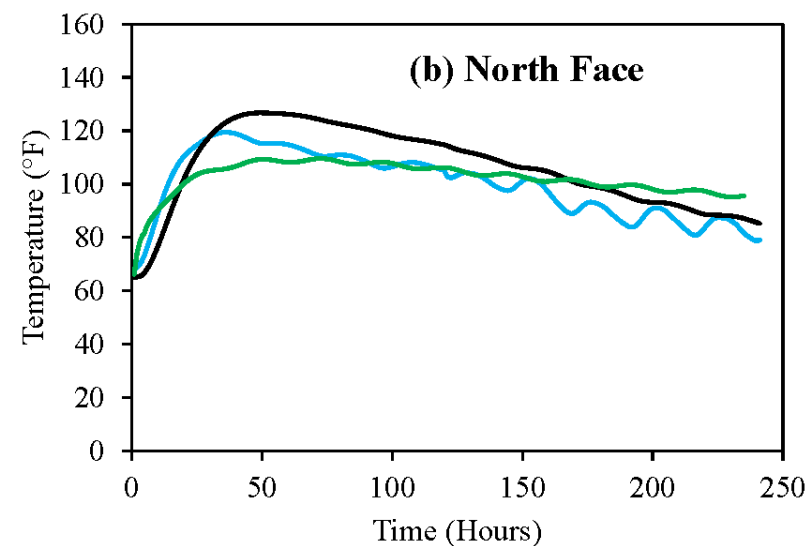
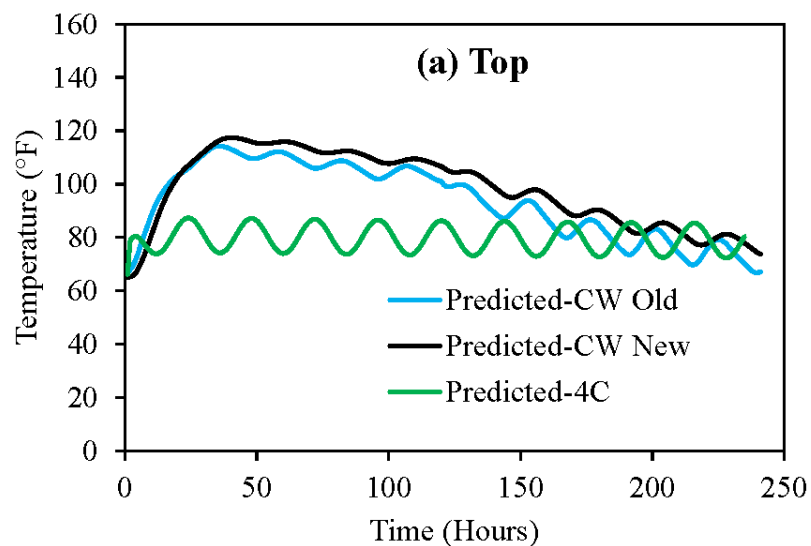


**Figure 7.14. Differential temperature comparisons for Mix 2**

As observed for Mix 1, and for Mix 2 as well, the ConcreteWorks predictions of maximum temperature at the top and north face of the footing are higher than that predicted by 4C. The ConcreteWorks prediction of maximum temperature at the top is 117°F. The ConcreteWorks predicted temperature differential between the core and the top are within the specified limits; however, that predicted by 4C exceeds the limit for a short period of time around 40–50 hours.

The prediction of the differential between the core and north face are all well within the limits. A high degree of replacement of cement by fly ash (45%) in Mix 2 resulted in the generation of less heat of hydration as compared to Mix 1. Therefore, the ConcreteWorks and 4C predictions of maximum temperature and temperature differentials are also lower in this case. Figure 7.15 presents the cracking probability predictions.

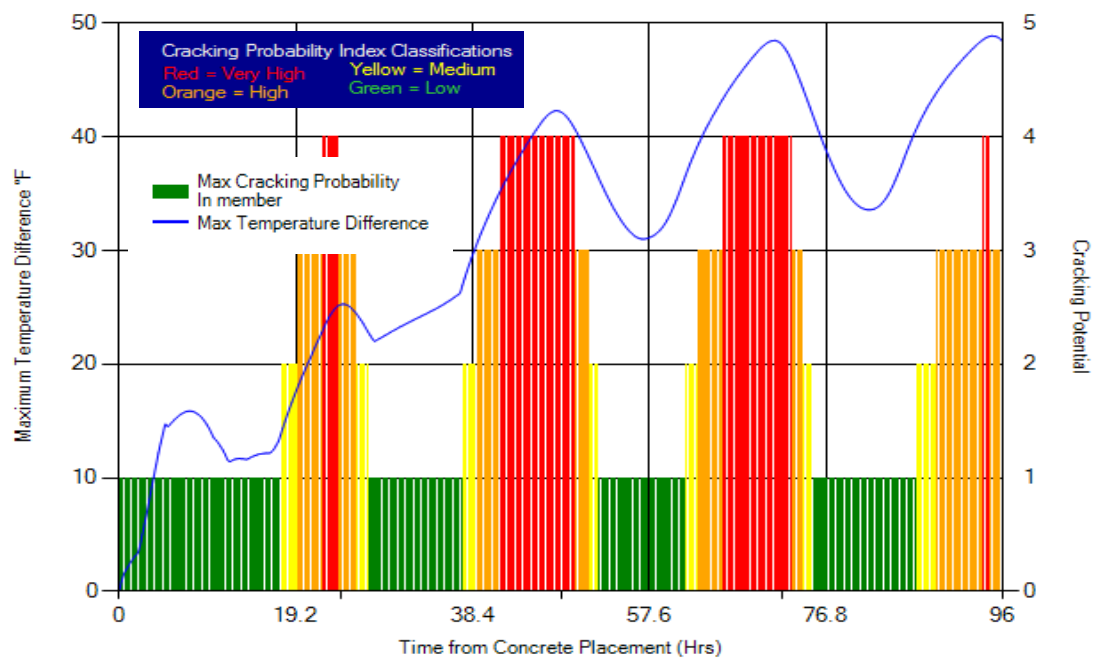


**Figure 7.15. Cracking probability prediction for Mix 2**

If this mix is used for casting, the cracking probability for the footing is predicted to be low in the initial 20 hours and increases to very high around 40–50 and 65–70 hours after casting.

### *Mix 3 (IS-20FA)*

The cementitious materials used in Mix 3 were Type IS (20) cement containing 20% grade 100 ground granulated blast furnace slag and 20% of C fly ash added to the concrete mix. Hence, the SCM replacement was 40% by weight of the total cement content in the concrete mix. The maximum temperature profile of the core of the bridge footing for Mix 3 as predicted by ConcreteWorks and 4C is presented in Figure 7.16.

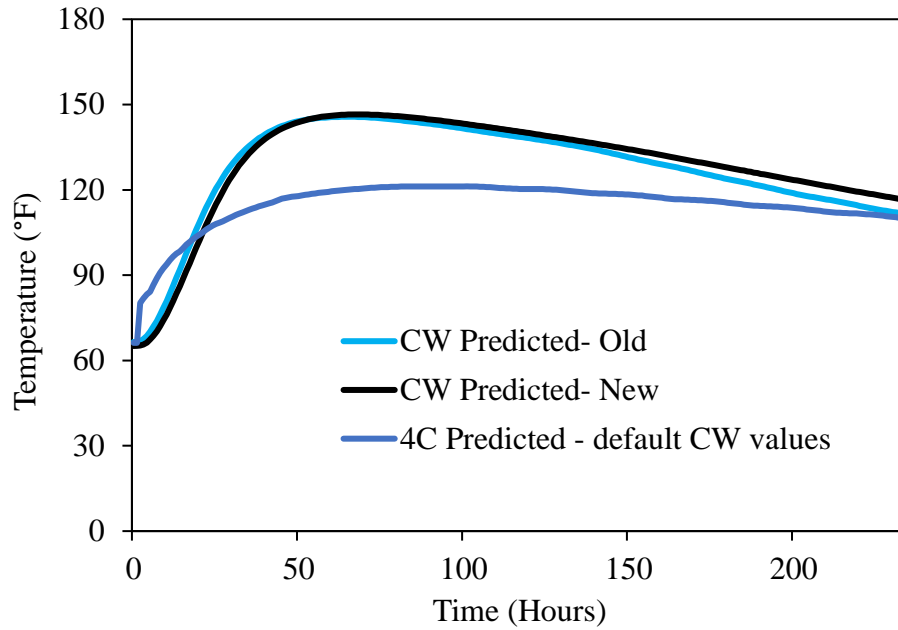


**Figure 7.16. Temperature at the core of footing (Mix 3)**

The maximum temperature predicted for Mix 3 was 145.7, 146.5, and 121.2°F by old ConcreteWorks, new ConcreteWorks, and 4C, respectively.

The temperature profile at other thermocouple locations such as the top and north face, as well as their temperature differentials with the core of the footing, are shown in Figure 7.17.

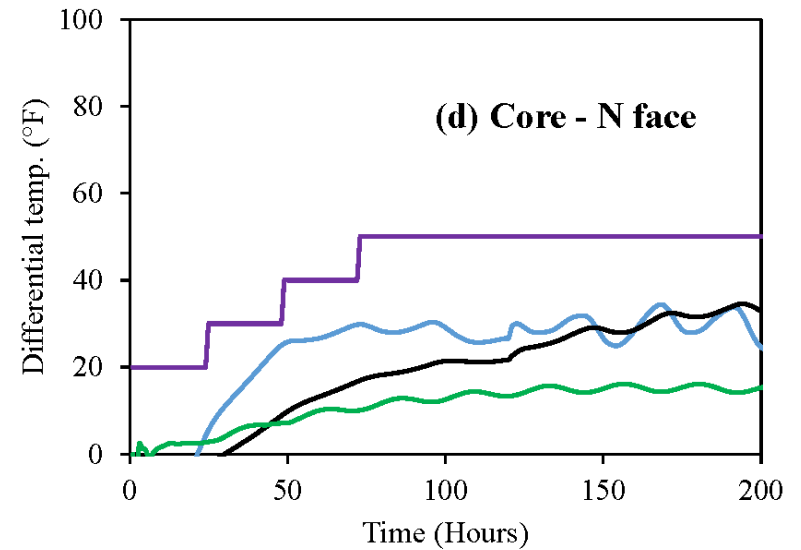
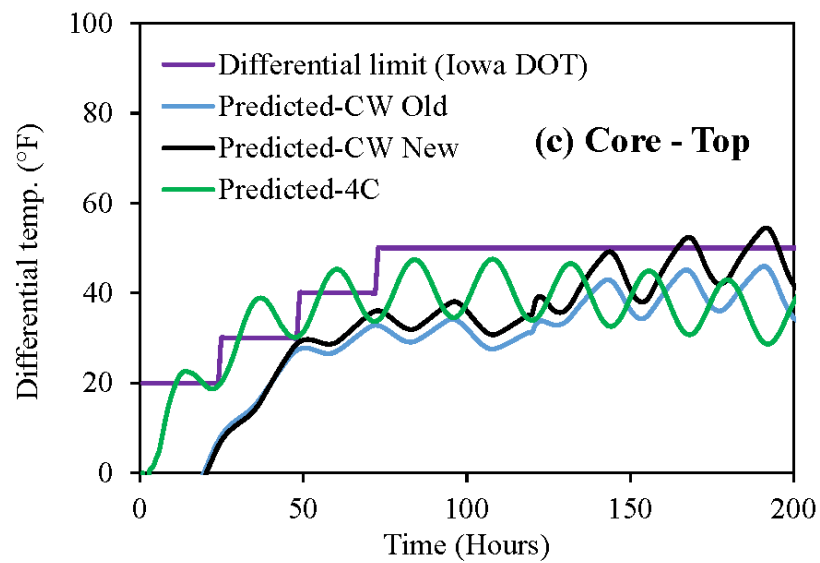
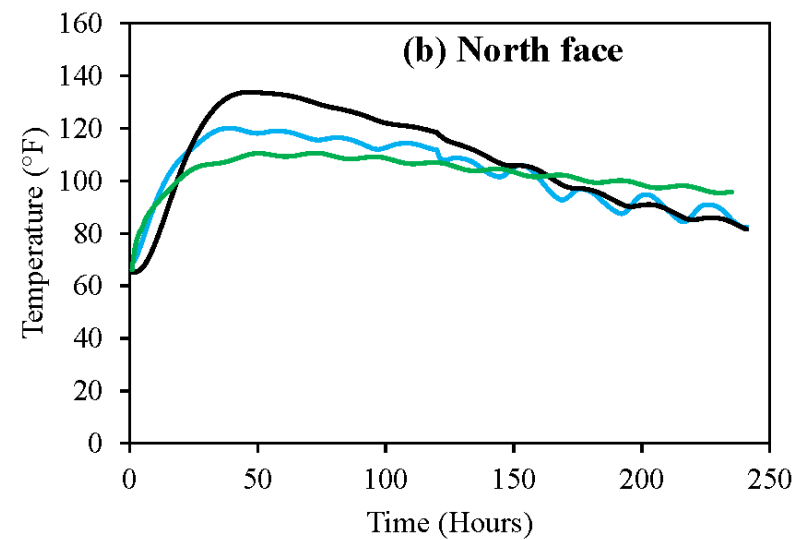
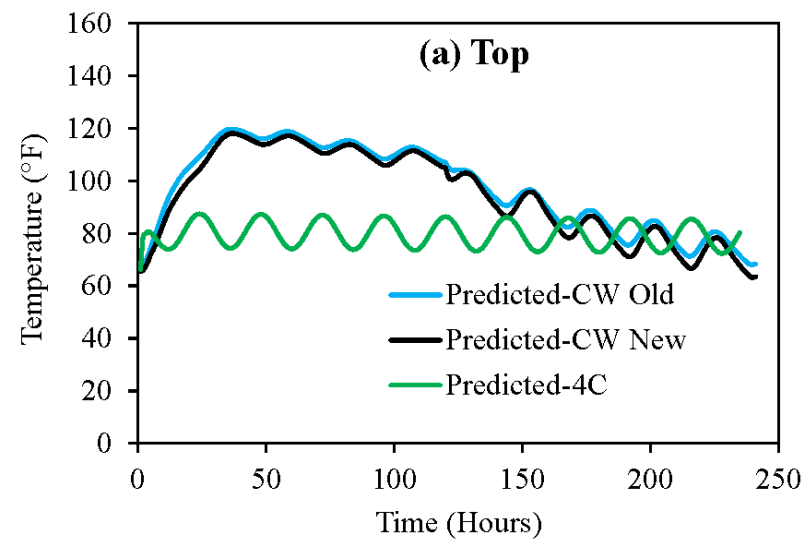


**Figure 7.17. Differential temperature comparisons for Mix 3**

Similar to the observations for Mixes 1 and 2, the 4C predictions of temperature at the top are less than those for ConcreteWorks predictions. From the figure, it is observed that the temperature at the top reduces after around 120 hours when the insulation blanket is removed. The new ConcreteWorks prediction of maximum temperature at the top is 118°F. As shown in Figure 7.17(c) and 7.17(d), the ConcreteWorks prediction of the temperature differential between core and the two faces (top and north) are within the Iowa DOT specified limits; however, that predicted by 4C goes off-spec for a short period of time around 40–50 hours. The cracking probability predicted by ConcreteWorks is shown in Figure 7.18.

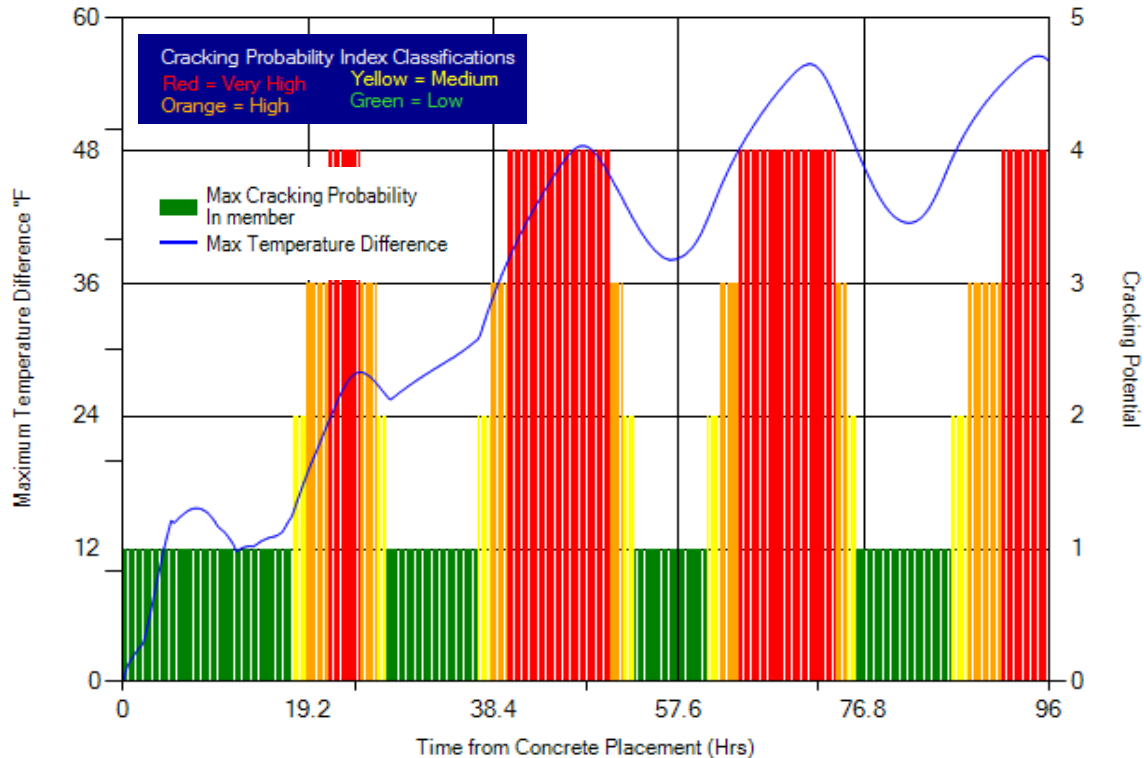


**Figure 7.18. Cracking probability prediction for Mix 3**

Similar to the previous two mixes, the cracking probability is predicted to be very high at approximately 20–25, 38–50, and 65–70 hours after concrete placement.

#### *Mix 4 (I/II-20FA-30S)*

The cementitious materials used for Mix 4 were Type I/II cement, 20% Class C fly ash, and 30% slag. Hence, the SCM replacement was 50% by weight of the total cement content in the concrete mix. The maximum temperature profile of the core of the bridge footing for Mix 4 as predicted by ConcreteWorks and 4C is presented in Figure 7.19.

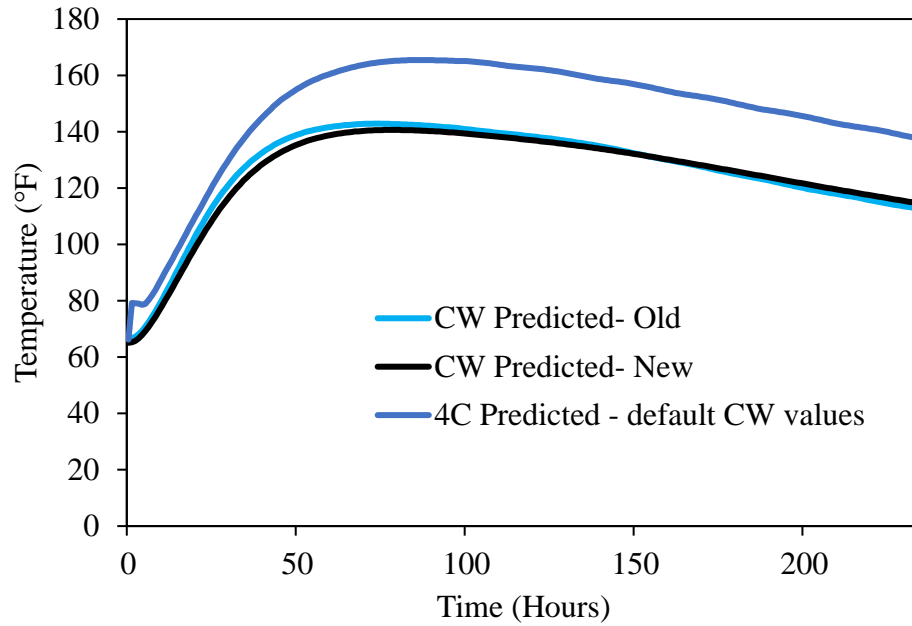


**Figure 7.19. Temperature at the core of footing (Mix 4)**

The maximum temperature predicted for Mix 4 was 142.8, 140.6, and 165.4°F by old ConcreteWorks, new ConcreteWorks, and 4C, respectively. It is observed from Figure 7.19 that the maximum temperature predicted by 4C at the core of the footing is much higher than that predicted by ConcreteWorks. The temperature profile at other thermocouple locations such as the top and north face, as well as their temperature differentials in the core of the footing, are shown in Figure 7.20.



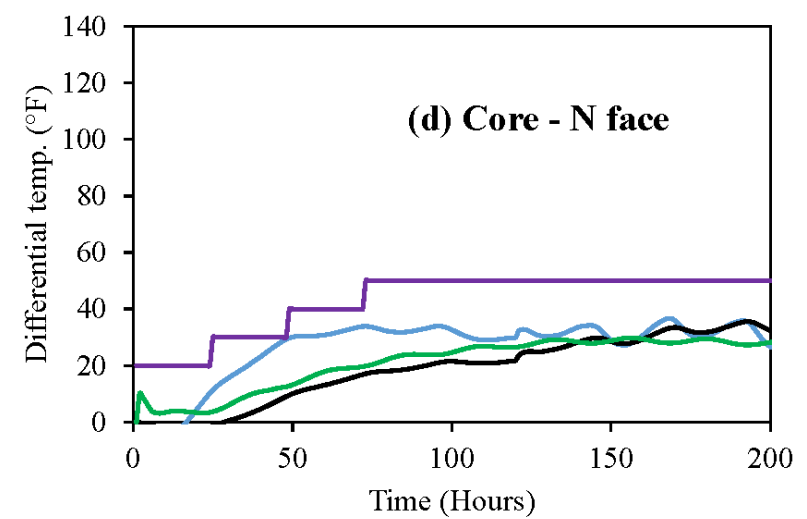
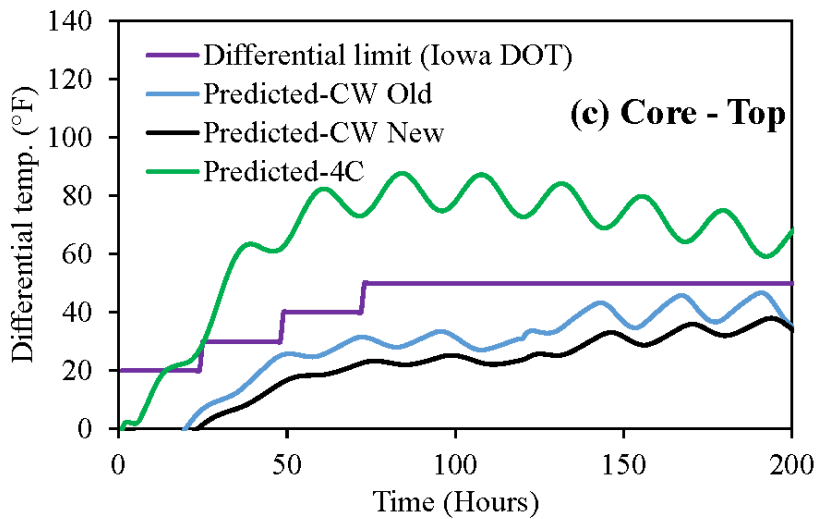
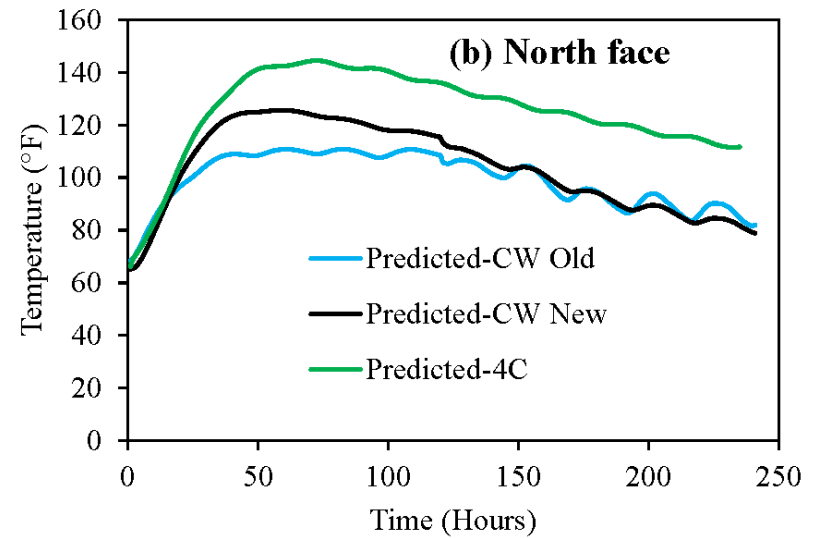
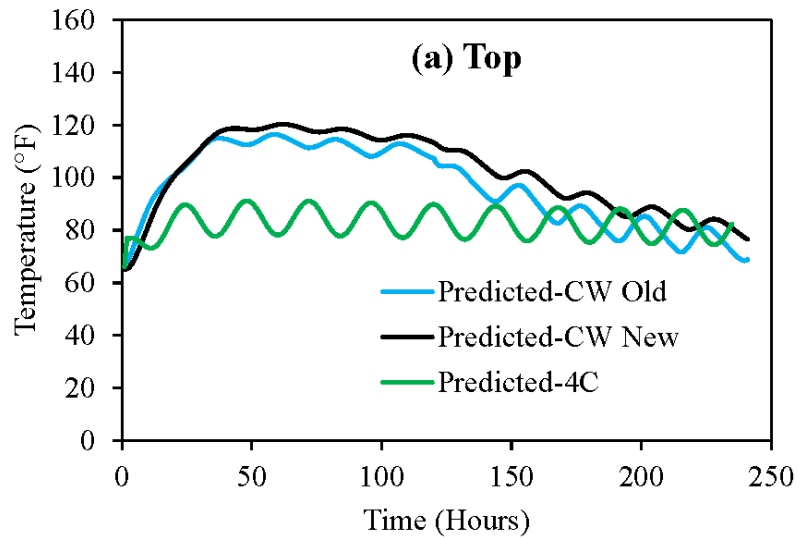


**Figure 7.20. Differential temperature comparisons for Mix 4**

The ConcreteWorks predictions of maximum temperature at the top of the footing are higher than that predicted by 4C. However, the 4C prediction of temperature at the north face is higher. The ConcreteWorks predicted temperature differential between the core and the top are within the specified limits; however, that predicted by 4C exceeds the limit, which is noteworthy. The prediction of the differential between the core and north face by all three programs are all well within the limits. One of the reasons for a higher prediction by 4C might be the use of a high amount of slag in this mix.

The cracking probability predicted by the new ConcreteWorks for the rectangular footing with Mix 4 is presented in Figure 7.21.

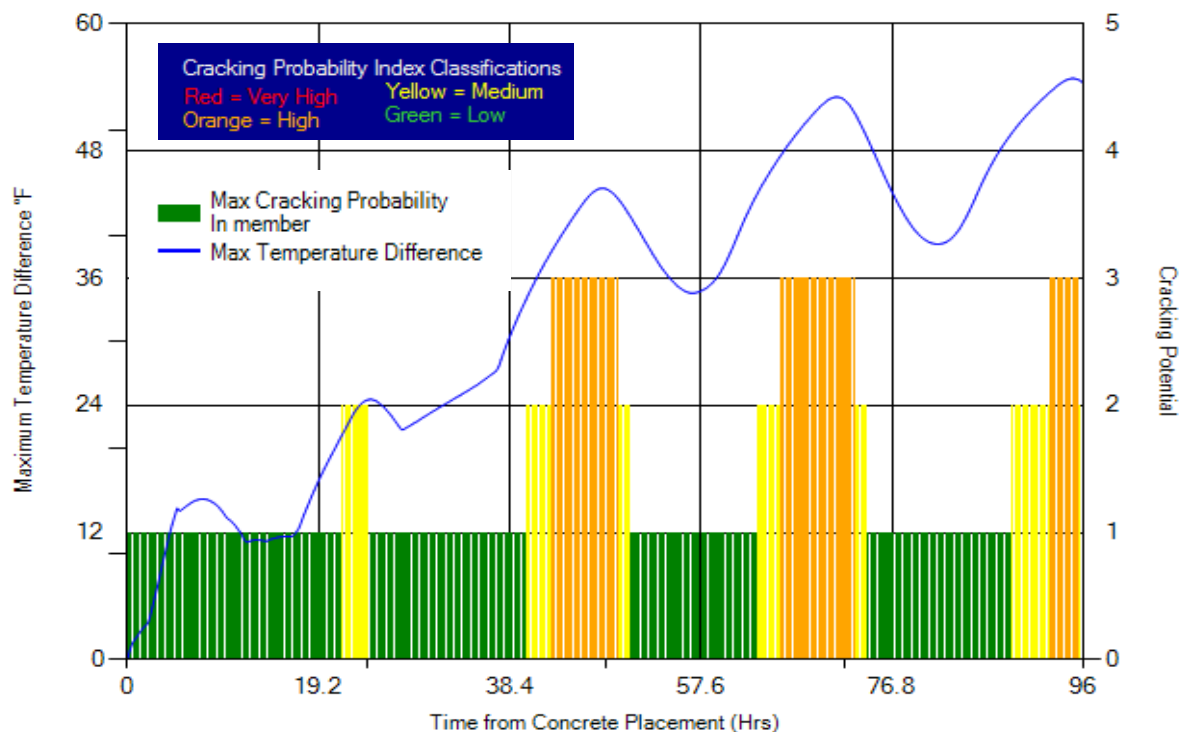


**Figure 7.21. Cracking probability prediction for Mix 4**

As shown, the cracking probability most of the time is low to medium. At approximately 40–50 and 65–72 hours after concrete placement, the probability is high.

### *Comparisons*

The new ConcreteWorks thermal analysis results for four concrete mixes, as presented in the previous sections, were compared with each other and with 4C. The parameters considered for comparisons were core temperature, temperature differential, maturity, and cracking probability. Figure 7.22 shows the temperature profile of all four mixes (as predicted by the new ConcreteWorks) at the core of the rectangular footing.

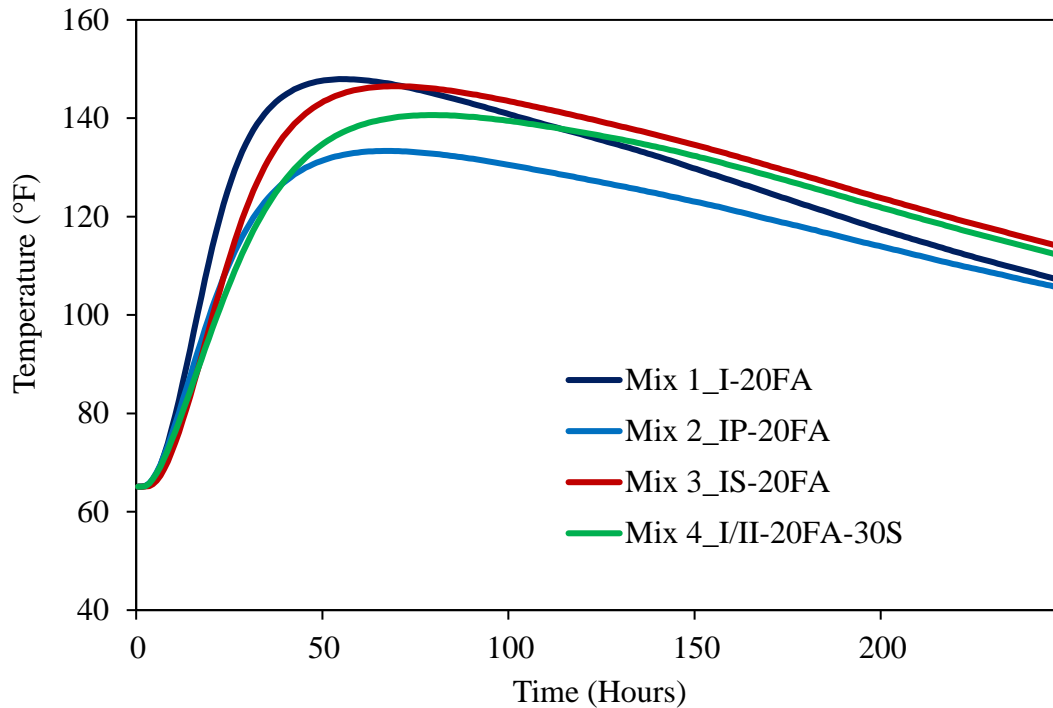


**Figure 7.22. Maximum temperature comparison of laboratory mixes**

The maximum temperature predicted by ConcreteWorks as well as 4C is presented in Table 7.3.

**Table 7.3. Maximum temperature comparisons for laboratory mixes**

| Mix                 | Max Concrete Temp. (°F) |        |
|---------------------|-------------------------|--------|
|                     | ConcreteWorks           | 4C     |
| Mix 1_I-20FA        | 147.96                  | 141.80 |
| Mix 2_IP-20FA       | 133.36                  | 119.81 |
| Mix 3_IS-20FA       | 146.52                  | 121.24 |
| Mix 4_I/II-20FA-30S | 140.65                  | 165.43 |

From the temperature profiles and data shown in Figure 7.22 and Table 7.3, it is observed that the temperature development in the footing is different for each of the four mixes. The ConcreteWorks predicted maximum temperature is the lowest for Mix 2 (133.36°F) containing a total of 45% fly ash and the highest for Mix 1 (148°F) containing only 20% fly ash. Even though Mixes 3 and 4 contain a high amount of fly ash and slag, the predicted maximum temperature remains relatively high. The predicted times to reach the maximum temperature for Mixes 1–4 are 55, 66, 68, and 78 hours, respectively. The 4C predictions of the parameters discussed above are different. The prediction of maximum temperature is the lowest for Mix 2 (120°F), but it is the highest for Mix 4 (165°F) containing 20% fly ash and 30% slag.

Figure 7.23 shows the differential temperature profile for the footing as predicted by ConcreteWorks for all four mixes.

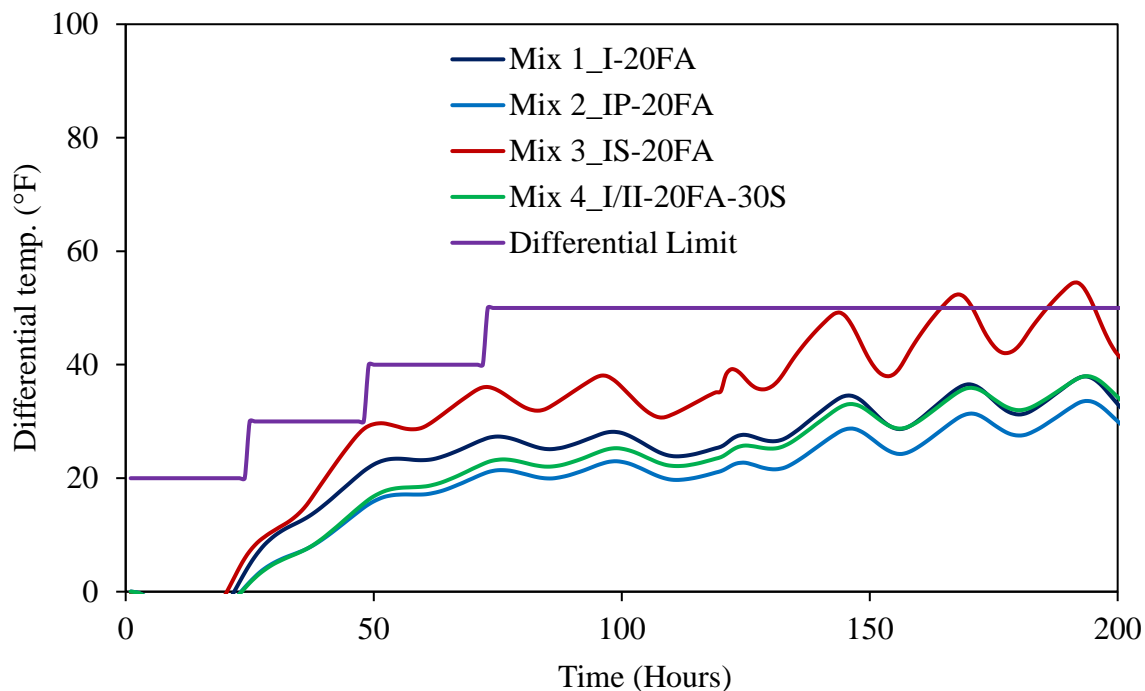


**Figure 7.23. Maximum temperature differential comparison of laboratory mixes**

Also shown in the figure are the limits on differential temperature specified by the Iowa DOT. Similar to the maximum temperature prediction, the predicted differential temperature is also the lowest for Mix 2. However, the differential temperature is the highest for Mix 3. The temperature differential prediction for all mixes is within the Iowa DOT specified limits. The predictions also show that the concrete mixes containing slag (Mix 3 and Mix 4) furnish a higher maximum temperature as well as a higher temperature differential compared to the other mixes not containing slag. A delayed interaction of the cement hydration product and slag might be responsible for increasing the temperature at the core of the footing and thereby the temperature differential also.

As explained in the previous section on Analysis of the Field Mix, ConcreteWorks also predicts the maturity and compressive strength as outputs. The predicted values of the maturity (TTF) and compressive strength for all four mixes are plotted in Figure 7.24 and compared with the measured values.

It can be observed from the figure that the predicted values are higher than the measured ones for all four mixes.

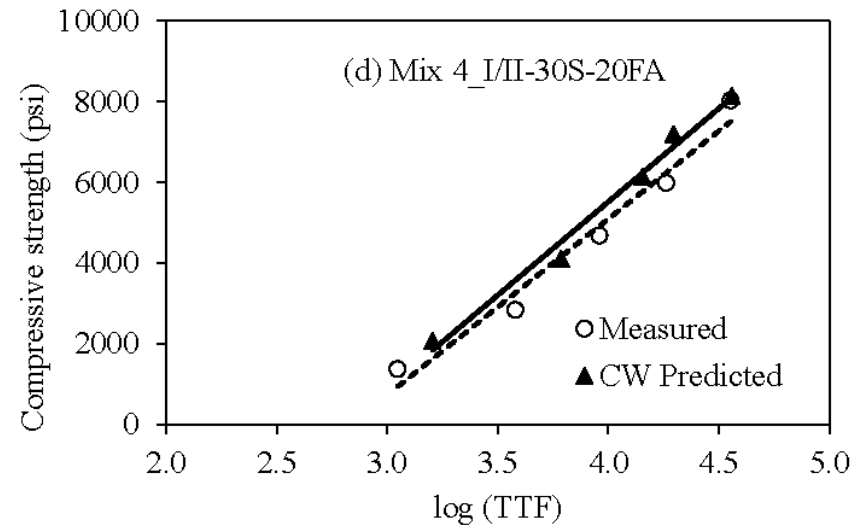
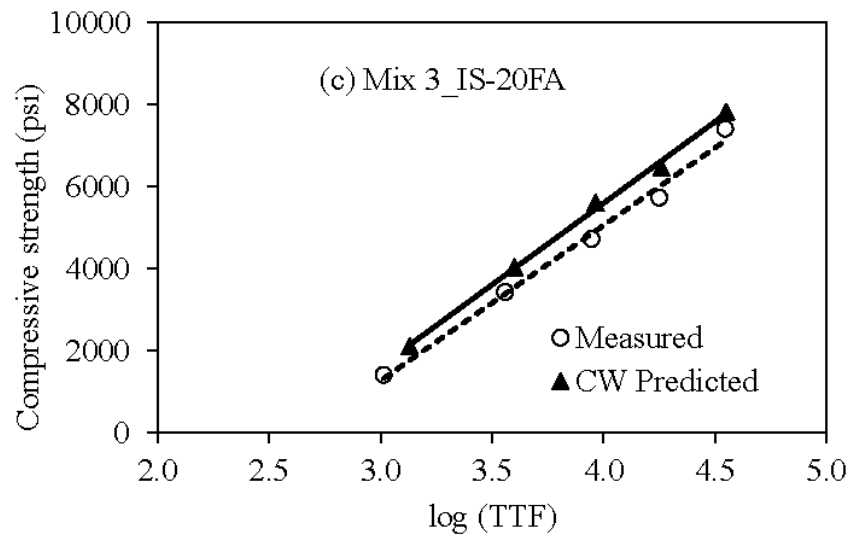
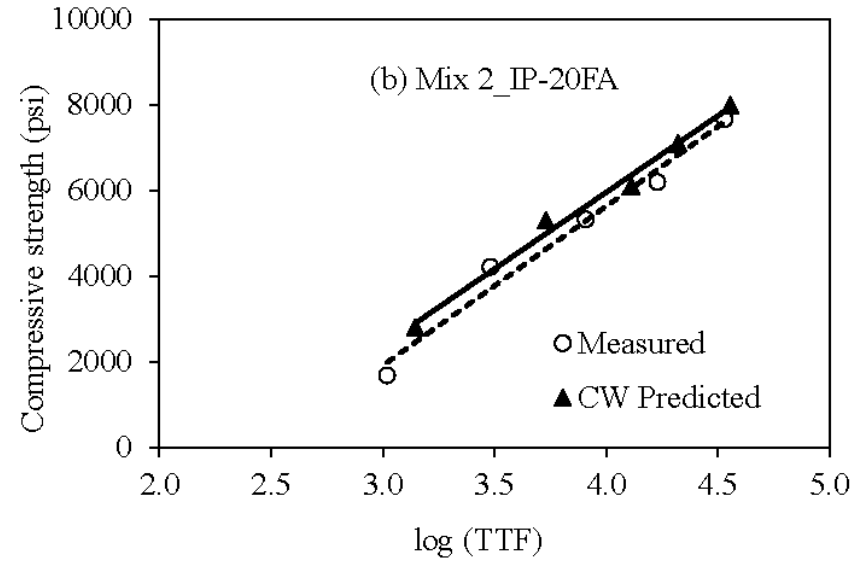
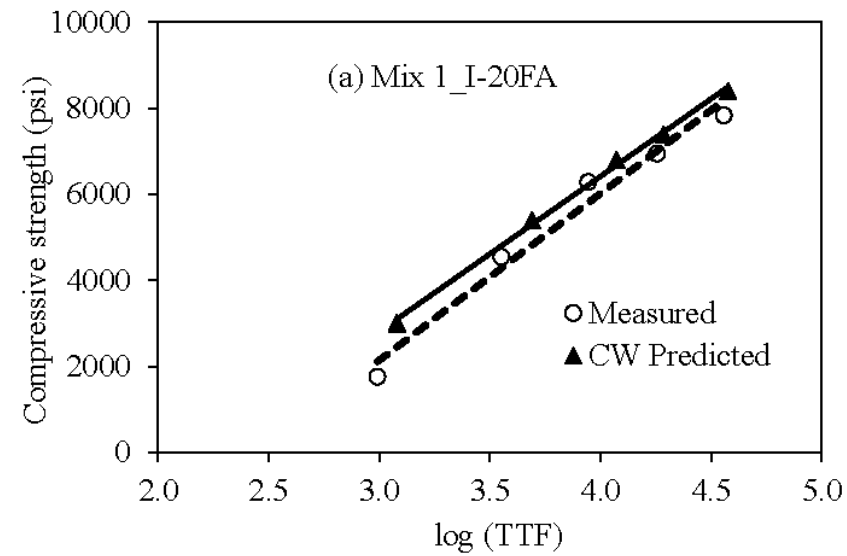


**Figure 7.24. Maturity and compressive strength comparison of laboratory mixes**

## 8. WORKSHOP AND SOFTWARE DOWNLOAD DETAILS

A hands-on workshop on Mass Concrete Fundamentals was conducted by the Iowa DOT under the lead of Ahmad Abu-Hawash November 7–8, 2019. About 40 people (engineers, contractors, and consultants) from Iowa attended the workshop over the two days. Three specialists—from the DOT, a consulting firm, and academia—presented on various topics related to mass concrete, including mass concrete specifications, fundamentals, predictions, and applications (see Table 8.1).

**Table 8.1. Presentations at the Mass Concrete Fundamentals workshop**

| <b>Presentation topic</b>                            | <b>Presenter</b>                      | <b>Presentation download link</b>                                                                                                                                                                                                             |
|------------------------------------------------------|---------------------------------------|-----------------------------------------------------------------------------------------------------------------------------------------------------------------------------------------------------------------------------------------------|
| Overview of mass concrete and temperature management | John Gajda<br>MJ2 Consulting,<br>PLLC | <a href="https://iowadot.gov/bridge/MassConcrete/Presentations/Gajda%20Mass%20Concrete%20Fundamentals%20handouts.pdf">https://iowadot.gov/bridge/MassConcrete/Presentations/Gajda%20Mass%20Concrete%20Fundamentals%20handouts.pdf</a>         |
| Iowa DOT mass concrete specification                 | Curtis Carter<br>Iowa DOT             | <a href="https://iowadot.gov/bridge/MassConcrete/Presentations/Curtis%20Carter%20MassConcWorkshop.pdf">https://iowadot.gov/bridge/MassConcrete/Presentations/Curtis%20Carter%20MassConcWorkshop.pdf</a>                                       |
| ConcreteWorks software for Iowa use                  | Kyle Riding<br>University of Florida  | <a href="https://iowadot.gov/bridge/MassConcrete/Presentations/Riding%20IDOT%20ConcreteWorks%20Training%20Nov%202019.pdf">https://iowadot.gov/bridge/MassConcrete/Presentations/Riding%20IDOT%20ConcreteWorks%20Training%20Nov%202019.pdf</a> |

Along with the theoretical and practical knowledge of mass concrete, the attendees worked step-by-step with the modified ConcreteWorks software on individual computers (see Figure 8.1).

The modified ConcreteWorks software is available from the Iowa DOT Bridges and Structures website at the bottom of this webpage: <https://iowadot.gov/bridge/Mass-Concrete-Fundamentals-November-2019>.

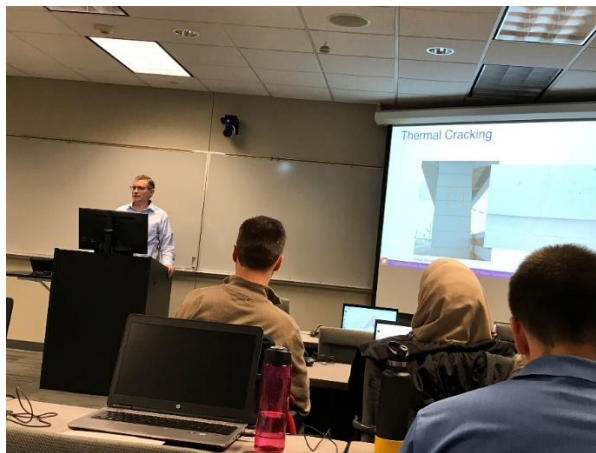


**Figure 8.1. Mass concrete fundamentals workshop**

## 9. CONCLUSIONS AND RECOMMENDATIONS

The input and output parameters of ConcreteWorks that needed to be modified for Iowa's use were identified in this study. The key properties of typical Iowa concrete mixes required by ConcreteWorks for thermal predictions were tested. The Iowa environmental data and Iowa DOT temperature differential limits for mass concrete were incorporated into the modified ConcreteWorks program. Thermal analyses were conducted on a real-time mass concrete project (the I-35 NB to US 30 WB [Ramp H] bridge) using both the unmodified and modified ConcreteWorks software, as well as 4C-Temp&Stress software, and the predicted temperature developments were compared with those monitored from the field site.

A summary of the features in the modified ConcreteWorks software includes the following.

1. Some default input values in the ConcreteWorks software have been updated based on the results obtained from this research project (both laboratory and field applications). They are available for use when analyzing Iowa mass concrete and can also be changed when measured data are available.
2. A soil initial temperature model has been added, which makes the predictions by the new ConcreteWorks more accurate.
3. The thermal analysis has been extended to up to 31 days. However, the cracking probability can be generated for only up to 7 days.
4. The environmental data for eight cities in Iowa are pre-incorporated in ConcreteWorks. They can be selected and used as environmental input data, as required by the software, for Iowa mass concrete temperature analysis. If changes are necessary, these environmental parameters can be manually entered.
5. The new ConcreteWorks can generate the profiles of temperature development at any selected point and temperature differential between any two selected points on a mass concrete member. The generated results can also be compared with the Iowa DOT limits incorporated into the software.

Some observations were made during the present study:

1. Some prediction models used in ConcreteWorks and the 4C program are quite different and thereby furnish different results. For example, the thermal conductivity, specific heat, and heat of hydration simulation processes in the software are different. 4C overestimates both the maximum temperature and differential temperature as with the footing analyzed in this study.



2. Among all three tools used (4C and new and old ConcreteWorks) for temperature analysis of the Pier 4 footing of the I-35 NB to US 30 WB bridge, the new ConcreteWorks predicted the closest value of the maximum temperature (149.
3. 16°F) to that measured in the field (149.00°F). The new ConcreteWorks prediction of the time to reach the maximum temperature (52 hours) is also close to that of the field-measured value (50 hours).
4. The measured temperature difference between the core and top of the footing was within the Iowa DOT limits for most of the early-age period. The 4C prediction of this parameter was relatively high in comparison to both ConcreteWorks predictions and the field measurements. However, the new ConcreteWorks prediction was very similar to the measured profile.
5. The new ConcreteWorks predicted slightly higher values of maturity and compressive strength than those measured from the field concrete; this is conservative from the perspective of factor of safety.
6. Comparing the new ConcreteWorks predictions of temperature profiles of the four concrete mixes tested in the laboratory, the maximum temperature was observed to be the lowest in Mix 2 (133.36°F) containing a total of 45% fly ash and the highest in Mix 1 (148°F) containing only 20% fly ash. Even though Mixes 3 and 4 contained a high amount of fly ash and slag, the predicted maximum temperature was not low if these two mixes were used. The predicted times to reach the maximum temperature for Mixes 1–4 were 55, 66, 68, and 78 hours, respectively.
7. ConcreteWorks furnished a higher maximum temperature and a higher differential temperature for mixes containing slag (Mix 3 and 4) when compared with the mix with no slag (Mix 2).
8. Overall, the new ConcreteWorks predicts the early-age temperature profile, maturity, and strength of Iowa mass concrete quite well.

Recommendations for an effective use of the modified ConcreteWorks and for further research are as follows.

1. The modified ConcreteWorks can be used for the analysis of the temperature development profile and the cracking probability of a range of mass concrete elements, such as rectangular/partially submerged footing, rectangular/T-shaped bent cap, and rectangular/circular column.
2. The modified ConcreteWorks can be used to generate the temperature development profile at any point and temperature differential between any two points in the mass concrete member.

The generated results can also be compared with the Iowa DOT temperature differential limits incorporated in the software.

3. The weblink for the ConcreteWorks workshop conducted during this project can serve as a resource for engineers that are interested in learning how to use the software. The ConcreteWorks Operator's Manual developed during this project can also serve as a reference to help users input data and interpret results properly. Additional workshops/short courses can be conducted to teach potential users how to use the manual and further understand the software.
4. Some of the default values (material properties, hydration parameters, formwork insulation, etc.) can be further modified if the measured data are available. It was observed in this study that compared to portland cement and fly ash containing mixes, the concrete mixes containing slag might exhibit a higher adiabatic temperature rise if used in mass concrete construction. Considering the interaction of slag and portland cement, further research can be performed to investigate the heat generation in slag-containing concrete mixes. A new model can also be developed to predict the temperature development profile of mass concrete members where such mixes are used. In addition, limestone cement is increasingly used in Iowa but not included in the present study. Investigation into the thermal behavior of mass concrete containing limestone cement may be necessary in the very near future.
5. In a bridge foundation design and construction, cofferdams are built to form watertight enclosures surrounding excavations. These enclosures normally consist of sheet piling driven around the perimeter of the excavation. A concrete seal coat is placed within the sheet piling, and the bridge footing is then built on the seal coat slab. A concern was raised in the present study on how the temperature profile of the seal coat slab can affect the early-age temperature development in the footing placed above it. Currently, the ConcreteWorks software doesn't have the capability to predict the concrete temperature of seal coat slabs. This demands further study.

## REFERENCES

- ACI Committee 207. 2006. *Guide to Mass Concrete*. ACI 207.1R-05. American Concrete Institute, Farmington Hills, MI.
- ASTM C177. 2004. *Standard Test Method for Steady-State Heat Flux Measurements and Thermal Transmission Properties by Means of the Guarded-Hot-Plate Apparatus*. ASTM International, West Conshohocken, PA.
- ASTM C192. 2016. *Standard Practice for Making and Curing Concrete Test Specimens in the Laboratory*. ASTM International, West Conshohocken, PA.
- Bai, H. 2013. Validation of Cylindrical Pavement Specimen Thermal Conductivity Protocol. MS thesis. Iowa State University, Ames, IA.
- Barber, E. S. 1957. Calculation of Maximum Pavement Temperatures from Weather Reports. *Highway Research Board Bulletin*, No. 168, pp. 1–8.
- Carlson, J. D., R. Bhardwaj, P. E. Phelan, K. E. Kaloush, and J. S. Golden. 2010. Determining Thermal Conductivity of Paving Materials Using Cylindrical Sample Geometry. *Journal of Materials in Civil Engineering*, Vol. 22, No. 2, pp. 186–95.
- De Schutter, G. and L. Taerwe. 1996. Degree of Hydration-Based Description of Mechanical Properties of Early Age Concrete. *Materials and Structures*, Vol. 29, No. 335.
- Emanuel, J. H. and J. L. Hulsey. 1977. Prediction of the Thermal Coefficient of Expansion of Concrete. *ACI Journal Proceedings*, Vol. 74, No. 4, pp. 149–155.
- Folliard, K. 2010. 3. *Heat of Hydration and Thermal Stress Analysis*. Training Materials presentation slides. University of Texas Concrete Durability Center, Center for Transportation Research, University of Texas at Austin, TX.  
[https://library.ctr.utexas.edu/digitized/products/5-4563-01-P1\\_PDFsOnly.zip](https://library.ctr.utexas.edu/digitized/products/5-4563-01-P1_PDFsOnly.zip).
- Meeks, C. and K. Folliard. 2013. *ConcreteWorks Implementation: Final Report*. Center for Transportation Research, University of Texas at Austin, TX.
- Poole, J. L. 2007. Modeling Temperature Sensitivity and Heat Evolution of Concrete. PhD dissertation. University of Texas at Austin, TX.
- Poole, J. L., K. A. Riding, K. J. Folliard, M. C. G. Juenger, and A. K. Schindler. 2007. Methods for Calculating Activation Energy for Portland Cement. *Materials Journal*, Vol. 104, No. 1, pp. 303–311.
- Riding, K. A. 2007. Early Age Concrete Thermal Stress Measurement and Modeling. PhD dissertation. University of Texas at Austin, Austin, TX.
- Riding, K. A., J. L. Poole, A. K. Schindler, M. C. G. Juenger, and K. J. Folliard. 2006. Evaluation of Temperature Prediction Methods for Mass Concrete Members. *Materials Journal*, Vol. 103, No. 5, pp. 357–65.
- Riding, K. A., J. L. Poole, K. J. Folliard, M. C. G. Juenger, and A. K. Schindler. 2011. New Model for Estimating Apparent Activation Energy of Cementitious Systems. *Materials Journal*, Vol. 108, No. 5, pp. 550–557.
- Riding, K. A., J. L. Poole, A. K. Schindler, M. C. G. Juenger, and K. J. Folliard. 2014. Statistical Determination of Cracking Probability for Mass Concrete. *Journal of Materials in Civil Engineering*, Vol. 26, No. 9, pp. 1–13.
- Riding, K., A. Schindler, P. Pesek, T. Drimalas, and K. Folliard. 2017. *ConcreteWorks V3 Training/User Manual (P1) ConcreteWorks Software (P2)*. Center for Transportation Research, University of Texas at Austin, Austin, TX.

- Schindler, A. K. 2002. Concrete Hydration, Temperature Development, and Setting at Early-Ages. PhD dissertation. University of Texas at Austin, TX.
- Schindler, A. K. 2004. Effect of Temperature on Hydration of Cementitious Materials. *Materials Journal*, Vol. 101, No. 1, pp. 72–81.
- Shaw, J. J., C. T. Jähren, K. Wang, and J. L. Li. 2011. *Iowa Mass Concrete for Bridge Foundation Study – Phase I*. Institute for Transportation, Iowa State University, Ames, IA. [https://intrans.iastate.edu/app/uploads/2018/03/mass\\_concrete\\_i\\_w\\_cvr.pdf](https://intrans.iastate.edu/app/uploads/2018/03/mass_concrete_i_w_cvr.pdf).
- Shaw, J. J., C. T. Jähren, K. Wang, and J. L. Li. 2014. *Iowa Mass Concrete for Bridge Foundation Study – Phase II*. Institute for Transportation, Iowa State University, Ames, IA. [https://intrans.iastate.edu/app/uploads/2018/03/mass\\_concrete\\_ii\\_w\\_cvr2.pdf](https://intrans.iastate.edu/app/uploads/2018/03/mass_concrete_ii_w_cvr2.pdf).
- Van Breugel, K. 1998. Prediction of Temperature in Hardening Concrete. In *Prevention of Thermal Cracking in Concrete at Early Ages*. RILEM Technical Committee 119, E & Fh Spon, London, pp. 51–74.
- Viviani, M. 2005. Monitoring and Modelling of Construction Materials During Hardening. PhD dissertation. Swiss Federal Institute of Technology, Zürich, Switzerland.

## APPENDIX A. CALIBRATION OF ISOTHERMAL CALORIMETER

Steps of the calibration procedure are as follows:

1. Using a multimeter, resistance  $R$  of the calibration inserts (1500 Ohm) are checked.
2. To initiate calibration, the environmental chamber is first set at the desired temperatures—10, 20, 30, and 40°C—one by one.
3. After the desired temperature is obtained, the baseline is recorded for a minimum of 24 hours. The average reading for each cell is the baseline,  $V_0$ .
4. The calibration insert is inserted into cell 1 with connections to a power source but no power applied, and the lid of the calorimeter chamber is closed completely.
5. A standard voltage  $V_{ref}$  of 15 V is applied over the calibration insert in one of the cells and output voltages measured in the calorimeter are recorded.
6. When the output voltage stays constant, usually after 4 hours, the average of the constant voltages is taken as  $V_1$ .
7. Standard voltage is turned off and the calorimeter is allowed to stabilize.
8. The above steps are repeated for all other cells and at other temperatures.
9. The calibration factor is then calculated as follows.

$$P = \frac{V_{ref}^2}{R}$$

$$CF = \frac{P}{V_1 - V_0}$$

Table A.1 presents the calculated values of calibration factors used in this study for eight channels of the calorimeter at 10, 20, 30, and 40°C.

**Table A.1. Calibration factors for eight channels of isothermal calorimeter**

| Temperature,<br>°C | Calibration Factor, mW/mV |       |       |       |       |       |       |       |
|--------------------|---------------------------|-------|-------|-------|-------|-------|-------|-------|
|                    | Ch1                       | Ch2   | Ch3   | Ch4   | Ch5   | Ch6   | Ch7   | Ch8   |
| 10                 | 13.01                     | 12.73 | 13.18 | 13.60 | 13.85 | 13.00 | 13.24 | 13.26 |
| 20                 | 12.61                     | 12.36 | 13.16 | 13.09 | 13.04 | 12.69 | 12.85 | 12.88 |
| 30                 | 12.27                     | 11.95 | 12.85 | 13.10 | 13.32 | 12.62 | 13.06 | 13.12 |
| 40                 | 12.34                     | 12.39 | 12.88 | 13.16 | 13.17 | 12.69 | 12.94 | 13.03 |

## **APPENDIX B. STEPS FOR BUILDING A SEMI-ADIABATIC CALORIMETER**

Steps for building a semi-adiabatic calorimeter are using a standard 24 in. diameter drum 36 in. high follow.

1. Using a galvanized steel sheet, construct a cylindrical chamber 7 in. in diameter and 14 in. high to hold the concrete sample (see Figure B.1).



**Figure B.1. Specimen holder**

2. Measure the inner height of the drum, divide it into 3, and mark those dimensions so that the steel chamber/concrete sample will be at the center of the drum and the insulation will be adequate.
3. Drill a hole in the drum at one third of the height from the bottom. This is required in order to take the thermocouple wires out to connect them to the data logger (see Figure B.2).



**Figure B.2. Thermocouple wires through drilled hole**

4. Three Type T thermocouples are placed. One thermocouple is to measure the temperature of concrete (MID), another to measure the temperature at the surface of the steel chamber (EXT1), and the third one an inch away from the surface of the steel chamber (EXT2) into the insulation.

5. For routing the MID thermocouple wire out of the concrete specimen, a small hole is drilled at the top of the steel chamber as shown in Figure B.3.



**Figure B.1. Cut-off at steel chamber edge**

6. Mix and place the insulation foam into the drum. Following the manufacturer's guide, mix the insulation foam in small amounts.
7. Fill the bottom third of the drum while holding the steel chamber in place. Then, fill the remaining portion of the drum such that the foam lines up with the top of the steel chamber as shown in Figure B.4.



**Figure B.4. Use of foam sealant**

8. As seen in Figure B.5, use “great stuff” insulation foam sealant to fill any holes.





**Figure B.5. Alignment of foam with steel chamber**

9. Cut an acrylic sheet to make the smooth top cover, and use high-temperature silicone to finish the edges (Figure B.6).



**Figure B.6. Acrylic sheet finish**

10. Once the foam insulation is finished, it is required to prepare the top cover. A neoprene sponge is used for this purpose. Cut a circular piece of sponge to create a smooth contact area between the bottom and top cover of the drum.
11. The final constructed calorimeter looks like that shown in Figure B.7.



**Figure B.7. Semi-adiabatic calorimeter**

## APPENDIX C. CALIBRATION OF SEMI-ADIABATIC CALORIMETER

The heat loss from the semi-adiabatic calorimeter must be measured and corrected for. Accurate calculation of the adiabatic temperature rise requires proper calibration of the instrument. In this research, de-ionized water was used as the calibration medium since its thermal properties are known and also easy to use. The calibration protocol described in Poole 2007 was used for the calorimeter, and the heat loss was computed.

Steps of the calibration procedure are as follows:

1. One 6×12 in. cylinder mold is taken and its weight is recorded.
2. De-ionized water is heated to 70–75°C, filled in the cylinder, and has its weight recorded.
3. The cylinder is placed inside the drum calorimeter.
4. All three thermocouples are connected to the Pico Technology data logger (USB TC-08) through the male connectors, which further connects to the computer through the USB cable.
5. The following steps (a-d) are then used to calculate the calibration factors ( $C_{f1}$ ,  $C_{f2}$ ).
  - a) Record the time ( $t$  in hr.), water temperature ( $T_w$  in °C), and the temperature difference between the two external thermocouples ( $T_d$  in °C) at 15-minute intervals for 160 hours. The first 5 hours of data are not used since the interior of the calorimeter has to first stabilize with the higher temperature of the test specimen.
  - b) Calculate the change in temperature of water ( $\Delta T_w$ ) at each time,  $t$ , and record sum of the changes in temperature ( $\Sigma \Delta T_w$ ).
  - c) Model the change in temperature of water using its known density,  $\rho_w$ , and specific heat,  $C_{p,w}$ , with the calibration factors ( $C_{f1}$  and  $C_{f2}$ ) using the following two equations.

$$\Delta q_h = T_d \cdot (-C_{f1} \cdot \ln(t) + C_{f2})$$

Where,  $\Delta q_h$ =heat transfer (J/h·m<sup>3</sup>),  $T_d$ =temperature difference between thermocouples EXT 1 and EXT 2,  $C_{f1}$ =calibration factor (W/°C),  $C_{f2}$ =calibration factor (W/°C), and  $t$ =time elapsed from start of test (hrs)

$$\Sigma \Delta T_w^* = \Sigma \frac{\Delta q_h \cdot \Delta t}{\rho_w \cdot C_{p,w} \cdot V_w}$$

Where,  $\Sigma \Delta T_w^*$ =the sum of the modeled changes in water temperature (°C),  $\rho_w$ =density of water (1,000 kg/m<sup>3</sup>),  $C_{p,w}$ =specific heat of water (4,186 J/kg°C),  $V_w$ =volume of water sample (m<sup>3</sup>), and  $\Delta t$ =time step(s).

- d) A regression analysis using the R-squared method with the Solver function in Excel is performed to match the modeled change in water temperature to the measured change in

water temperature. The Solver function generates the best-fit calibration factors ( $C_{f1}$  and  $C_{f2}$ ), which are used to model the change in water temperature.

Note: The researchers found the calculated heat loss from the first calibration procedure to be more than the expected. A 1.5 in. thick styrofoam insulating sheet was used below the top Aeromarine insulating lid to minimize the heat loss from the calorimeter. The calibration performed on the modified semi-adiabatic calorimeter produced better results with comparatively less heat loss. The values of the calibration factors are presented in Table C.1.

**Table C.1. Calibration factors for semi-adiabatic calorimeter**

| <b>Factor</b> | <b>Value</b> |
|---------------|--------------|
| $C_{f1} =$    | 0.0197 W/°C  |
| $C_{f2} =$    | 0.3970 W/°C  |

## **APPENDIX D. PROCEDURE TO ASSEMBLE THE THERMAL CONDUCTIVITY TEST SETUP**

The procedure to assemble the thermal conductivity test setup is explained below.

1. Specimen Preparation – Cylindrical specimen of 4 inches diameter and 6 inches height is prepared with a 0.5-in. hole through the center. For casting the specimen, a 4×8 in. cylindrical mold is commonly used along with a 0.5-in. diameter iron rod to create the hole in the center of the specimen (Figure D.1). Figure D.2 shows two 1-in. thick iron disks that are used—one each at the top and bottom.



**Figure D.1. Specimen preparation**



**Figure D.2. Iron disks for holding the rod**

2. While demolding after 24 hours, the rod and disks are pulled out.
3. The specimens are cured in the moist room for 28 days. After curing, the specimens are dried in the oven at 105°C for 24 hours and then these are tested for thermal conductivity.
4. The concrete specimen is placed on a 1.5-in. thick, 6-in. diameter, styrofoam insulation sheet. Another sheet of same dimensions is placed at the top after assembling the complete test setup.

5. A total of eight temperature sensors (Type K thermocouples) are installed. The location of sensors are as follows:
  - a) One sensor at one third from the top into the core of the specimen (Core top)
  - b) One sensor at one third from the bottom into the core of the specimen (Core bottom)
  - c) Five sensors at the surface of the specimen (S1, S2, S3, S4, and S5)
  - d) One sensor to measure the room temperature
6. The sensors at the surface are installed first. These sensors are pasted using a commonly used black electrical tape.
7. Silicone-based high thermal conductivity paste ( $k = 2.3 \text{ W/m-K}$ ) manufactured by Omega Engineering, Inc. is poured evenly into the central 0.5-in. diameter core of the specimen. The paste is injected using a plastic tube sleeve. Effort should be made to spread the paste as evenly and thinly as possible.
8. After the paste is poured, a cartridge heater (resistance =  $57.9 \Omega$ ) of 0.375-in. diameter and 6 in. height is inserted into the core.
9. Two central thermocouples (core top and core bottom) are attached to the heater with a separation of thin silver foil. This is done to ensure that the temperature data recorded by the thermocouples are that of the concrete inner surface and not that of the heater.
10. The thermocouples are connected to a Pico Technology data logger (USB TC 08) for recording temperature development during the test.
11. The heater is connected to a voltage regulator, which is connected to a power source.
12. A multimeter is also connected in series for measuring the applied voltage.
13. The resistance of the heater is measured and a predetermined voltage of 21.7 V is applied to the heater.
14. The data recording starts at this point.

## APPENDIX E. CALIBRATION OF THERMAL CONDUCTIVITY APPARATUS

It was required to check the accuracy of test method so that the test results could be validated. For this purpose, an ultra-high molecular weight polyethylene (UHMWPE) material was selected as a “known” reference (Figure E.1) sample since it has a low thermal conductivity range.



**Figure E.1. Reference material (UHMWPE)**

The UHMWPE manufactured by San Diego Plastics, Inc. was used, the thermal conductivity of which was given as 0.42–0.51 W/m-K by the manufacturer.

The material was of the same dimensions as that of concrete cylindrical specimens: a 4×6 in. cylinder with a 0.5-in. core through the center. Before performing the test on concrete samples, a tests on this reference material were first performed using an input heater voltage of 21.7 V (power=8.13 W). Four separate runs were conducted for the reference UHMWPE sample. In between each run, the test setup was completely disassembled and then reassembled. The data were recorded using the same Pico Technology data logger. The steady-state mean thermal conductivity value of the polyethylene sample was calculated to be 0.44 W/m-K with a 95% confidence interval of 0.43, 0.45, which is well within the range provided by the manufacturer. Figure E.2 shows the recorded data of the temperature sensors and the thermal conductivity values of four experimental runs.

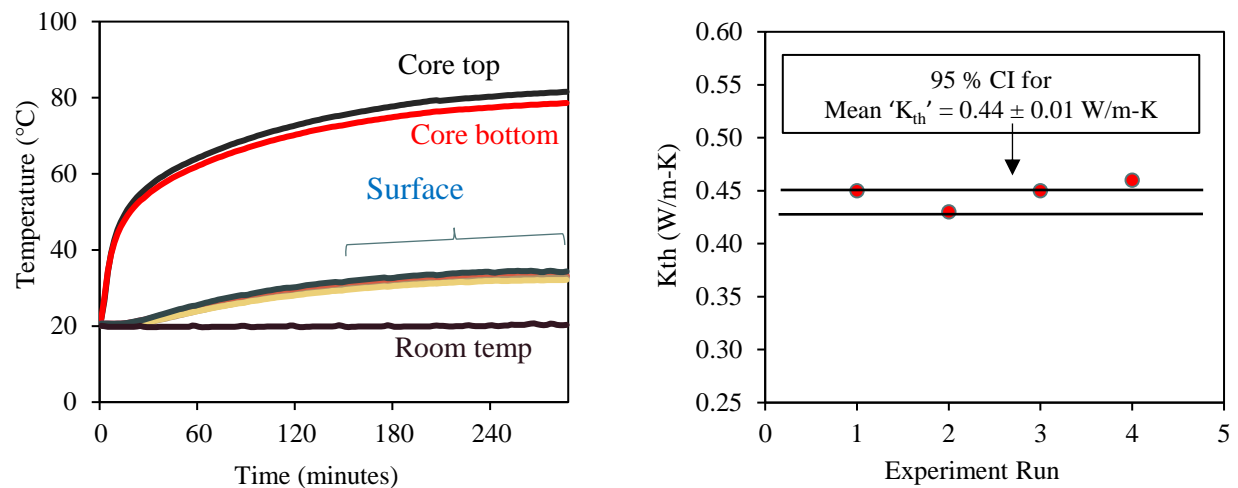


**Figure E.2. Thermal conductivity test for UHMWPE with temperature development during the test (left) and measured  $k$  of four test runs (right)**





**THE INSTITUTE FOR TRANSPORTATION IS THE FOCAL POINT FOR TRANSPORTATION  
AT IOWA STATE UNIVERSITY.**

**InTrans** centers and programs perform transportation research and provide technology transfer services for government agencies and private companies;

**InTrans** contributes to Iowa State University and the College of Engineering's educational programs for transportation students and provides K–12 outreach; and

**InTrans** conducts local, regional, and national transportation services and continuing education programs.



**IOWA STATE  
UNIVERSITY**

Visit [InTrans.iastate.edu](https://InTrans.iastate.edu) for color pdfs of this and other research reports.